AFRL-IF-RS-TR-1998-123
Final Technical Report
July 1998

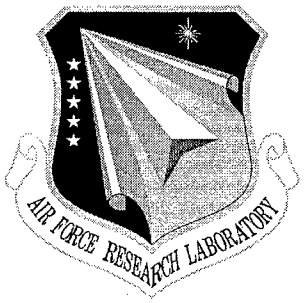

COMPARISON OF TIME AND TRANSFORM DOMAIN INTERFERENCE MITIGATION TECHNIQUES

Rensselaer Polytechnic Institute

Gary J. Saulnier and Catalina A. Silva

APPROVED FOR PUBLIC RELEASE; DISTRIBUTION UNLIMITED.

AIR FORCE RESEARCH LABORATORY
INFORMATION DIRECTORATE
ROME RESEARCH SITE
ROME, NEW YORK

This report has been reviewed by the Air Force Research Laboratory, Information Directorate, Public Affairs Office (IFOIPA) and is releasable to the National Technical Information Service (NTIS). At NTIS it will be releasable to the general public, including foreign nations.

AFRL-IF-RS-TR-1998-123 has been reviewed and is approved for publication.

APPROVED: Michael J. Medley

MICHAEL J. MEDLEY
Project Engineer

FOR THE DIRECTOR:

WARREN H. DEBANY, JR., Technical Advisor
Information Grid Division
Information Directorate

If your address has changed or if you wish to be removed from the Air Force Research Laboratory Rome Research Site mailing list, or if the addressee is no longer employed by your organization, please notify AFRL/IFGC, 525 Brooks Road, Rome, NY 13441-4505. This will assist us in maintaining a current mailing list.

Do not return copies of this report unless contractual obligations or notices on a specific document require that it be returned.

REPORT DOCUMENTATION PAGE	Form Approved OMB No. 0704-0188

1. AGENCY USE ONLY *(Leave blank)*	2. REPORT DATE	3. REPORT TYPE AND DATES COVERED
	July 1998	Final Apr 97 - Sep 97

4. TITLE AND SUBTITLE

COMPARISON OF TIME AND TRANSFORM DOMAIN INTERFERENCE MITIGATION TECHNIQUES

5. FUNDING NUMBERS

C - F30602-97-1-0142
PE - 61102F
PR - 2304
TA - C7
WU - 01

6. AUTHOR(S)

Gary J. Saulnier and Catalina A. Silva

7. PERFORMING ORGANIZATION NAME(S) AND ADDRESS(ES)

Rensselaer Polytechnic Institute
110 Eighth Street
Troy NY 12180-3590

8. PERFORMING ORGANIZATION REPORT NUMBER

N/A

9. SPONSORING/MONITORING AGENCY NAME(S) AND ADDRESS(ES)

Air Force Research Laboratory/IFGC
525 Brooks Road
Rome NY 13441-4505

10. SPONSORING/MONITORING AGENCY REPORT NUMBER

AFRL-IF-RS-TR-1998-123

11. SUPPLEMENTARY NOTES

Air Force Research Laboratory Project Engineer: Michael J. Medley/IFGC/(315) 330-4830

12a. DISTRIBUTION AVAILABILITY STATEMENT

Approved for public release; distribution unlimited.

12b. DISTRIBUTION CODE

13. ABSTRACT *(Maximum 200 words)*

Many methods have been proposed for suppressing interference in a direct sequence spread spectrum signal, including time domain adaptive filtering and transform domain excision. This report presents Monte Carlo simulation results which directly compare the performance of predictive and two-sided adaptive filters, time domain adaptive correlation, transform domain excision with modulated lapped transforms and time domain correlation, and transform domain excision with modulated lapped transforms and transform domain excision. Comparisons are made for a number of different jammers, including fixed and swept-frequency (i.e. chirp) tones, narrowband Gaussian interference, and pulsed tone and narrowband Gaussian Interference. The performance of all the systems is compared under identical jamming conditions. Simulations were performed using the Signal Processing WorkSystem (SPW) Prom Alta Group of Cadence Design Systems, Inc. The results indicate that the transform domain excision with the modulated lapped transform and time domain correlation may provide the best compromise in implementation complexity and performance over the range of interferers considered.

14. SUBJECT TERMS	15. NUMBER OF PAGES
Adaptive Filtering, Transform Domain Processing, Modulated Lapped Transforms, Interference	106
	16. PRICE CODE

17. SECURITY CLASSIFICATION OF REPORT	18. SECURITY CLASSIFICATION OF THIS PAGE	19. SECURITY CLASSIFICATION OF ABSTRACT	20. LIMITATION OF ABSTRACT
UNCLASSIFIED	UNCLASSIFIED	UNCLASSIFIED	UL

Standard Form 298 (Rev. 2-89) (EG)
Prescribed by ANSI Std. 239.18
Designed using Perform Pro, WHS/DIOR, Oct 94

CONTENTS

LIST OF FIGURES iii

LIST OF TABLES v

EXECUTIVE SUMMARY 1

1.- Introduction 2

1.1- Spread Spectrum Systems 2

1.2- Report Overview 8

2.- System Description 9

2.1- Modulator and Channel 9

2.2- Jammers. 14

2.2.1- Stationary Tone Jamming (Jammer 1) 14

2.2.2- Swept Tone and Chirp Jamming (Jammer 2) 14

2.2.3- Narrowband Gaussian Jamming (Jammer 3) 19

2.2.4- Pulsed Tone and Pulsed Gaussian Jamming (Jammer 4) 19

2.2.5- Summary 23

2.3- Communication Receivers 23

2.3.1- Adaptive Filters 23

2.3.2- Modulated Lapped Transforms - Transform Domain Excision (MLT-TDE) 26

2.3.3- Adaptive Correlator 30

2.3.4- Modulated Lapped Transforms - Transform Domain Excision and Detection (MLT-TDED) 33

2.3.5- Computational Complexity 36

3.- Implementation 37

3.1- Signal Processing WorkSystem (SPW) 37

3.2- Parameters 37

3.3- Simulations 38

4.- Results 39

4.1- Results for Jammer 1 39

4.2- Results for Jammer 2 47

4.2.1- Swept Tone 47

4.2.2- Chirp Jamming 55

4.3- Results for Jammer 3 63

4.4- Results for Jammer 4 71

4.4.1- Pulsed Tone 71

4.4.2- Pulsed Gaussian Jamming 78
5.- Conclusions and Discussions 87
5.1- Conclusions 87
5.1.1- Adaptive Filters 87
5.1.2- MLT-Transform Domain Exciser 87
5.1.3- Adaptive Correlator 88
5.1.4- MLT-Transform Domain Excision and Detection 88
5.1.5- Additional Comments 88
5.2- Future Research 89
6.- Bibliography 90

LIST OF FIGURES

Figure 1.1: Illustration of Power Spectral Density for Spread Spectrum System 5
Figure 2.1: Block Diagram for the Modulator and Channel 10
Figure 2.2: PN Sequence Waveform 11
Figure 2.3: Random Data Waveform 12
Figure 2.4: Gaussian Random Noise Waveform 13
Figure 2.5: Block Diagram for the Jammer Systems 15
Figure 2.6: Stationary Tone Jamming Waveform 16
Figure 2.7: Swept Tone Waveform 17
Figure 2.8: Chirp Jamming Waveform 18
Figure 2.9: Narrowband Gaussian Jamming Waveform 20
Figure 2.10: Pulsed Tone Jamming Waveform 21
Figure 2.11: Pulsed Gaussian Jamming Waveform 22
Figure 2.12: Predictive Transversal Filter 25
Figure 2.13: Illustration of the Excision Process 27
Figure 2.14: Block Diagram for the Filters and MLT-TDE Receiver Systems 29
Figure 2.15: Adaptive Correlator Receiver Structure 31
Figure 2.16: Receiver Employing MLT Domain Excision and Detection 34
Figure 2.17: Block Diagram for the Correlator and MLT-TDED Receiver Systems 35
Figure 4.1 : BER vs. Eb/No for Jammer 1 - Filters / MLT-TDE 40
Figure 4.2 : BER vs. Eb/No for Jammer 1 - Corr / MLT-TDED 41
Figure 4.3 : BER vs. JSR for Jammer 1 - Filters / MLT-TDE 42
Figure 4.4 : BER vs. JSR for Jammer 1 - Corr / MLT-TDED 42
Figure 4.5 : BER vs. Jammer Frequency for Jammer 1 - Filters / MLT-TDE 45
Figure 4.6 : BER vs. Jammer Frequency for Jammer 1 - Corr / MLT-TDED 46
Figure 4.7 : BER vs. Eb/No for Jammer 2-Triang - Filters / MLT-TDE 47
Figure 4.8 : BER vs. Eb/No for Jammer 2-Triang - Corr / MLT-TDED 48
Figure 4.9 : BER vs. JSR for Jammer 2-Triang - Filters / MLT-TDE 49
Figure 4.10 : BER vs. JSR for Jammer 2-Triang - Corr / MLT-TDED 49
Figure 4.11 : BER vs. Sweep Frequency for Jammer 2-Triang - 1-S Filter 52
Figure 4.12 : BER vs. Sweep Frequency for Jammer 2-Triang - 2-S Filter 53
Figure 4.13 : BER vs. Sweep Frequency for Jammer 2-Triang - MLT-TDE 53
Figure 4.14 : BER vs. Sweep Frequency for Jammer 2-Triang - Corr 54
Figure 4.15 : BER vs. Sweep Frequency for Jammer 2-Triang - MLT-TDED 54

Figure 4.16 : BER vs. Eb/No for Jammer 2-Ramp - Filters / MLT-TDE 55
Figure 4.17 : BER vs. Eb/No for Jammer 2-Ramp - Corr / MLT-TDED 56
Figure 4.18 : BER vs. JSR for Jammer 2-Ramp - Filters / MLT-TDE..... 57
Figure 4.19 : BER vs. JSR for Jammer 2-Ramp - Corr / MLT-TDED 57
Figure 4.20 : BER vs. Sweep Frequency for Jammer 2-Ramp - 1-S Filter 60
Figure 4.21 : BER vs. Sweep Frequency for Jammer 2-Ramp - 2-S Filter..... 61
Figure 4.22 : BER vs. Sweep Frequency for Jammer 2-Ramp - MLT-TDE..... 61
Figure 4.23 : BER vs. Sweep Frequency for Jammer 2-Ramp — Corr..... 62
Figure 4.24 : BER vs. Sweep Frequency for Jammer 2-Ramp - MLT-TDED..... 62
Figure 4.25 : BER vs. Eb/No for Jammer 3 - Filters / MLT-TDE 63
Figure 4.26 : BER vs. Eb/No for Jammer 3 - Corr / MLT-TDED 64
Figure 4.27 : BER vs. JSR for Jammer 3 - Filters / MLT-TDE 65
Figure 4.28 : BER vs. JSR for Jammer 3 - Corr / MLT-TDED 65
Figure 4.29 : BER vs. Jammer Frequency for Jammer 3 - Filters / MLT-TDE 68
Figure 4.30 : BER vs. Jammer Frequency for Jammer 3 - Corr / MLT-TDED..... 69
Figure 4.31 : BER vs. Jammer Bandwidth for Jammer 3 - Filters / MLT-TDE 70
Figure 4.32 : BER vs. Jammer Bandwidth for Jammer 3 - Corr / MLT-TDED 70
Figure 4.33 : BER vs. Eb/No for Jammer 4-Tone - Filters / MLT-TDE 71
Figure 4.34 : BER vs. Eb/No for Jammer 4-Tone - Corr / MLT-TDED 72
Figure 4.35 : BER vs. JSR for Jammer 4-Tone - Filters / MLT-TDE 73
Figure 4.36 : BER vs. JSR for Jammer 4-Tone - Corr / MLT-TDED 74
Figure 4.37 : BER vs. Jammer Frequency for Jammer 4-Tone - Filters / MLT-TDE 77
Figure 4.38 : BER vs. Jammer Frequency for Jammer 4-Tone - Corr / MLT-TDED..... 78
Figure 4.39 : BER vs. Eb/No for Jammer 4-NB - Filters / MLT-TDE 79
Figure 4.40 : BER vs. Eb/No for Jammer 4-NB - Corr / MLT-TDED 80
Figure 4.41 : BER vs. JSR for Jammer 4-NB - Filters / MLT-TDE 81
Figure 4.42 : BER vs. JSR for Jammer 4-NB - Corr / MLT-TDED 81
Figure 4.43 : BER vs. Jammer Frequency for Jammer 4-NB - Filters / MLT-TDE 84
Figure 4.44 : BER vs. Jammer Frequency for Jammer 4-NB - Corr / MLT-TDED 85
Figure 4.45 : BER vs. Jammer Bandwidth for Jammer 4-NB - Filters / MLT-TDE 86
Figure 4.46 : BER vs. Jammer Bandwidth for Jammer 4-NB - Corr / MLT-TDED 86

LIST OF TABLES

Table 2.1: Summary of Main Parameters for Modulator and Channel 9
Table 2.2: Summary of Main Parameters for Jammers 23
Table 2.3: Computational Complexity for the Different Communication Receiver Systems 36
Table 3.1: Simulations Performed 38
Table 4.1: Jammer 1 - Filters / MLT-TDE - Parameters Used for Each Value of JSR 43
Table 4.2: Jammer 1- Corr / MLT-TDED - Parameters Used for Each Value of JSR 44
Table 4.3: Jammer 2 Triangle - Filters / MLT-TDE - Parameters Used for Each Value of JSR .. 50
Table 4.4: Jammer 2 Triangle - Corr / MLT-TDED - Parameters Used for Each Value of JSR .. 51
Table 4.5: Jammer 2 Ramp - Filters / MLT-TDE - Parameters Used for Each Value of JSR 58
Table 4.6: Jammer 2 Ramp - Corr / MLT-TDED - Parameters Used for Each Value of JSR..... 59
Table 4.7: Jammer 3 - Filters / MLT-TDE - Parameters Used for Each Value of JSR 66
Table 4.8: Jammer 3- Corr / MLT-TDED - Parameters Used for Each Value of JSR..... 67
Table 4.9: Jammer 4 Tone - Filters / MLT-TDE - Parameters Used for Each Value of JSR 75
Table 4.10: Jammer 4 Tone - Corr / MLT-TDED - Parameters Used for Each Value of JSR..... 76
Table 4.11: Jammer 4 Noise - Filters / MLT-TDE - Parameters Used for Each Value of JSR 82
Table 4.12: Jammer 4 Noise - Corr / MLT-TDED - Parameters Used for Each Value of JSR 83

EXECUTIVE SUMMARY

Many methods have been proposed for suppressing interference in a direct sequence spread spectrum signal and many have been shown to be effective for particular jamming conditions. However, it has been difficult to compare the performance of these techniques because, in most cases, they have been studied separately using different channel conditions. The objective of this effort was to perform a direct comparison of a number of techniques by evaluating their performance for identical interferers. The particular techniques under consideration were predictive and two-sided transversal adaptive filters, the time domain adaptive correlator, transform domain excision using modulated lapped transforms and transform domain detection, and transform domain excision using modulated lapped transforms and time domain correlation. The interferers included fixed and variable frequency tones, swept tones (chirps), narrowband Gaussian interference, pulsed tones and pulsed narrowband Gaussian interference. This collection of interferers is sufficiently varied to test the ability to each technique to resolve interference in both frequency and time. Additionally, in comparing the techniques, the computational complexity was taken into account, such that direct comparison is made between interference suppression techniques of similar complexity. In particular, whenever possible, the parameters of the interference suppressor, such as the order of the adaptive filter and length of the transform, were selected to make the complexity nearly equivalent. The comparisons are based on bit-error-rate performance obtained through Monte Carlo simulation. Simulations were performed using the Signal Processing WorkSystem (SPW) from AltaGroup of Cadence Design Systems, Inc.

The simulation results indicate that the performance, in terms of low bit error rate, of the different receiver systems depends heavily on the jamming signal and parameters used, and therefore there is no "ideal" structure in the sense of a particular system that would be able to handle any type of situation. Nevertheless, the LMS filter systems, 'particularly the two-sided filter, present excellent performance in removing the interference when the channel introduces fixed-tone jamming, while the tracking capabilities of the MLT with transform domain excision and detection structure are remarkable.

CHAPTER 1

Introduction

Spread spectrum techniques were initially conceived for military usage, due to their ability to reduce the effects of strong jamming and provide some level of security. However, civilian applications may also benefit from it, such as the use of this system for mobile radio networks (radio telephony, packet radio, and amateur radio), and multiple-access communication (CDMA).

The processing gain of a direct sequence spread-spectrum system provides some degree of protection against narrowband interference. However, when the processing gain is unable to combat the jammer adequately, additional signal processing techniques can be employed to more effectively remove the interference.

Considerable amount of work has been performed on interference mitigation techniques involving time domain and frequency domain processing. The time domain study has been centered primarily on transversal filter structures, and the various adaptive algorithms that can be used with them. Transform domain processing has moved from initial work in frequency domain excision to include the consideration of different transforms. The purpose of this study is to accomplish a comparative study of different interference suppression techniques, and determine which technique is best suited for a given interference scenario.

1.1- Spread Spectrum Systems

Spread spectrum systems transmit the data using a much larger bandwidth than the minimum bandwidth required [1, 2]. The spectrum spreading is achieved before transmission employing a noise-like spreading code called pseudo-random or pseudo-noise sequence, that is independent of the message sent. In the receiver, the same code is used to despread, or correlate, the received data, which allows for the recovery of the original message. The widening of the bandwidth is realized through the use of modulation, which can be achieved using a variety of methods, including pseudo-noise (PN), frequency hopping (HP), time hopping (TH), and hybrid combinations of these techniques. In pseudo-noise direct-sequence modulation, a pseudo-randomly generated sequence is used to produce phase transitions in the carrier containing the data. Frequency hopping involves a shift in the carrier's frequency in a pseudo-random way, while in time hopping, bursts of signal are originated at pseudo-random times. In all these techniques, the idea behind the term pseudo-random is random in appearance, but that can be reproduced by authorized receivers.

An important attribute of a spread-spectrum communication system is its capability to reject externally generated interfering (jamming) signals with finite power, whether intentional or not. The transmitted signal assumes a wideband noise-like appearance, and therefore is hard to detect from the background noise.

A pseudo-noise (PN) sequence is defined as a random binary coded sequence, usually periodic, of 1s and 0s with certain autocorrelation properties. Such sequences can be generated by simple mechanisms, particularly a linear feedback shift register. Maximum-length sequences present many of the properties observed in truly random binary sequences. They are always periodic with a period of $N = 2^m - 1$, where m is the length of the shift register. In an augmented PN sequence, one additional 0 bit is generated, thereby increasing the period to $N = 2^m$. Typically, each bit interval is subdivided into N short intervals called chips. The longer the period of the spreading code, the closer will the transmitted signal be to a truly random wave, and the harder it will be to detect. However, the price for a better protection against interference is increased transmission bandwidth, system complexity, and processing delay.

In order to better illustrate the previous concepts, the PN direct sequence spread-spectrum modulation operation is described in the remainder of this section:

The transmitted message $b(t)$ is multiplied by a wideband PN waveform $c(t)$,

$$m(t) = b(t)\ c(t). \tag{1.1}$$

Thus, if the data is narrowband and the PN sequence is wideband, the product signal $m(t)$ will have its spectrum bandwidth about the same as the PN sequence, as it equals the convolution of the spectra of the two component signals. If it is assumed that

$$b(t) = \sqrt{E_s} \sum_k b_k\ p\left(t - k\,T_b\right), \tag{1.2}$$

where T_b is the bit duration, T_c is the chip duration, E_s is the energy per symbol, $p(t)$ is a basic pulse shape, and b_k the binary digits. $N = \dfrac{T_b}{T_c}$ is the number of chips per data bit.

It follows that the power spectral density of the message $b(t)$ is given by

$$S_{bb}(f) = \frac{1}{T_b} \left|P(f)\right|^2 \sum_{n=-\infty}^{\infty} R_{bb}(n)\ e^{-j2\pi n f T_b}, \tag{1.3}$$

and assuming that its autocorrelation function, $R_{bb}(n) = \delta_n$, the delta function,

$$S_{bb}(f) = T_b\ \sin c^2(\pi f T_b), \tag{1.4}$$

and that $c(t)$ and $b(t)$ are independent:

$$S_{mm}(f) = S_{cc}(f) \otimes S_{bb}(f), \tag{1.5}$$

where $S_{mm}(f)$ and $S_{cc}(f)$ are the power spectral densities of the signals $m(t)$ and $c(t)$ respectively.

For $N >> 1$, $S_{cc}(f)$ is much wider than $S_{bb}(f)$, therefore

$$S_{mm}(f) \approx \frac{E_s}{T_b} S_{cc}(f). \tag{1.6}$$

The received signal is modeled as

$$r(t) = m(t) + n(t) + i(t) \tag{1.7}$$

where $n(t)$ is wideband noise and $i(t)$ a narrowband interference component. To recover the data $b(t)$, the received signal $r(t)$ is applied to a demodulator, employing the same PN sequence used in the transmitter and, assuming that the receiver operates in perfect synchronism with the transmitter,

$$\begin{aligned} z(t) &= c(t)\, r(t) \\ &= c^2(t)\, b(t) + c(t)\, n(t) + i(t)\, c(t) \\ &= b(t) + n'(t) + i(t)\, c(t), \end{aligned} \tag{1.8}$$

where $c^2(t) = 1$ and $n'(t)$ is a new wideband noise component. If $n(t)$ is zero-mean WGN, then $n'(t)$ is likewise a zero-mean WGN process with double-sided noise spectral density $\frac{N_o}{2}$ Watts/Hz.

Similarly, the despread interference component is

$$\begin{aligned} i'(t) &\equiv c(t)\, i(t) \\ &= i(t) \sum_k c_k\, p(t - k T_c) \end{aligned} \tag{1.9}$$

where c_k represents the binary digits.

The multiplication operation brings the data signal down to its original bandwidth while spreading the noise and interference to a wide bandwidth, as shown in Figure 1.1.

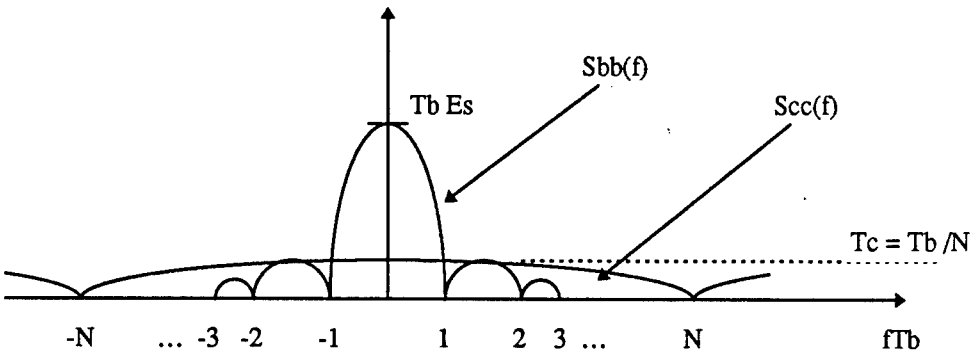

Figure 1.1: Illustration of Power Spectral Density for Spread Spectrum System

Subsequent lowpass filtering may reject large amounts of the spread noise and interference, making possible the recovery of the original message. At the receiver, the ratio of the spread signal-to-noise ratio, SNR_I, to the signal-to-noise ratio after despreading, SNR_o, is defined as the processing gain G_p, i.e.,

$$G_p = \frac{SNR_I}{SNR_o}, \tag{1.10}$$

and is a measure of the amount of performance improvement that is achieved through the use of spread spectrum. The processing gain can be approximated by taking the ratio of the spread bandwidth to the data information bandwidth (rate), i.e.,

$$G_p \approx \frac{BW_{spread}}{R_{info}}. \tag{1.11}$$

If $i(t)$ is orthogonal to $c(t)$ then after subsequent integration (matched filtering), the interference component can be eliminated. Otherwise, $i'(t)$ is a wideband component whose effect after subsequent low-pass filtering is the same as if $i'(t)$ were Gaussian with power spectral density

$$S_{i'i'}(f) = S_{ii}(f) \otimes S_{cc}(f)$$

$$= \frac{E_I}{N}. \tag{1.12}$$

Assuming that $i(t)$ is narrowband relative to $c(t)$, with E_I the interference energy in a bit interval, and $S_{i'i'}(f)$ and $S_{ii}(f)$ the power spectral densities of the signals $i'(t)$ and $i(t)$ respectively.

Finally

$$n''(t) \equiv n'(t) + i'(t) \tag{1.13}$$

can be considered Gaussian with power spectral density

$$\frac{N_o'}{2} = \frac{N_o}{2} + \frac{E_I}{N} = \frac{N_o}{2}\left[1 + \frac{2E_I}{NN_o}\right]. \tag{1.14}$$

For binary antipodal signaling, the bit error probability is

$$P_b = Q\left(\sqrt{\frac{2E_b}{N_o\left[1+\frac{2E_I}{N\,N_o}\right]}}\right) \tag{1.15}$$

where E_b is the energy per bit. Suppose that the jammer has average energy E_I but only on a fraction ρ of a bit interval. The noise spectral density is then

$$\frac{N_0'}{2} = \frac{N_o}{2} + \frac{E_I/\rho}{N} \tag{1.16}$$

when the jammer is on, and

$$\frac{N_0'}{2} = \frac{N_o}{2} \tag{1.17}$$

when the jammer is off. The error probability is then

$$P_b = (1-\rho)\,Q\left(\sqrt{\frac{2E_b}{N_o}}\right) + \rho\,Q\left(\sqrt{\frac{2E_b}{N_o\left[1+\frac{2E_I/\rho}{N\,N_o}\right]}}\right), \tag{1.18}$$

where $Q(x) = \frac{1}{\sqrt{2\pi}}\int_x^\infty e^{-t^2/2}\,dt$ is named the tail function.

Suppose that $E_I / N >> N_o / 2$, i.e. the processing gain is insufficient to render interference negligible. Then

$$P_b \approx \rho \; Q\left(\sqrt{\frac{\rho\, E_b}{E_I / N}}\right). \tag{1.19}$$

An intelligent jammer will maximize this by choice of ρ. The maximum value of $x\,Q\left(\sqrt{x}\right)$ can be seen at $x = 1.44$ with maximum value 0.1657. The maximum value of ρ is then

$$\rho^* = \min\left\{1; \frac{1.44}{E_b / E_I'}\right\} \tag{1.20}$$

where $E_I' \equiv E_I / N$. The corresponding error probability is

$$P_b^* = \frac{0.1657}{E_b / E_I'}, \tag{1.21}$$

which decreases only algebraically in E_b / E_I'.

For full-time jammer, the error probability is

$$P_b = Q\left(\sqrt{\frac{2E_b}{N_o\left[1+\frac{2E_I'}{N_o}\right]}}\right) \tag{1.22}$$

and if $E_I' \equiv E_I / N >> N_o / 2$, then

$$P_b \approx Q\left(\sqrt{\frac{E_b}{E_I'}}\right) \tag{1.23}$$

$$\leq \frac{1}{2}\, e^{-\frac{1}{2}(E_b/E_I')} \tag{1.24}$$

which decreases exponentially in E_b / E_I'.

1.2- Report Overview

An elementary way to fight noise and interference is to increase the signal power. However, raising power is costly and can damage instruments. Noise modulation, i.e. utilization of noise-like signal as a carrier, is very suitable for anti-jamming and security issues. Nevertheless, despite the fact that spread-spectrum modulation techniques inherently present interference suppression capabilities, these can be enhanced considerably by processing the received signal.

The purpose of this report is to perform a direct comparison of time domain and frequency domain interference suppression techniques. Simulations will be performed using the Signal Processing WorkSystem (SPW) from AltaGroup of Cadence Designs, Incorporated. The overall goal will be to determine the performance of a number of interference suppression techniques under different interference conditions. The four individual techniques studied are time domain adaptive transversal filtering, transform domain excision, time domain adaptive correlator receiver, and transform domain excision and detection. A direct head-to-head comparison of the performance of the techniques for a set of "typical" interference types will been performed, in order to decide which technique is best for different applications. The types of interference that will be considered are stationary tone jamming, swept tone and chirp jamming, narrowband Gaussian jamming, pulsed tone and pulsed Gaussian jamming. The performance measures that will be used include the bit-error-rate (BER), tracking performance, and implementation complexity.

In chapter 2, the different systems are described, beginning with the modulator and channel, followed by the various jammer types, and finally the four communication receiver structures are explained. Besides, the implementation complexity for the receiver systems is calculated. In chapter 3, the Signal Processing WorkSystem (SPW) and the three performance measures are presented, along with a description of the simulations to be performed. In chapter 4, the results of the simulations executed for each of the structures with the different types of jammers are presented, along with the curves showing the bit error rates obtained. Finally, in chapter 5, the discussions and conclusions of this report are exposed, making a direct comparison among the different interference suppression techniques analyzed.

CHAPTER 2

System Description

In the following chapter, the different systems built in this report are described.

2.1- Modulator and Channel

A block diagram showing the modulator and channel (without jamming) can be seen in Figure 2.1. Binary Phase Shift Keying (BPSK) baseband signal and direct sequence spread-spectrum modulation are used for this system.

The pseudo-noise (PN) sequence, after conversion of 0s and 1s to -1s and 1s, is shown in Figure 2.2. A value of 6 is used for the length of the shift register, with a resulting period of $N = 2^m - 1 = 2^6 - 1 = 63$. The random data consists of random 1s and 0s binary bits (see Figure 2.3), whose sampling frequency equals the period of the PN sequence, and bit rate is set to $1.0\ Hz$. The logical 0s and 1s are converted to real-number outputs for both sequences: when the input is true (high; > 0), the output is set to 1.0; when the input is false (low; ≤ 0), the output is set to -1.0. The PN sequence is then used to modulate the random data. A Gaussian random noise (see Figure 2.4) is added, using a value of $E_b / N_0 = 6.0\ dB$ for the following parameters,

$$\mu = Mean = 0.0 \tag{2.1}$$

$$\sigma^2 = Variance = 10^{\frac{10\log_{10}\frac{2^m-1}{2} - E_b/N_o}{10}} = 10^{\frac{10\log_{10}\frac{2^6-1}{2} - 6.0}{10}} = 7.91244. \tag{2.2}$$

Table 2.1 summarizes the main parameters used to design the communication channel.

PN Sequence	m = Shift Register = 6 N = Period = 63 Chip Rate = 63 Hz
Random Data	Sampling Frequency = 63.0 Hz Bit Rate = 1.0 Hz
Gaussian Random Noise	E_b/N_o = 6.0 dB μ = Mean = 0.0 σ^2 = Variance = 7.91244

Table 2.1: Summary of Main Parameters for Modulator and Channel

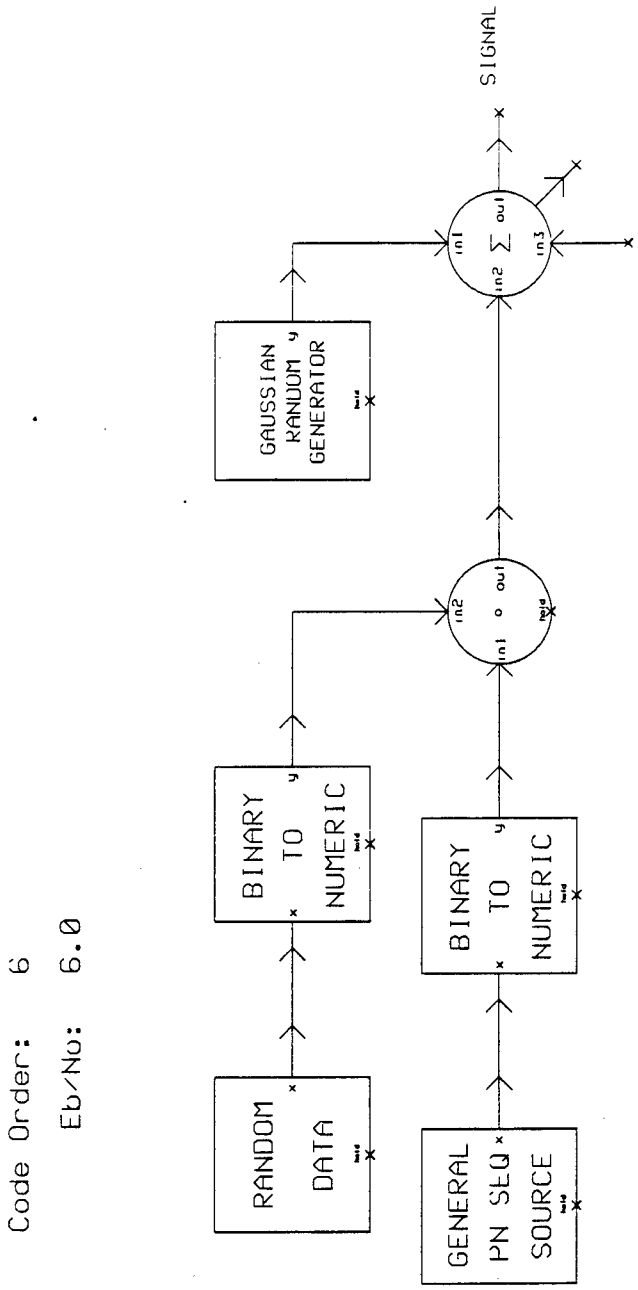

Figure 2.1: Block Diagram for the Modulator and Channel

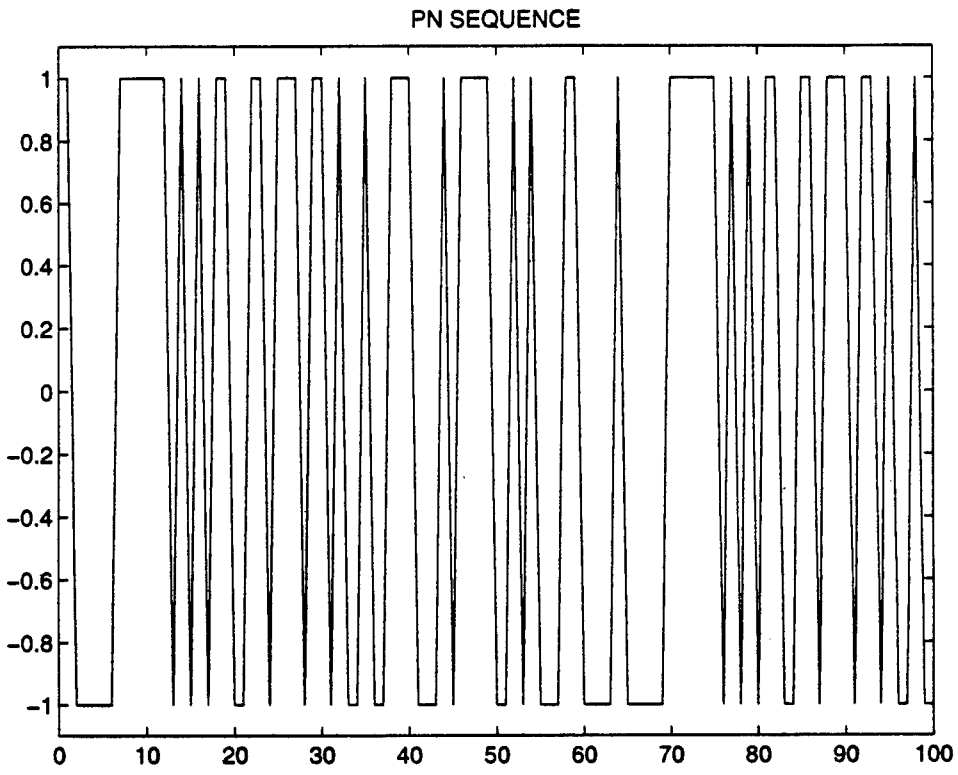

Figure 2.2: PN Sequence Waveform

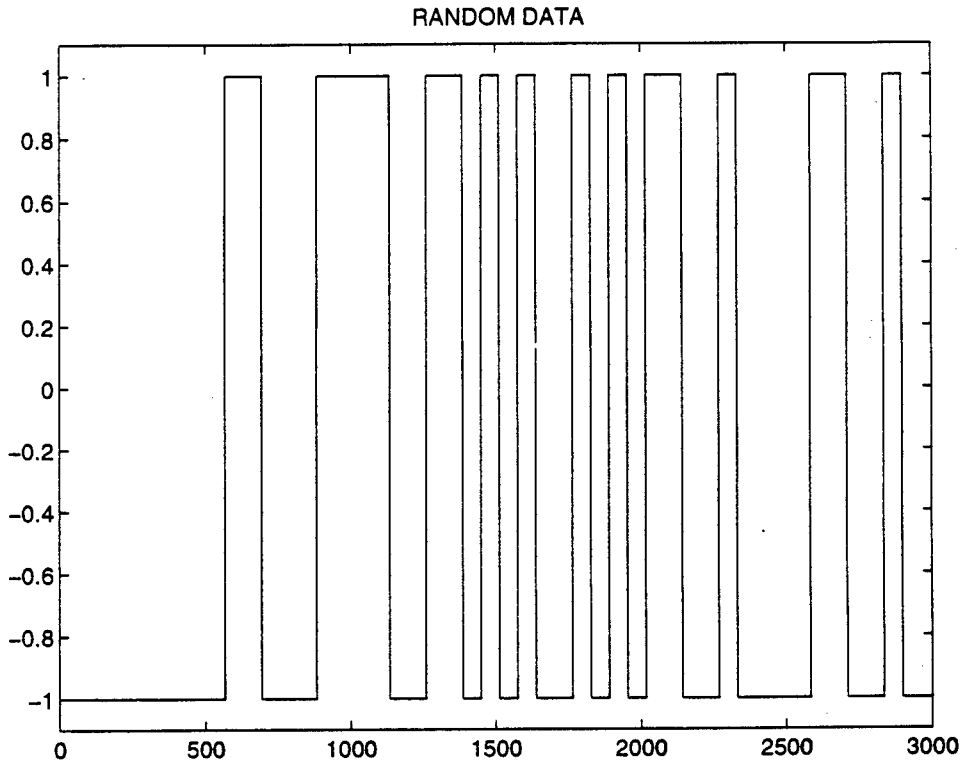

Figure 2.3: Random Data Waveform

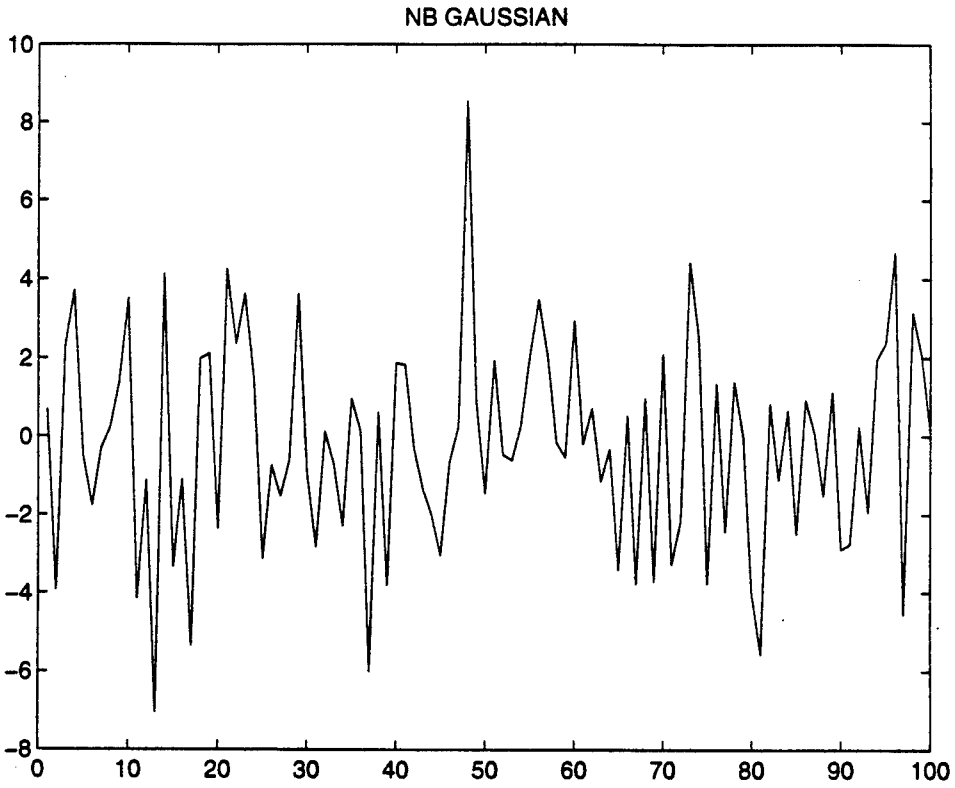

Figure 2.4: Gaussian Random Noise Waveform

2.2- Jammers

Interference is unwanted energy from systems other than the transmitter. It occurs in radio communication when the receiver gets two or more signals in the same frequency band; however, it may also come from multipath propagation or electromagnetic transmission cables. Contaminating noise normally has an additive effect, meaning that noise adds to the information-bearing signal at different points in the system. The sources of contamination are generally classified as human interference or naturally occurring noise, like the unavoidable thermal noise [2].

In this report, four different types of jammers are considered, and can be seen in figure 2.5 [2,13].

2.2.1- Stationary Tone Jamming (Jammer 1). A sinusoid of fixed frequency is used as the jammer (Figure 2.6). It is the easiest of all jamming signal to generate, and can be modeled as

$$j[n] = A_j \cos[2\pi\ f_T n + \theta\ ], \tag{2.3}$$

with its power defined relative to that of the desired signal by the jammer-to-signal ratio (JSR)

$$JSR = \frac{A_j^2}{2P_s}. \tag{2.4}$$

The sampling frequency is set to a normalized value of $1.0\ Hz$, and the amplitude (power) of the jammer is calculated as

$$A_T = 1.414 \times 10^{\frac{JSR}{20}} = 1.414 \times 10^{\frac{20}{20}} = 14.14. \tag{2.5}$$

Both the frequency and strength of this jammer are parameters to be varied.

2.2.2- Swept Tone and Chirp Jamming (Jammer 2). In the case of a swept tone, the frequency of the sinusoid is varied using a triangular wave (Figure 2.7), while for chirp jamming the frequency is varied using a ramp wave (Figure 2.8). Here, the jammer sweeps through the frequency band of the transmitted signal, meaning that its frequency is now constantly changing, and therefore the communication receiver systems must also be constantly changing to track the jammer. This jammer can also be represented by equation (2.3), with a moving value for f_T. The value of JSR can also be calculated according to equation (2.4), while the sweep frequency should allow the jammer frequency to sweep back and forth many times. The frequency range, variation rate and power are the parameters to be varied for this type of jammer.

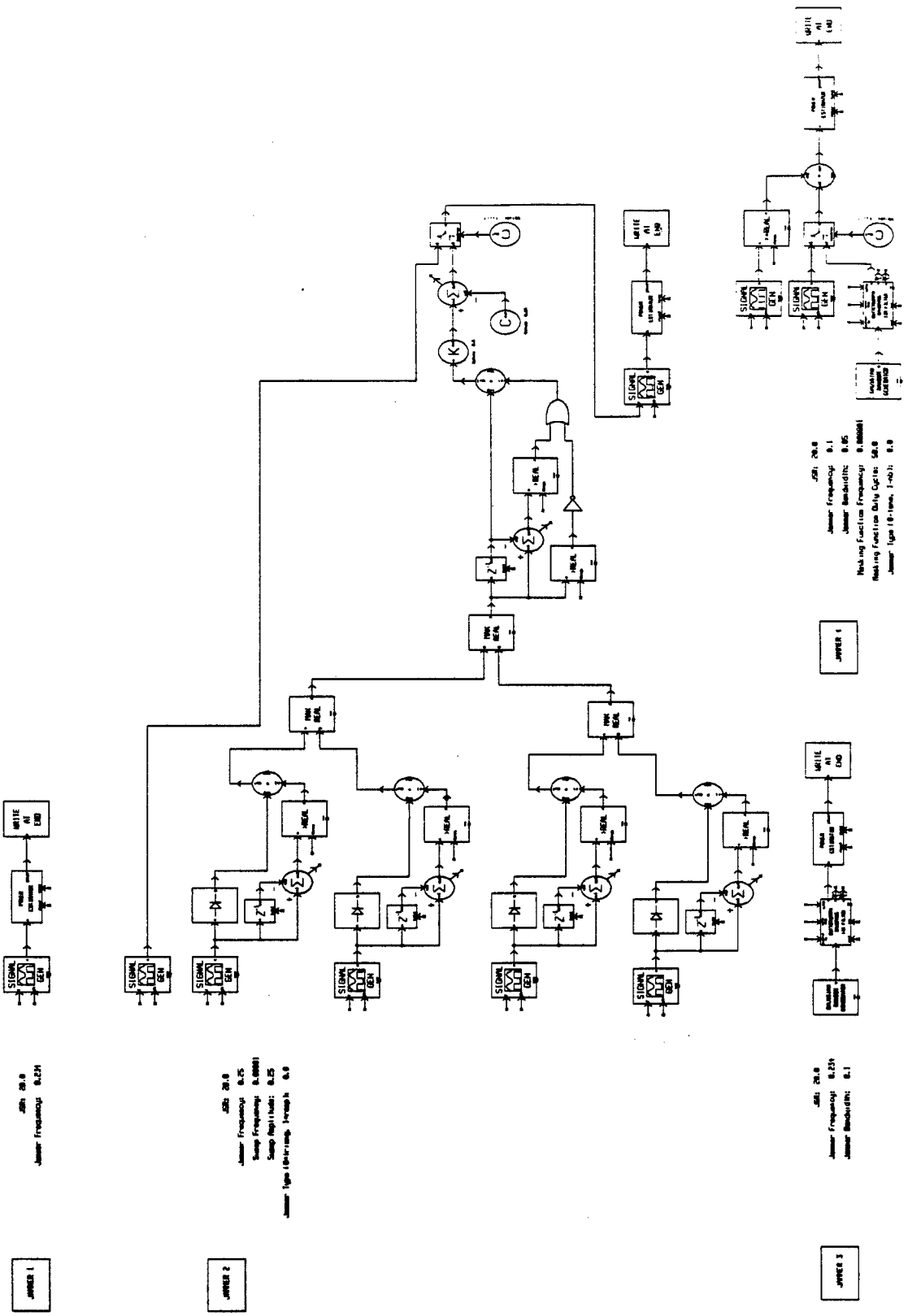

Figure 2.5: Block Diagram for the Jammer Systems

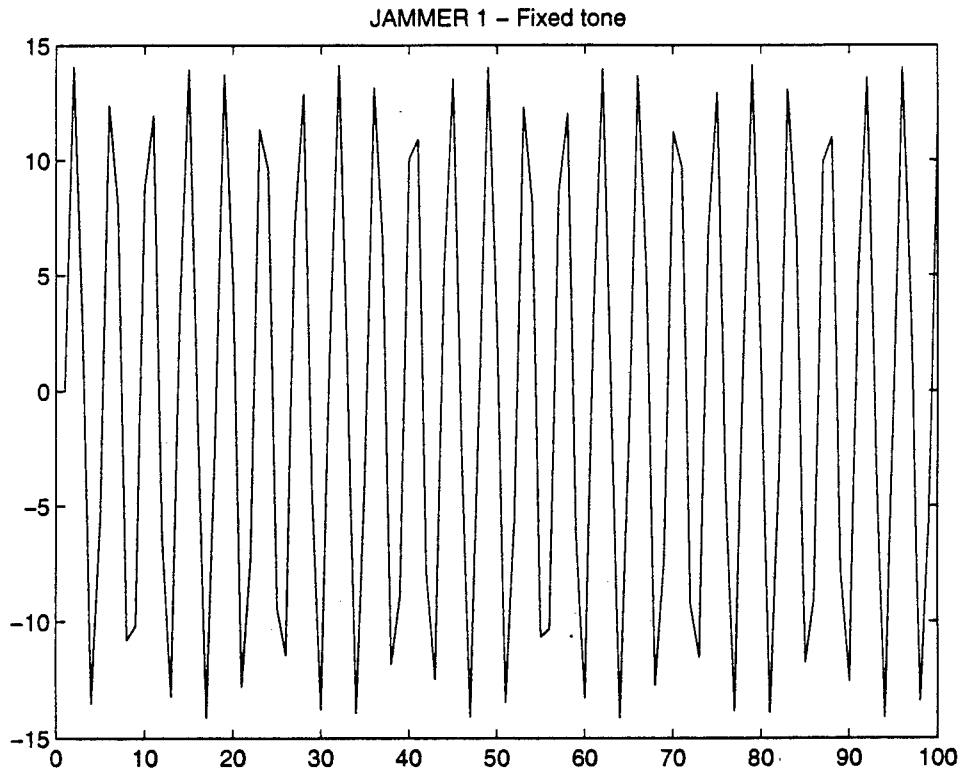

Figure 2.6: Stationary Tone Jamming Waveform

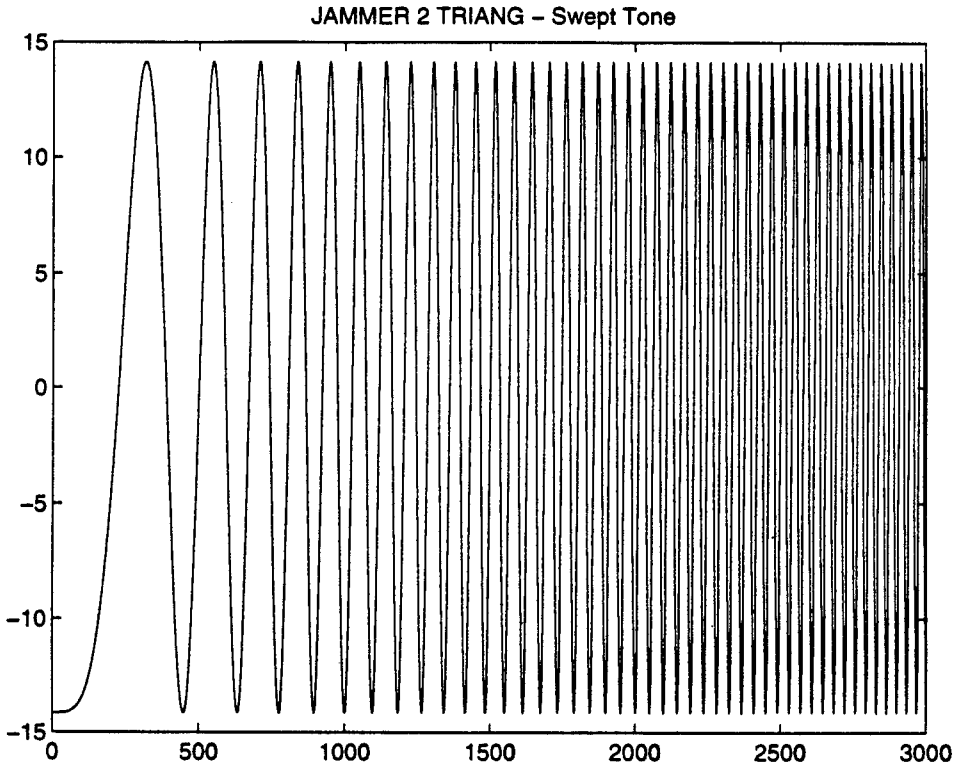

Figure 2.7: Swept Tone Waveform

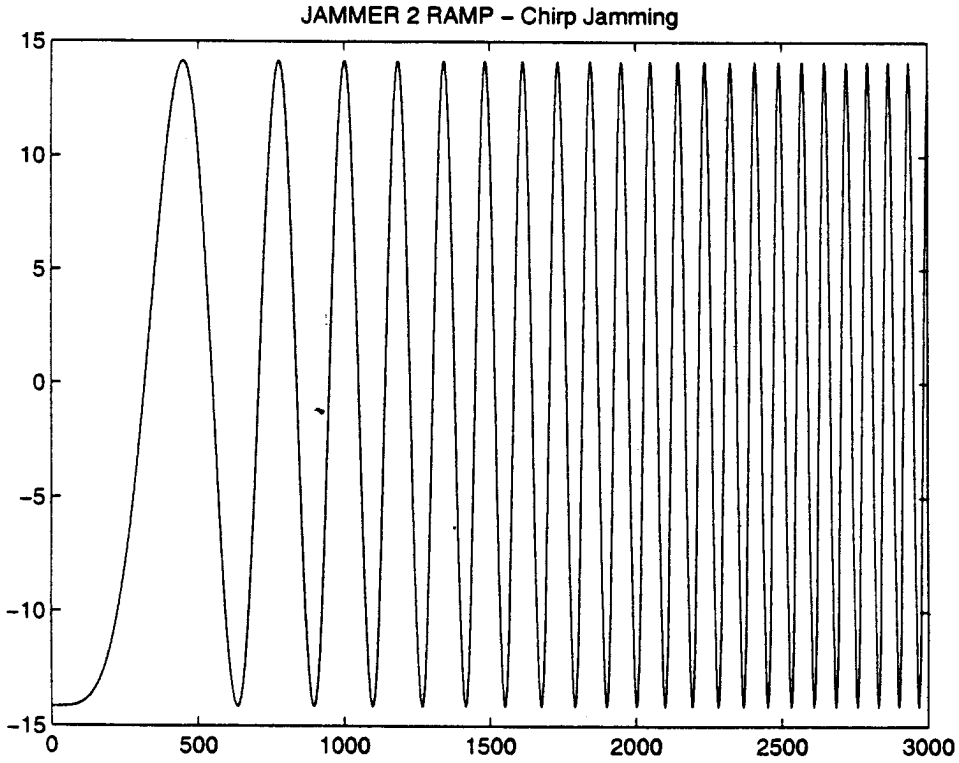

Figure 2.8: Chirp Jamming Waveform

2.2.3- Narrowband Gaussian Jamming (Jammer 3). The output from a white noise generator with a Gaussian distribution is passed through a narrowband filter to produce the interference (Figure 2.9). This class of jammer is a brute-force jammer that does not exploit any knowledge of the antijam communication system except for its spread bandwidth.

Denoting the total interference power as A_{nb}^2, the jammer-to-signal ratio is given by

$$JSR = \frac{A_{nb}^2}{P_s}. \tag{2.6}$$

The filter is an IIR Butterworth bandpass filter, of order 10 and attenuation at passband edge $3\,dB$, while the sampling frequency is set to a normalized value of $1.0\,Hz$. The main parameters for this jammer are calculated as follows,

$$\mu = Mean = 0.0 \tag{2.7}$$

$$\sigma^2 = Variance = \frac{10^{\frac{JSR}{10}}}{2\,BW_J}. \tag{2.8}$$

Filter bandwidth and jammer power are the parameters to be varied.

2.2.4- Pulsed Tone and Pulsed Gaussian Jamming (Jammer 4). A pulse-shaped masking function is placed on tone (Figure 2.10), and Gaussian (Figure 2.11) jammers. The sampling frequency is set to a normalized value of $1.0\ Hz$, and the tone amplitude $A_T = 14.14$ is calculated according to equation (2.5). As to the Gaussian noise, the filter is an IIR Butterworth bandpass filter, of order 10 and attenuation at passband edge $3\ dB$. The masking function consists of a square wave varying from 0 to 1. The value of the quiescent frequency, i.e., the frequency of the masking function, has to be lower than $1/Period_{PN\,Seq} = 1/N = 1/63$, and is set to $0.000001\ Hz$. The duty cycle of the masking function is a parameter that specifies the percentage of time that the signal is high, rather than low, and is set to $Factor_{duty} = 50\,\%$.

The main parameters for this jammer are calculated as follows,

$$\mu = Mean = 0.0 \tag{2.9}$$

$$\sigma^2 = Variance = \frac{10^{\frac{JSR}{10}}}{2\,BW_J\,Factor_{duty}}. \tag{2.10}$$

The parameters of the original tone and Gaussian jammers are quantities to be varied.

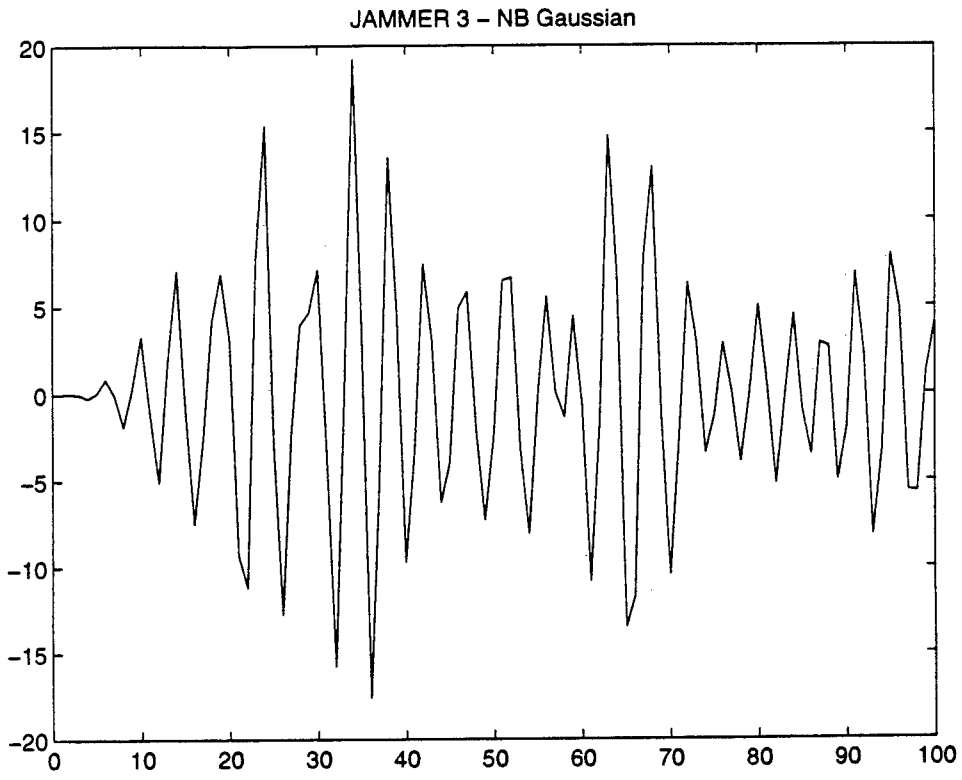

Figure 2.9: Narrowband Gaussian Jamming Waveform

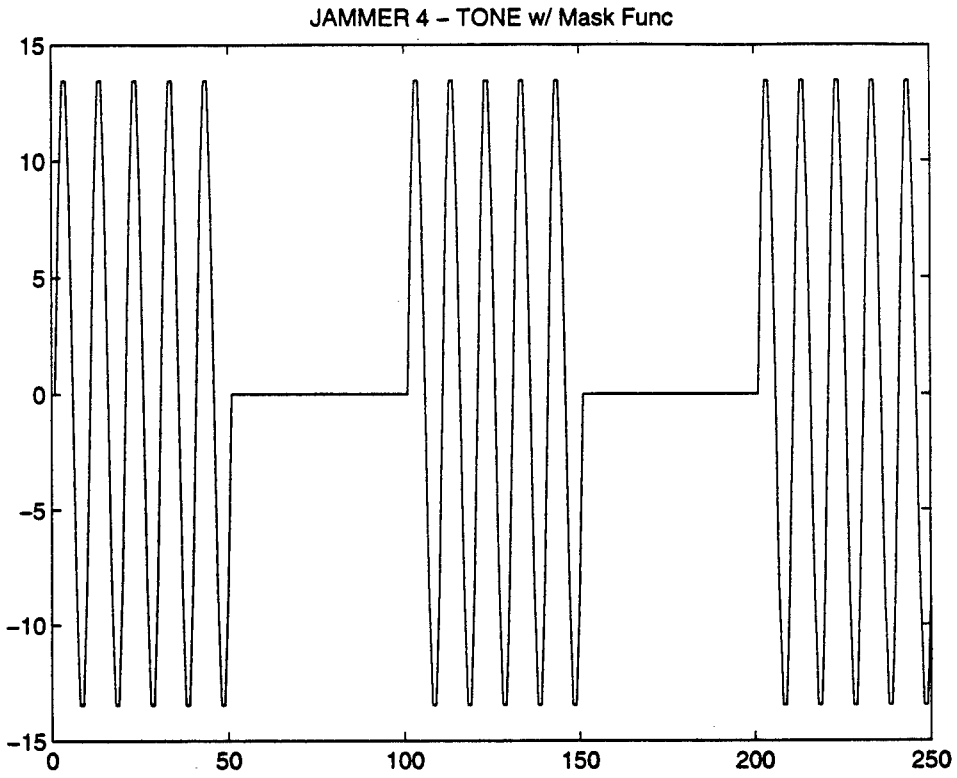

Figure 2.10: Pulsed Tone Jamming Waveform

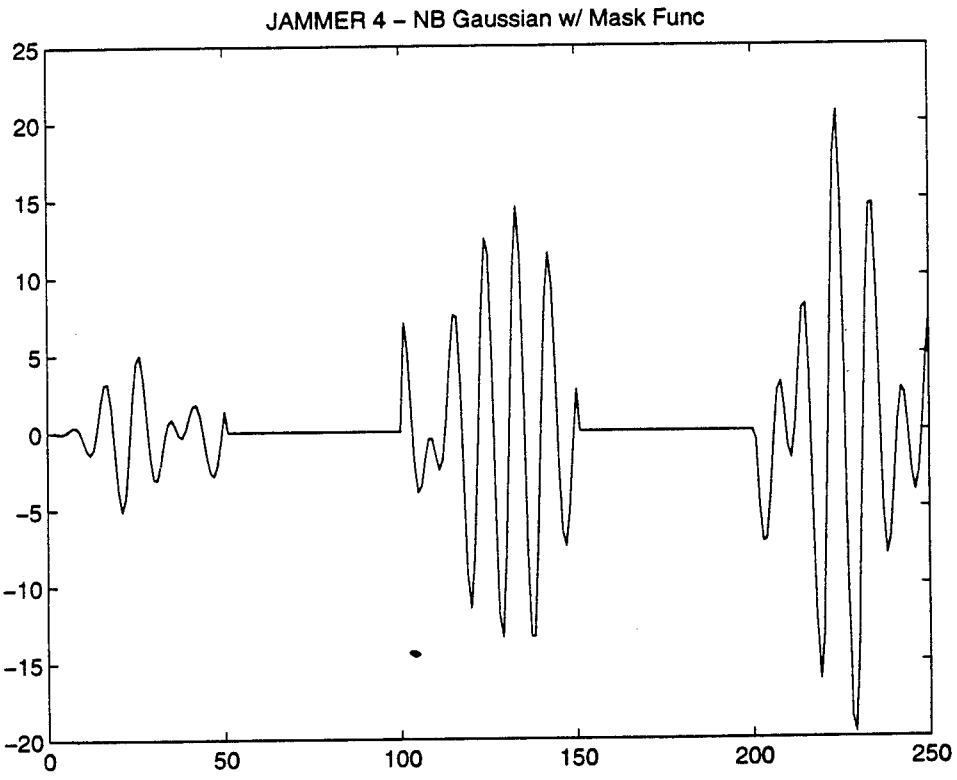

Figure 2.11: Pulsed Gaussian Jamming Waveform

2.2.5- Summary

Table 2.2 gives the default parameter values used for the different jammers. Unless otherwise indicated, these are the values that are used.

JAMMER 1	Eb/No = 6 dB JSR = 20.0 dB Jammer Frequency = 0.234 Hz
JAMMER 2	Eb/No = 6 dB JSR = 20.0 dB Sweep Frequency = 0.00001 Hz
JAMMER 3	Eb/No = 6 dB JSR = 20.0 dB Jammer Frequency = 0.234 Hz Jammer Bandwidth = 0.1 Hz
JAMMER 4	Eb/No = 6 dB JSR = 20.0 dB Jammer Frequency = 0.1 Hz Jammer Bandwidth = 0.05 Hz Masking Function Frequency = 0.000001 Hz Masking Function Duty Cycle = 50 %

Table 2.2: Summary of Main Parameters for Jammers

2.3- Communication Receivers

The communication receivers detect, demodulate and despread the received data signal. Besides, they perform additional processing in an effort to reconstruct or estimate the originally transmitted message symbol, contaminated by the jamming process.

2.3.1- Adaptive Filters

Filters are used in nearly any communication system, for the purpose of retrieving an information-bearing signal from unwanted contaminations such as interference, noise, and distortion products. When the correlation functions are unknown and the environment is non-stationary, adaptive filters can be an excellent alternative. These filters are self-designing devices whose coefficients are

updated according to a recursive algorithm, such that efficient transmission is maintained. The LMS (Least-Mean-Squared) algorithm is probably the best known of the adaptive filtering algorithms. A significant feature of the LMS algorithm is its simplicity. Indeed, this algorithm is iterative, i.e. it does not require information about the statistics of the incoming signal, but rather adapts on a step-by-step basis to converge to the optimal (in the mean-square sense) tap weights. In the direct sequence receiver application, an iteration occurs each time a new sample is input into the delay line, meaning that the system adapts once per chip of the signal [3, 4, 5].

Since both the data and the thermal noise are wideband signals, their future values cannot be easily predicted from their past values. However, the interference is a narrowband process, and hence can have its future values predicted from past values. Once its present value is predicted, it can be subtracted from the received signal. The same principle is used for the two-sided transversal filter, except that now the estimate of the current value of the interference is based upon both past and future values.

In figure 2.12 , a simple predictive adaptive filter interference suppression structure is shown. The received signal $x[k]$ is fed into a tapped delay structure having a tap spacing equal to the chip duration, T_c. Delayed input samples, $x[k-1]$, $x[k-2]$, ..., $x[k-N]$ are multiplied by a set of tap weights, w_1, w_2, ..., w_N , and the products are summed to form the signal $y[k]$. This output is then subtracted from the input signal to form an error signal, $\in[k]$. The tap weights are determined using the LMS adaptive algorithm which works to minimize the error signal, $\in[k]$. This adaptive process forces $y[k]$ to become an estimate of the current sample of the input signal, $x[k]$.

The LMS algorithm for adaptive filters is as follows

$$w_i[k+1] = w_i[k] + \mu \in [k]\, x[k-i]. \tag{2.11}$$

The term $\mu \in [k]\, x[k-i]$ represents the correction that is applied to the current estimate of the tap-weight vector, w_k.The adaptation constant μ is a parameter which determines the rate of convergence of the algorithm. Indeed, the LMS algorithm is convergent in the mean square if

$$0 < \mu < \frac{2}{Total\ Average\ Input\ Power}. \tag{2.12}$$

The larger the adaptation constant μ , the faster the tracking capability of the LMS algorithm, which is equivalent to the LMS algorithm having a short "memory". However, a large value of μ may imply a high excess mean-square error, sometimes called misadjustment, as limited data is applied to estimate the gradient vector. Therefore, a compromise must be reached between fast tracking and low excess mean-squared error. Hence, the parameter μ may be conceived as the memory of the LMS algorithm, since it decides on the weighting applied to the tap inputs.

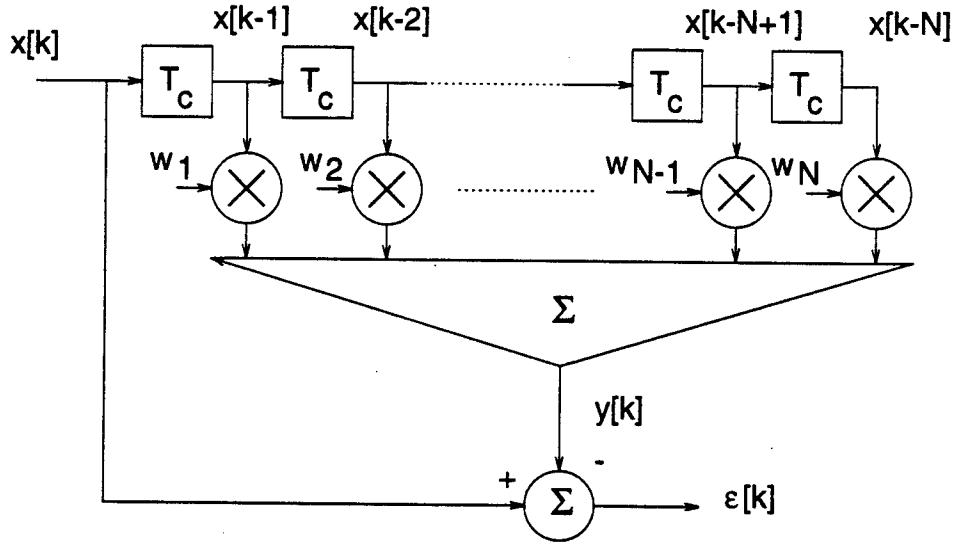

Figure 2.12: Predictive Transversal Filter

The inputs to the predictive filter are a delayed version of the signal, coming from the delay element, and the desired response, which is the signal coming directly from the channel. The filter length for the predictive LMS filter system is set to 7 taps. In the two-sided system, the signal is fed into a first LMS adaptive filter. The output of the second filter, whose inputs are a delayed version of the signal and the error feedback, is summed up with the output of the first filter and subtracted from the output of the first unit delay to form the error signal for both LMS filters. The filter length for the two-sided LMS adaptive filter system is set to 5 taps.

2.3.2- Modulated Lapped Transforms - Transform Domain Excision (MLT-TDE)

The basic idea behind transform domain processing is to compactly represent the interference energy in the transform domain, and then easily remove it. The transform should be selected such that the interference is nearly a delta function in the transform domain, while the desired signal is converted to a waveform whose spectrum is notably wide in comparison to the transformed interference's. A simple exciser can then remove the interferer, without significantly damaging the original signal. An inverse transform then recovers the almost interference-free desired signal [6, 7, 8]. Figure 2.7 illustrates the excision process.

The excision process is a fast adaptive algorithm that is performed prior to the correlation stage. It removes narrowband interference, adjusting the position of the notch (or notches) to suppress spectral components with large amount of energy, typically those that surpass a user-defined threshold. Its level can be established sufficiently high so that components are removed only when interference is present. However, if the interference is changing rapidly, the algorithm may not be able to track these variations. The performance of the excision process highly depends on the ability of the transform to compactly represent the interference.

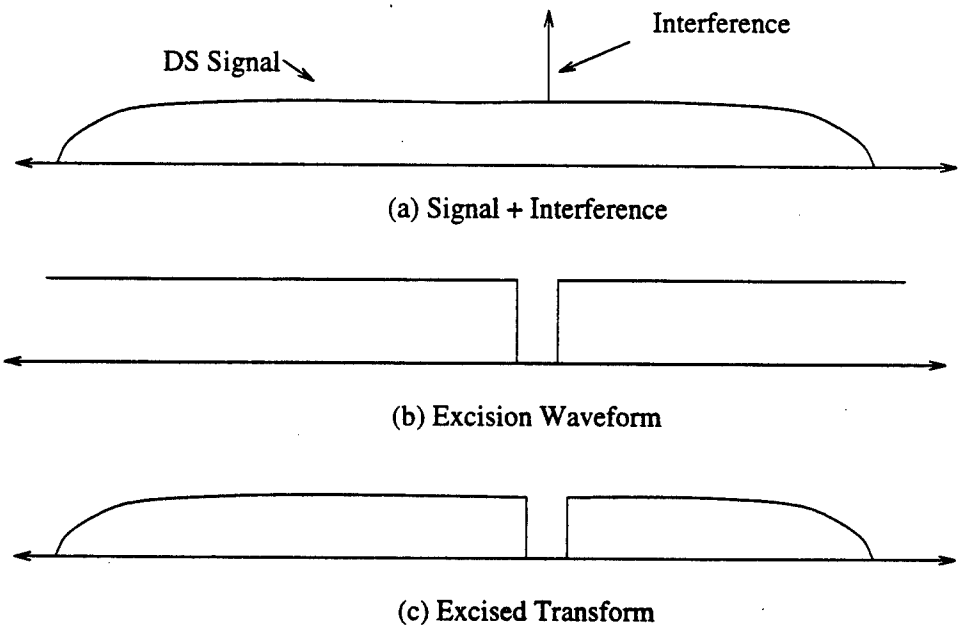

Figure 2.13: Illustration of the Excision Process

The Fast Fourier Transform (FFT) is not considered here, due to its considerable spectral overlap effects with large number of adjacent carriers. Instead, Lapped Transforms (LTs) and in particular Modulated Lapped Transforms (MLTs), are proposed [7]. The central reason for the introduction of LTs is found in one of the major disadvantages of traditional block transforms: the blocking effects, which are discontinuities in the reconstructed signal. Besides, LTs have higher coding gains than block transforms, and therefore higher signal-to-noise ratios. The basis functions of LTs are filters whose length L is equal to some even integer multiple of the number of filter bank subbands, i.e. $L = 2KM$, where M is the number of subbands and K is the overlapping factor. MLTs are considered as a subset of general LTs with $K = 1$, and they closely approximate the ideal filter system of unity passband gain and infinite stopband attenuation. A 2M-tap lowpass filter is used as a subband filter prototype and shifted in frequency to produce a set of orthogonal bandpass filters, which span the frequency domain. The lowpass prototype, $h[n]$, must satisfy the following

$$h[2M-1-n] = h[n] \qquad 0 \le n \le M-1 \tag{2.13}$$

and

$$h^2[n] + h^2[n+M] = 1 \qquad 0 \le n \le M/2-1. \tag{2.14}$$

The half-sine windowing function is used as the lowpass filter prototype,

$$h[n] = -\sin\left[\left(n+\frac{1}{2}\right)\frac{\pi}{2M}\right]. \tag{2.15}$$

The basis functions can then be described as

$$\psi_k[n] = h[n]\sqrt{\frac{2}{M}}\cos\left[\left(n+\frac{M+1}{2}\right)\left(k+\frac{1}{2}\right)\frac{\pi}{M}\right] \tag{2.16}$$

where $0 \le n \le 2M-1$ and $0 \le k \le M-1$.

In the MLT-TDE system, the narrowband interference is removed in the transform domain. The signal is brought to the transform domain via a modulated lapped transform. The transform domain excision is then performed, regulated by two parameters, the threshold and the notch width. The exciser block cancels any components, and a user-defined number of bins around the components, that exceed a preset threshold. Next, the signal is brought back to the time domain via an inverse modulated lapped transform. The vector length for the system is set to 32 points.

In both the adaptive filters and MLT-TDE systems, the receiver does not need to be synchronized with the transmitter. Both receivers can be seen in Figure 2.14.

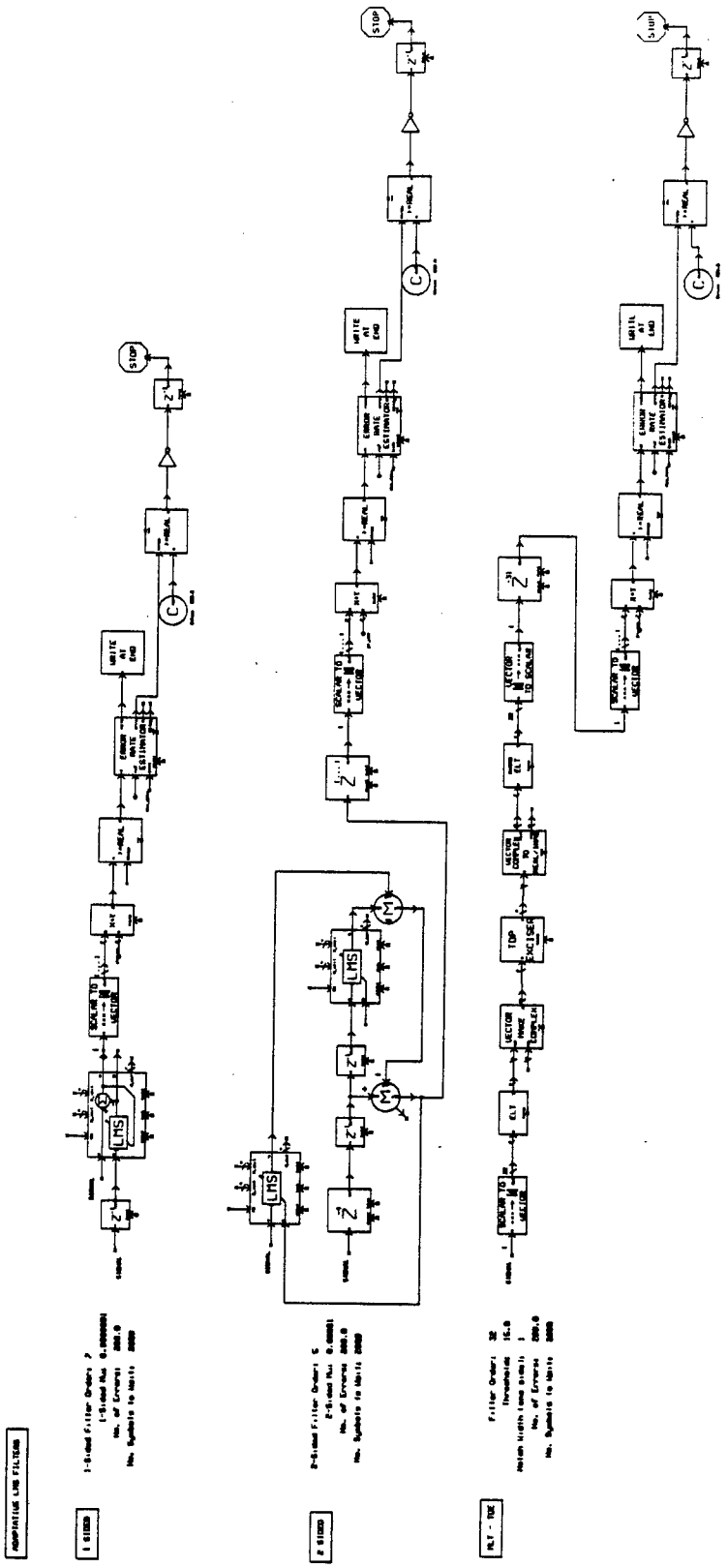

Figure 2.14: Block Diagram for the Filters and MLT-TDE Receiver Systems

2.3.3- Adaptive Correlator

An adaptive correlator is a system that performs the following functions: it detects the transmitted data, removes interference, and compensates for multipath. Consequently, the resulting receiver would consist of a 3 tapped-delay line structure in cascade: the LMS adaptive filter to remove interference, the correlator to despread the signal, and a linear combiner; still, a single filter may be used to perform all three tasks [9, 10].

There are two stages of operation:

During the training period, a known data sequence is transmitted and a synchronized version of this signal is generated in the receiver where it is used as the desired response.

When the training is completed, the adaptive equalizer is switched to its second mode of operation, the decision-directed mode. The system is operated by aligning a data bit in the adaptive correlator, summing the products of the tap weights and signal samples, and comparing the result to the original transmitted data bit. The error between the output of the adaptive correlator and the transmitted data bit is then used to adapt the tap weights according to the LMS algorithm, in order to minimize the mean-square error. If the length of the correlator is the same as that of the data bit, timing has to be synchronized between the receiver and the transmitter, and the adaptation has to be exactly one correlator tap per received signal sample, since the adaptive algorithm is accomplished once per data bit. In a direct sequence spread spectrum signal in AWGN, the adaptive correlator will converge to the standard correlator receiver by in fact learning the transmitter's spreading sequence and the channel. When interference is present, the adaptive correlator will tend to suppress the interference. However, the adaptive correlator can jump to the wrong polarity, producing high error rates by inverting all the bits after the jump occurs.

Figure 2.8 is a block diagram of the adaptive correlator receiver. The receiver is a fractionally-spaced linear equalizer having a tap spacing, t_s, that is some fraction of the chip period and a total duration, $N_s\ t_s$, that equals the data bit period or more. During the operation of the receiver, the contents of the delay line will be advanced by a full data bit period between iterations of the adaptive algorithm. As a result, a particular tap of the tapped delay line will always correspond to a received signal sample taken at the same time within the data bit period.

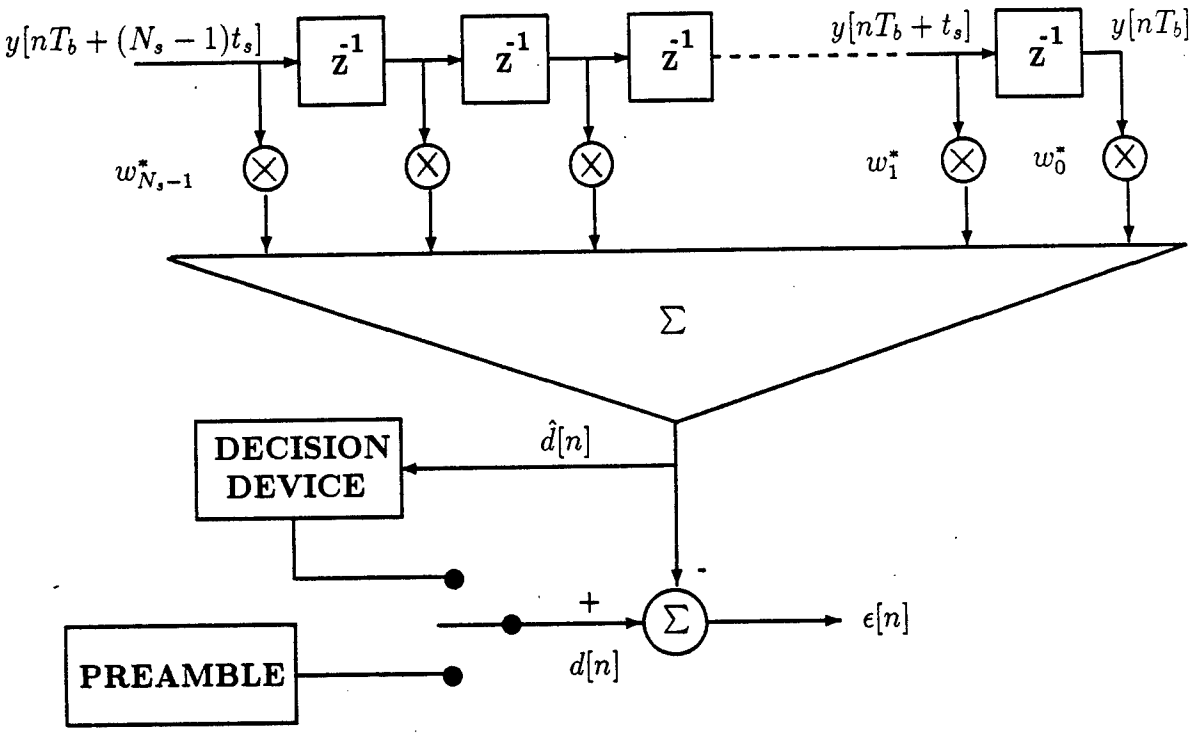

Figure 2.15: Adaptive Correlator Receiver Structure

The signal is fed into a Least Mean-Squared (LMS) adaptive filter. The output of the filter is then subtracted from the original signal data to form the error feedback of the filter. A clock holds the filter operation for a period of 63 iterations (period of the PN sequence), making the correlator adapt once every data bit. The filter length is therefore set to the same value as the period of the PN sequence, 63 taps.

The signal samples in the delay line can be expressed as the vector $\underline{y}[n]$,

$$\underline{y}[n]=\left(y\left[nT_b\right], y\left[nT_b + t_c\right], \ldots, y\left[nT_b + (L_c - 1)\, t_c\right]\right)^T \tag{2.17}$$

where T_b is the data bit period, t_c is the chip period, and L_c is the length of the spreading sequence in chips. Likewise, the tap weights can be represented as a vector,

$$\underline{w}[n] = \left(w_o[n], w_1[n], \ldots, w_{N_s-1}[n]\right)^T . \tag{2.18}$$

The output of the filter $d'[n]$ is found by taking the dot product

$$d'[n] = \underline{y}^T[n]\, \underline{w}^* = \underline{w}^H\, \underline{y}[n] . \tag{2.19}$$

The output is compared to the desired input to the filter, $d[n]$, which is the transmitted data bits obtained during the training period. The difference between $d'[n]$ and $d[n]$ is the error signal $\in$; the tap weights of the filter are selected to minimize its value. For the theoretical analysis, we will consider a channel containing only white Gaussian noise and a single tone interferer. The power at the receiver due to the transmitted signal is equal to P_s, and the spreading code is $\underline{c}$. The received vector $\underline{y}[n]$ is

$$\underline{y}[n] = X[n]\sqrt{P_s}\, \underline{c} + \underline{j}[n] + \underline{n}[n] . \tag{2.20}$$

According to the analysis in [10], the data bit energy to one-sided noise power spectral density (E_b / N_o) is

$$\frac{E_b}{N_o} = \frac{L_c\, P_s}{\sigma^2} , \tag{2.21}$$

the jammer-to-signal power ratio (JSR) is

$$JSR = \frac{A_J^2}{P_s} , \tag{2.22}$$

and the minimum mean square error is

$$\in = \frac{1}{1 + \dfrac{E_b}{N_o} - \left[\dfrac{P_s\, A_J^2}{\sigma^2\left(\sigma^2 + L_c\, A_J^2\right)}\right] \underline{c}^T\, \underline{e}\, \underline{e}^H\, \underline{c}} \tag{2.23}$$

where $\underline{e}^H\, \underline{e} = \underline{c}^T\, \underline{c} = L_c$.

2.3.4- Modulated Lapped Transforms - Transform Domain Excision and Detection (MLT-TDED)

In the MLT-TDED system, an augmented PN sequence is used, generating a period of $N = 2^m = 64$; the random data sampling frequency also results in a value $64.0\ Hz$. All the vector lengths are set to 64 points in this system, instead of the 63-length used in the three previous receivers. The detection is performed in the transform domain without performing an inverse transform. Figure 2.9 illustrates a generic communications receiver employing MLT-TDED. In this system, the spectral coefficients of the observed data signal are point-wise multiplied with the weighting vector elements. The corresponding outputs are then correlated with the known transform domain reference vectors, using a dot product, to yield the decision variable. The excision process is performed using a 64 point-length vector.

For both the adaptive correlator and MLT-TDED receiver systems, timing has to be synchronized between the receiver and the transmitter, since the processes are accomplished once per data bit. Figure 2.17 presents both systems.

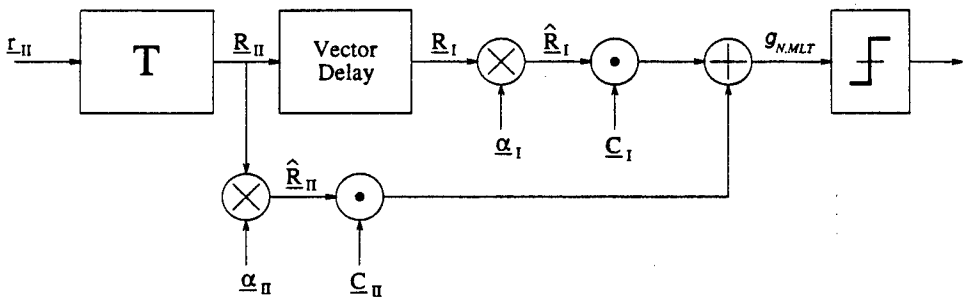

Figure 2.16: Receiver Employing MLT Domain Excision and Detection

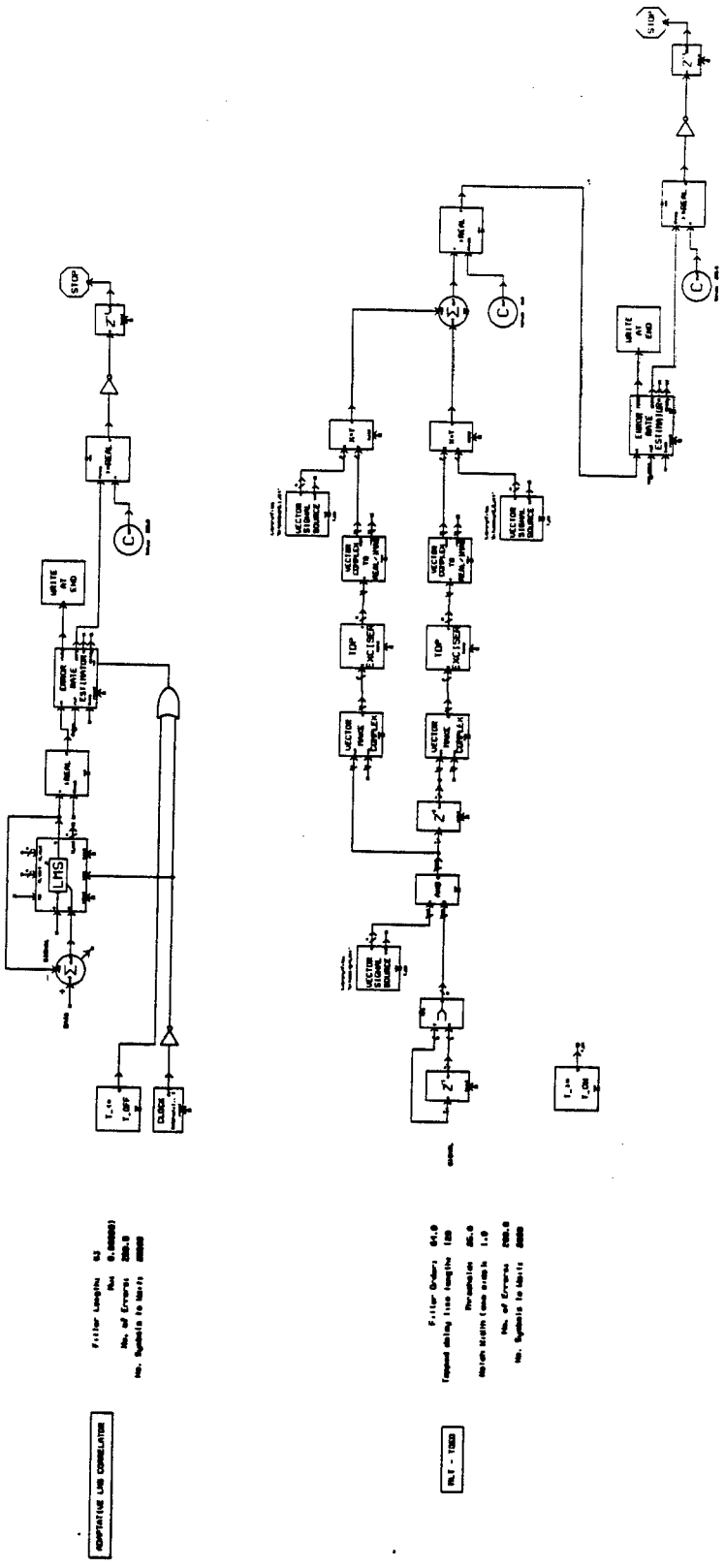

Figure 2.17: Block Diagram for the Correlator and MLT-TDED Receiver Systems

2.3.5- Computational Complexity

In Table 2.3, the computational complexity in terms of OpS (Operations per Sample) is calculated for the four different communication receiver systems.

The adaptive filters and MLT-based transform exciser are configured to have roughly the same complexity in order to make a fair comparison between the two structures. Therefore, the taps of the filters and the vector length used for the MLT-TDE system are selected to satisfy this requirement, attaining complexities of $28\ OpS$ for the predictive filter, $25\ OpS$ for the two-sided, and $29\ OpS$ for the MLT-TDE structure.

On another hand, the adaptive correlator and the MLT with transform domain excision and detection are constrained by the need to have the block size (vector length) equal the length of the data, as the receiver requires to be synchronized with the transmitter for these two structures. Values of $4\ OpS$ for the correlator and $17\ OpS$ for the MLT-TDED receiver are obtained.

Predictive LMS Filter	N_{PF} = Filter Order = 7 taps
	OpS = 4 N_{PF} = 28
Two-Sided Adaptive LMS Filter	N_{tsF} = Filter Order =5 taps
	OpS = 5 N_{tsF} = 25
MLT-TDE	$N_{MLT\text{-}TDE}$ = Vector Length = 32 points
	OpS = 9 + 4 $\log_2 N_{MLT\text{-}TDE}$ = 29
Adaptive Correlator	N_C = Filter Length = 63 taps
	OpS = 2 + 2 = 4
MLT-TDED	$N_{MLT\text{-}TDED}$ = Vector Length = 64 points
	OpS = 5 + 2 $\log_2 N_{MLT\text{-}TDED}$ = 17

Table 2.3: Computational Complexity for the Different Communication Receiver Systems

CHAPTER 3

Implementation

3.1- Signal Processing WorkSystem (SPW)

The Signal Processing WorkSystem (SPW) from the Alta Group of Cadence Design Systems, Inc. offers the possibility of capturing, simulating, testing and implementing a broad range of digital signal-processing (DSP) designs, like digital communication and radar systems. Its use goes from the evaluation of various architectural approaches to the design, development, simulation and fine-tuning of DSP algorithms. SPW consists of several modules, and contains different libraries. Besides, it can access directly DSP boards residing in the computers through the Code Generation System (CGS), which generates C code. These programs are then automatically downloaded to the computer, along with any required files, where they are compiled and downloaded into the DSP board for execution. This process shortens the time required to run the simulations.

3.2- Parameters

The three primary performance measures used are:

Bit-Error-Rate (BER). While signal-to-noise (SNR) improvement is often used as a measure of the performance of interference suppression techniques, BER might be a better parameter, since it takes into account both the level of interference suppression and the amount of distortion introduced into the spread spectrum signal. For its computation, the received data signal is compared with the original transmitted data signal, from which a bit error rate is generated, according to the following equation,

$$BER = \frac{\#\ Erroneous\ Bits}{\#\ Bits\ Sent}. \tag{3.1}$$

The theoretical performance for BPSK in AWGN is related to E_b / N_o $[dB]$ as

$$BER = \tfrac{1}{2}\ erfc\left(\sqrt{E_b / N_o}\right) \tag{3.2}$$

where $erfc$ is the complementary error function defined as

$$erfc\,(x) = \frac{2}{\sqrt{\pi}} \int_x^{\infty} e^{-t^2}\, dt\,. \tag{3.3}$$

Implementation Complexity. The implementation cost of a particular technique can greatly determine its applicability. Digital implementations of the various techniques are proposed, and their design complexity is determined in terms of operations/chip or operations/bit.

Tracking Performance. Many interference suppression techniques require time to learn the characteristics of the interference in order to remove it. In iterative adaptive systems, this learning period is often called the convergence time.

Clearly, there is significant interaction between the various performance measures. For instance, the BER and tracking performance of the time domain adaptive filter is a function of the number of taps which, in turn, affects the implementation complexity. Performance results will be organized in a manner which allows a fair comparison between the various techniques.

3.3- Simulations

The different simulations performed for the four jammer systems, using the previously described communication receivers, can be seen in Table 3.1.

Jammer 1	BER vs. E_b/N_o BER vs. JSR[1] BER vs. Jammer Frequency
Jammer 2	BER vs. E_b/N_o BER vs. JSR[1] BER vs. Sweep Frequency
Jammer 3	BER vs. E_b/N_o BER vs. JSR[1] BER vs. Jammer Frequency BER vs. Jammer Bandwidth
Jammer 4	BER vs. E_b/N_o BER vs. JSR[1] BER vs. Jammer Frequency BER vs. Jammer Bandwidth

Table 3.1: Simulations Performed

The simulations are run until the number of errors obtained reaches the value of 200.0. There is also a value for the number of symbols to wait before the system actually starts computing the BER. This parameter allows the system to stabilize before the computation of the BER begins. Its value is set to 2,000 for the adaptive transversal filters, MLT-TDE and MLT-TDED systems, while a value of 20,000 is used for the adaptive correlator receiver.

[1] The decision parameters for the different receiver systems, namely μ for the LMS algorithm, and notch and threshold for the excision process, are optimized for each value of JSR.

CHAPTER 4

Results

In the following chapter, the curves representing the Bit Error Rates associated with the four jammers, for the different parameters mentioned in Table 3.1, are shown.

The plots are presented in such a way that the LMS adaptive filters and the MLT-based transform domain excision are presented in the same figure, while the LMS adaptive correlator and the MLT-based transform domain excision and detection, are displayed together in another figure. This division filters/MLE-TDE and correlator/MLT-TDED is done in order to perform a better comparison between systems that present similar characteristics. Indeed, the LMS adaptive filters and the MLT-TDE system face similar implementation complexity, with a value of $28\ OpS$ for the predictive filter, $25\ OpS$ for the two-sided, and $29\ OpS$ for the MLT-TDE structure (refer to Table 2.3). On another hand, the correlator and MLT-TDED systems require less computation, with a value of $4\ OpS$ for the correlator, and $17\ OpS$ for the MLT-TDED receiver. Besides, in both the LMS adaptive filter and the MLT-TDE systems, the receiver does not need to be synchronized with the transmitter, while for the correlator and MLT-TDED structures, timing has to be synchronized.

4.1- Results for Jammer 1

This section presents the results obtained for each of the receiver structures when the channel introduces fixed-frequency tone jamming.

Figure 4.1 plots BER vs. E_b/N_o for the predictive and two-sided LMS filters and MLT-based transform domain exciser. Also, the performance of the BPSK baseband signal in AWGN alone (with no jamming), as well as the performance obtained without any interference suppression technique (raw error) are shown. For these simulations, the default parameters used for the jammer are $JSR = 20\ dB$ and a normalized frequency $f = 0.234\ Hz$. A value of $\mu = 0.0000001$ for the predictive and $\mu = 0.00001$ for the two-sided filter are used, while a $threshold = 15.0$ and $notch\ width = 1$ are employed for the MLT-transform domain exciser. These parameters were optimized in order to obtain the best performance for the receiver systems. As can be seen in the figure, all three suppression structures present similar performance, and a significant improvement over the no-suppression case.

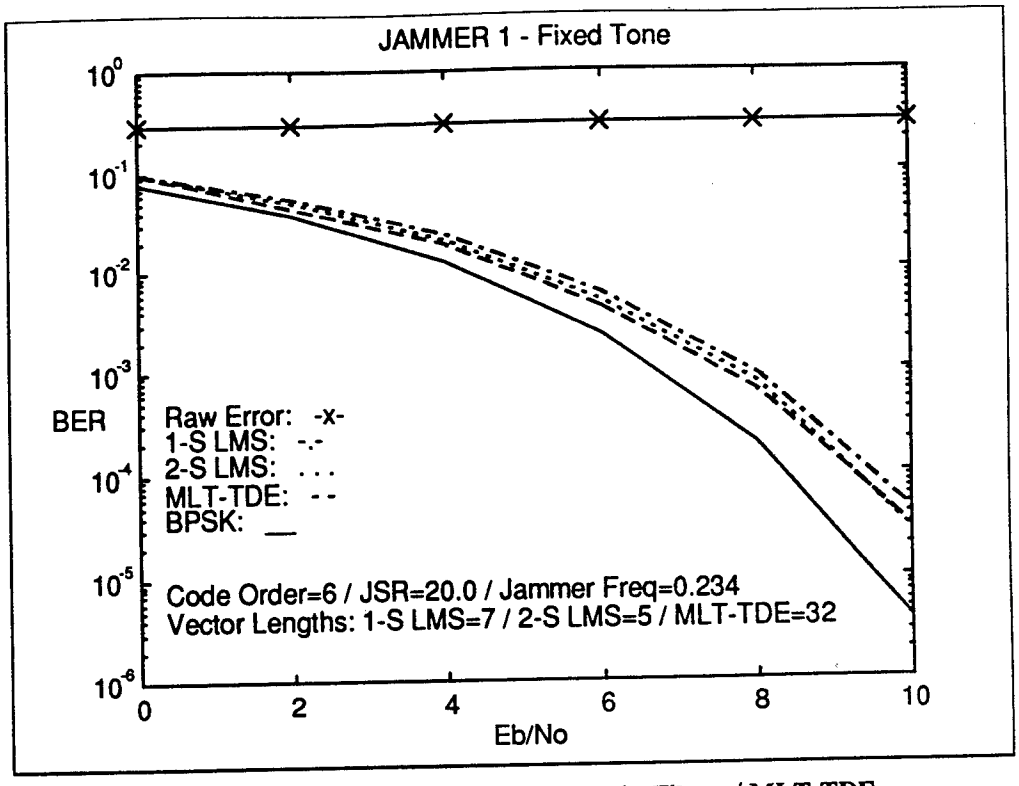

Figure 4.1 : BER vs. Eb/No for Jammer 1 - Filters / MLT-TDE

Figure 4.2 shows BER vs. E_b/N_o for the adaptive LMS correlator and MLT with transform domain excision and detection. Furthermore, the performance of BPSK baseband signal in AWGN alone and the one obtained without any interference suppression technique (raw error) are added. For these simulations, the default parameters used for the jammer are $JSR = 20\ dB$ and a normalized frequency $f = 0.234\ Hz$. A value of $\mu = 0.000001$ for the correlator, and $threshold = 25.0$ and $notch\ width = 1$ for the MLT-TDED system are used. These parameters were optimized in order to achieve best performance for the receivers. Note that both structures present similar results, and that their performance is closer to the AWGN-only results than the previous systems presented in Figure 4.1.

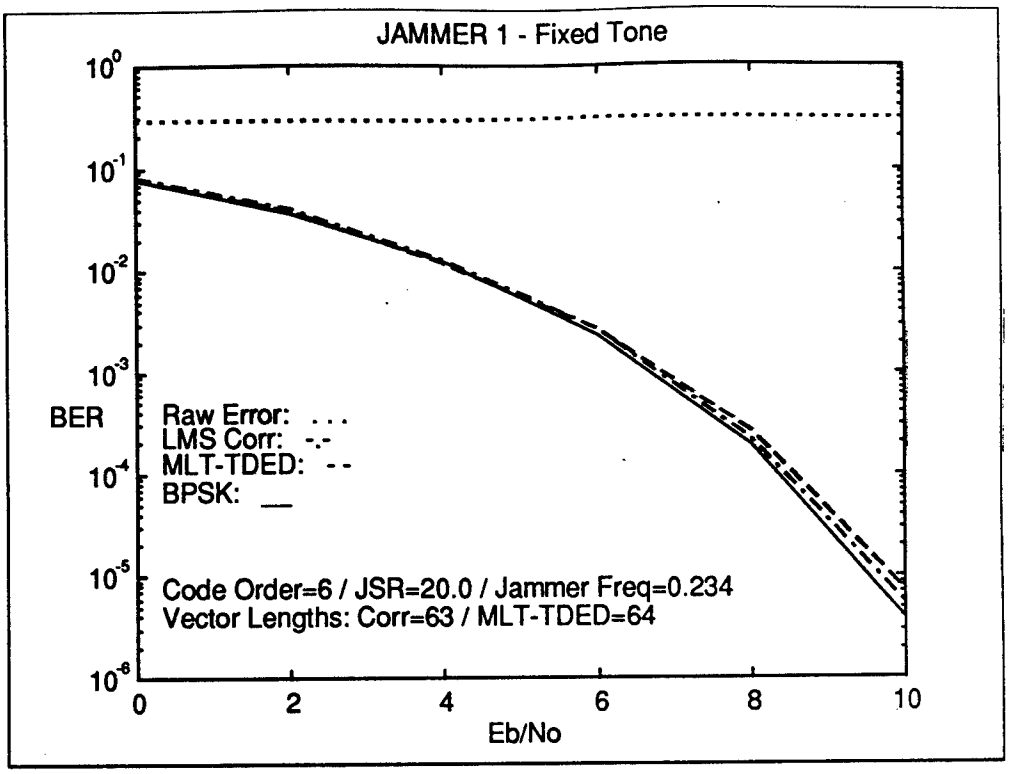

Figure 4.2 : BER vs. Eb/No for Jammer 1 - Corr / MLT-TDED

Figures 4.3 and 4.4 show the curves of BER vs. JSR for the different structures, using a value of $E_b / N_o = 6\,dB$ for the Gaussian noise in the channel and a normalized frequency $f = 0.234\,Hz$ for the jammer. In order to obtain these results, the parameters of the interference suppression techniques, i.e. the convergence factor μ for the adaptive filters and correlator, and exciser parameters for the MLT systems are optimized for each value of JSR, and can be seen in Tables 4.1 and 4.2. The figures indicate that the LMS filters provide the best performance, showing little dependence of BER on JSR, obtaining better results with the two-sided filter. The performance of all the other systems is relatively poor after values of $JSR \approx 30\,dB$, though the performance of the MLT-TDED structure is slightly better than the others.

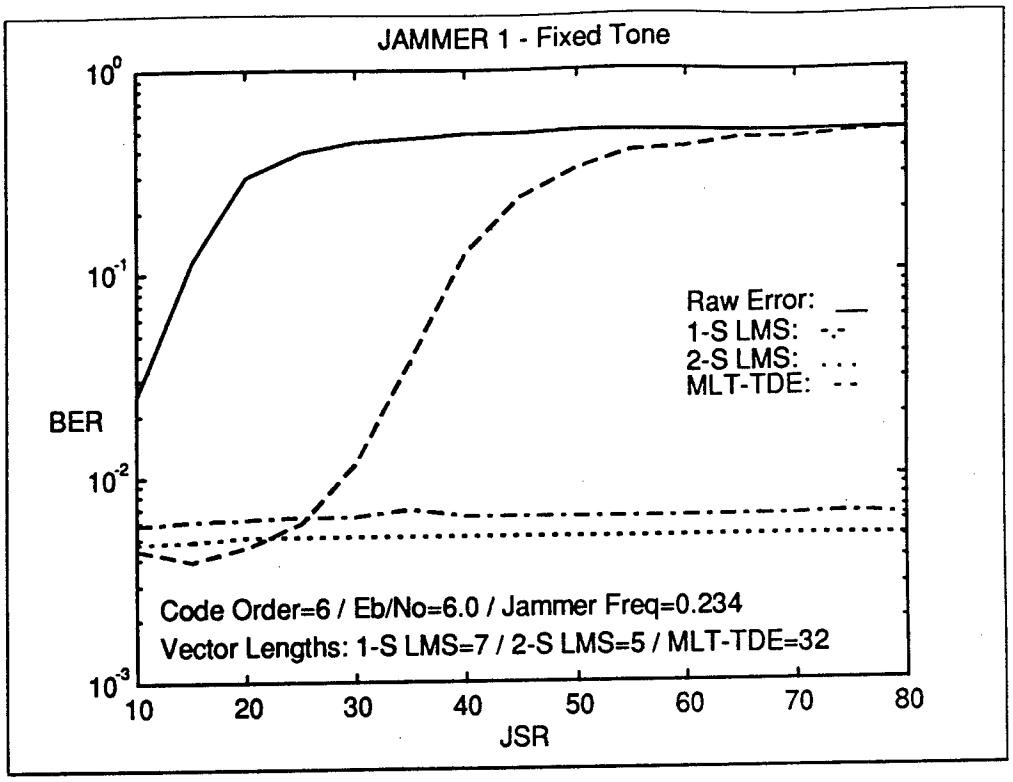

Figure 4.3 : BER vs. JSR for Jammer 1 - Filters / MLT-TDE

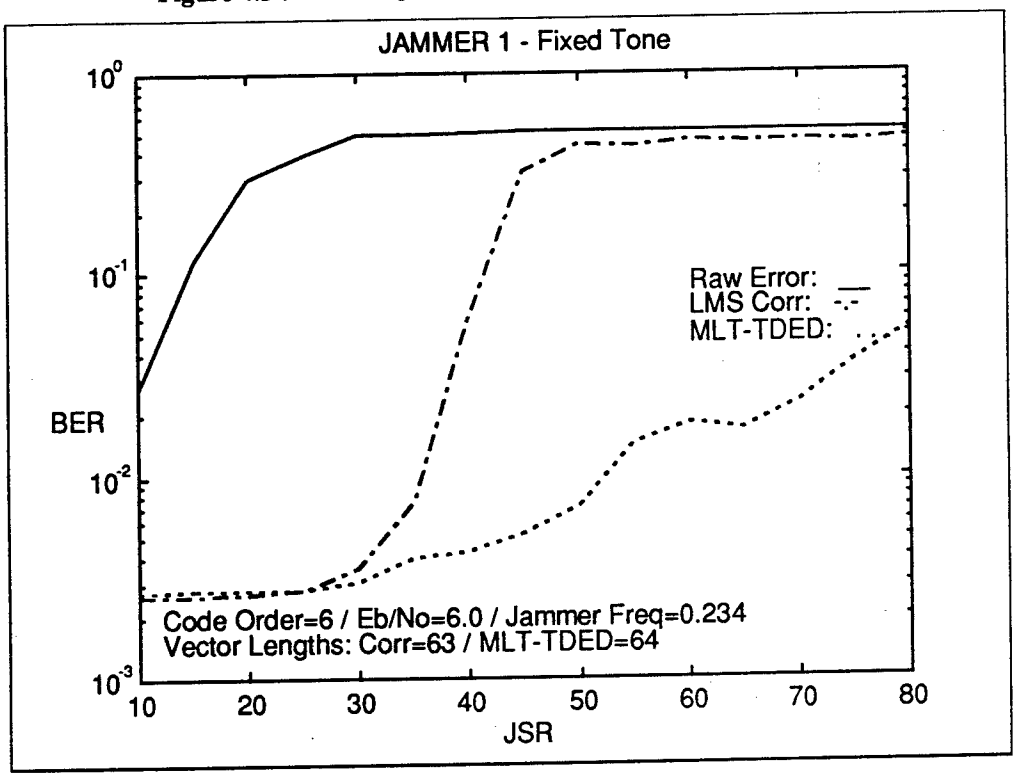

Figure 4.4 : BER vs. JSR for Jammer 1 - Corr / MLT-TDED

PREDICTIVE FILTER	TWO-SIDED FILTER	MLT-TDE
JSR = 10 dB μ = 0.000001 JSR = 15 dB μ = 0.000001 JSR = 20 dB μ = 0.0000001 JSR = 25 dB μ = 0.0000001 JSR = 30 dB μ = 0.00000001 JSR = 35 dB μ = 0.000000001 JSR = 40 dB μ = 0.000000001 JSR = 45 dB μ = 0.000000001 JSR = 50 dB μ = 0.0000000001 JSR = 55 dB μ = 0.0000000001 JSR = 60 dB μ = 0.0000000001 JSR = 65 dB μ = 0.00000000001 JSR = 70 dB μ = 0.00000000001 JSR = 75 dB μ = 0.00000000001 JSR = 80 dB μ = 0.000000000001	JSR = 10 dB μ = 0.0000001 JSR = 15 dB μ = 0.00001 JSR = 20 dB μ = 0.00001 JSR = 25 dB μ = 0.00001 JSR = 30 dB μ = 0.000001 JSR = 35 dB μ = 0.0000001 JSR = 40 dB μ = 0.0000001 JSR = 45 dB μ = 0.0000001 JSR = 50 dB μ = 0.00000001 JSR = 55 dB μ = 0.000000001 JSR = 60 dB μ = 0.000000001 JSR = 65 dB μ = 0.0000000001 JSR = 70 dB μ = 0.0000000001 JSR = 75 dB μ = 0.0000000001 JSR = 80 dB μ = 0.00000000001	JSR = 10 dB Threshold = 9.0 Notch Width = 1 JSR = 15 dB Threshold = 15.0 Notch Width = 1 JSR = 20 dB Threshold = 15.0 Notch Width = 1 JSR = 25 dB Threshold = 15.0 Notch Width = 1 JSR = 30 dB Threshold = 13.0 Notch Width = 0 JSR = 35 dB Threshold = 15.0 Notch Width = 0 JSR = 40 dB Threshold = 30.0 Notch Width = 1 JSR = 45 dB Threshold = 35.0 Notch Width = 1 JSR = 50 dB Threshold = 50.0 Notch Width = 1 JSR = 55 dB Threshold = 60.0 Notch Width = 3 JSR = 60 dB Threshold = 60.0 Notch Width = 4 JSR = 65 dB Threshold = 65.0 Notch Width = 4 JSR = 70 dB Threshold = 70.0 Notch Width = 4 JSR = 75 dB Threshold = 70.0 Notch Width = 4 JSR = 80 dB Threshold = 70.0 Notch Width = 4

Table 4.1: Jammer 1 - Filters / MLT-TDE - Parameters Used for Each Value of JSR

ADAPTIVE CORRELATOR	MLT-TDED
JSR = 10 dB μ = 0.000001 JSR = 15 dB μ = 0.000001 JSR = 20 dB μ = 0.000001 JSR = 25 dB μ = 0.000001 JSR = 30 dB μ = 0.000001 JSR = 35 dB μ = 0.000001 JSR = 40 dB μ = 0.000001 JSR = 45 dB μ = 0.0000001 JSR = 50 dB μ = 0.00000001 JSR = 55 dB μ = 0.00000001 JSR = 60 dB μ = 0.000000001 JSR = 65 dB μ = 0.000000001 JSR = 70 dB μ = 0.0000000001 JSR = 75 dB μ = 0.0000000001 JSR = 80 dB μ = 0.00000000001	JSR = 10 dB Threshold = 11.0 Notch Width = 1 JSR = 15 dB Threshold = 11.0 Notch Width = 1 JSR = 20 dB Threshold = 25.0 Notch Width = 1 JSR = 25 dB Threshold = 11.0 Notch Width = 1 JSR = 30 dB Threshold = 13.0 Notch Width = 1 JSR = 35 dB Threshold = 13.0 Notch Width = 1 JSR = 40 dB Threshold = 13.0 Notch Width = 2 JSR = 45 dB Threshold = 13.0 Notch Width = 2 JSR = 50 dB Threshold = 17.0 Notch Width = 2 JSR = 55 dB Threshold = 20.0 Notch Width = 2 JSR = 60 dB Threshold = 18.0 Notch Width = 4 JSR = 65 dB Threshold = 11.0 Notch Width = 4 JSR = 70 dB Threshold = 15.0 Notch Width = 4 JSR = 75 dB Threshold = 15.0 Notch Width = 4 JSR = 80 dB Threshold = 25.0 Notch Width =4

Table 4.2: Jammer 1- Corr / MLT-TDED - Parameters Used for Each Value of JSR

In figures 4.5 and 4.6, the curves representing BER vs. jammer frequency are shown, for the different receiver structures and for the raw error, where no interference suppression technique is incorporated. The plots only show a sampling of jammer frequencies with points taken at $f = 0.08\ Hz$, $f = 0.1\ Hz$, $f = 0.12\ Hz$, $f = 0.15\ Hz$, $f = 0.18\ Hz$, $f = 0.2\ Hz$, $f = 0.234\ Hz$, $f = 0.25\ Hz$, $f = 0.3\ Hz$, $f = 0.35\ Hz$, $f = 0.4\ Hz$, and $f = 0.45\ Hz$. If more frequencies were tested, the results would show more structure. For these simulations, the default parameters used are a value of $E_b / N_o = 6\ dB$ for the channel, and a value of $JSR = 20\ dB$ for the jammer. Magnitudes of $\mu = 0.0000001$ for the predictive and $\mu = 0.00001$ for the two-sided are used, while a $threshold = 15.0$ and $notch\ width = 1$ are employed for the MLT-transform domain exciser. The convergence parameter used for the adaptive correlator is $\mu = 0.000001$, and $threshold = 25.0$ and $notch\ width = 1$ for the MLT-TDED structure. It can be observed that only the MLT-TDED system is slightly dependent on jammer frequency.

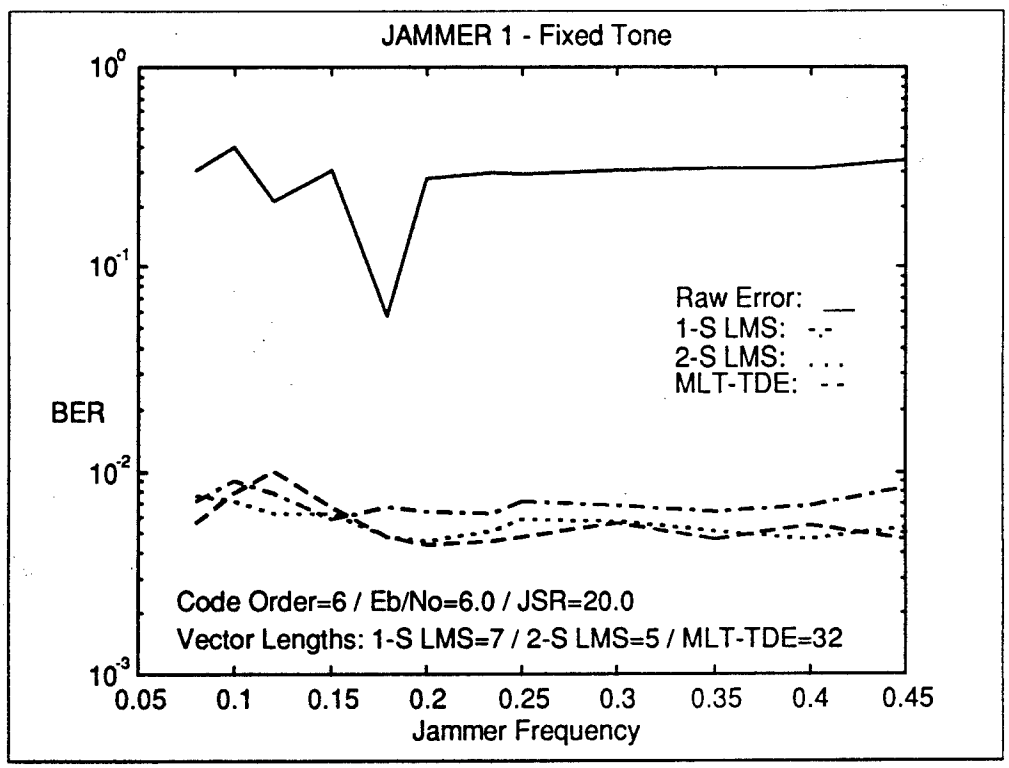

Figure 4.5 : BER vs. Jammer Frequency for Jammer 1 - Filters / MLT-TDE

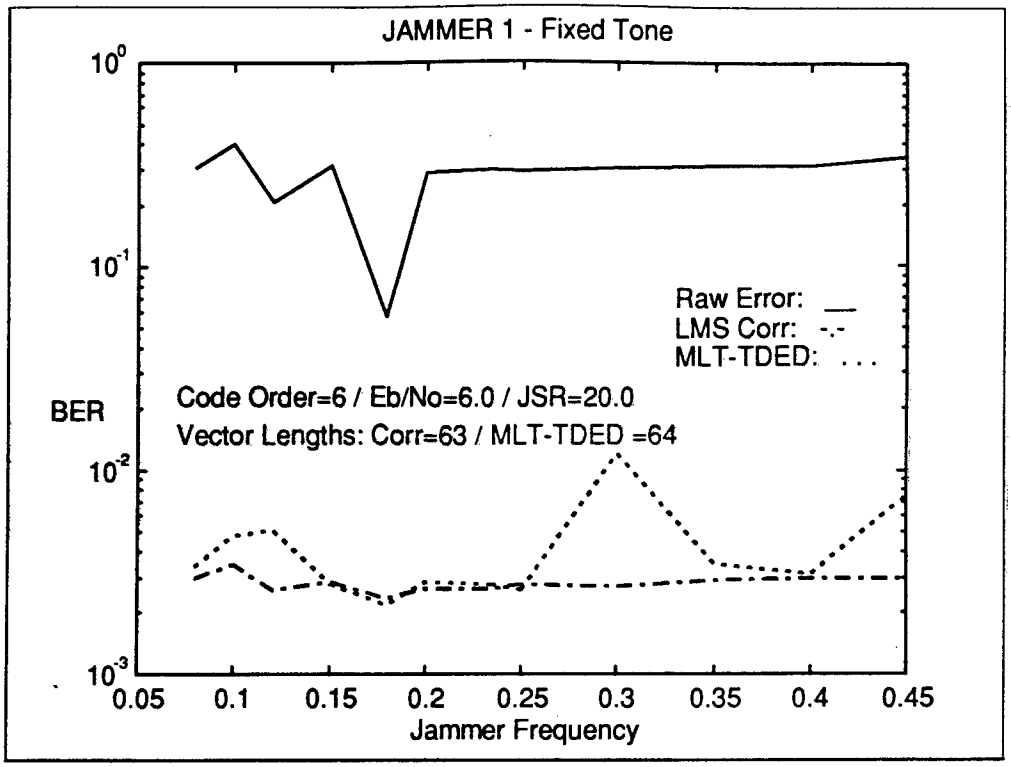

Figure 4.6 : BER vs. Jammer Frequency for Jammer 1 - Corr / MLT-TDED

4.2- Results for Jammer 2

4.2.1- Swept Tone

The interference used in the following section is the swept tone jammer, where a triangular wave is used to vary the tone frequency.

In Figure 4.7 and 4.8, BER vs. E_b/N_o for the different receiver systems can be observed. Also, the performance of BPSK baseband signal in AWGN, and the results related with the raw error are incorporated in the plots. For these simulations, the default parameters used for the swept jammer are $JSR = 20\ dB$, a normalized frequency $f = 0.25\ Hz$ and a sweep frequency $f_{sweep} = 0.00001\ Hz$. A value of $\mu = 0.00001$ for the predictive and $\mu = 0.0001$ for the two-sided filter are used, while the MLT-transform domain excision process is performed with $threshold = 13.0$ and $notch\ width = 1$. Values of $\mu = 0.00001$ for the correlator, and $threshold = 15.0$ and $notch\ width = 1$ for the MLT-TDED system are selected. All these values are optimized in order to obtain the best results for the systems. It can be noticed from Figure 4.7 that the adaptive LMS filters and the MLT-TDE structure introduce improvements, removing the interference and decreasing the BER. The predictive filter seems to perform slightly worse than the others. Figure 4.8 shows that the performance of the MLT-TDED system is pretty similar to the ones obtained with the two-sided filter and MLT-TDE receiver. On another hand, the adaptive correlator presents poor results in comparison to the other systems.

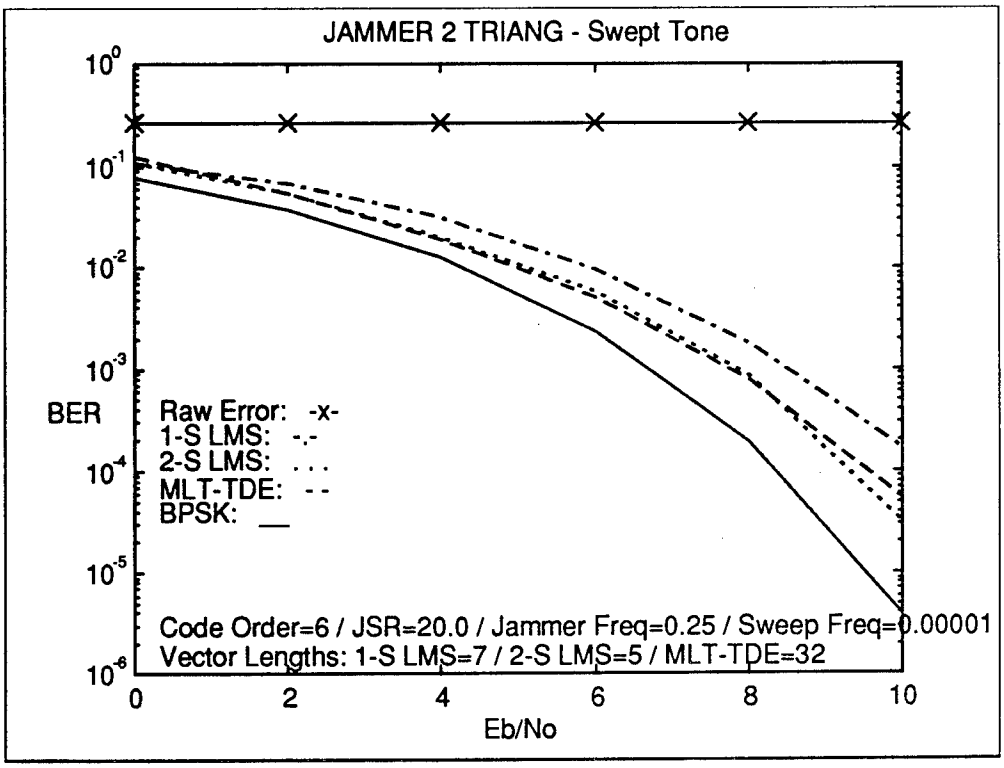

Figure 4.7 : BER vs. Eb/No for Jammer 2-Triang - Filters / MLT-TDE

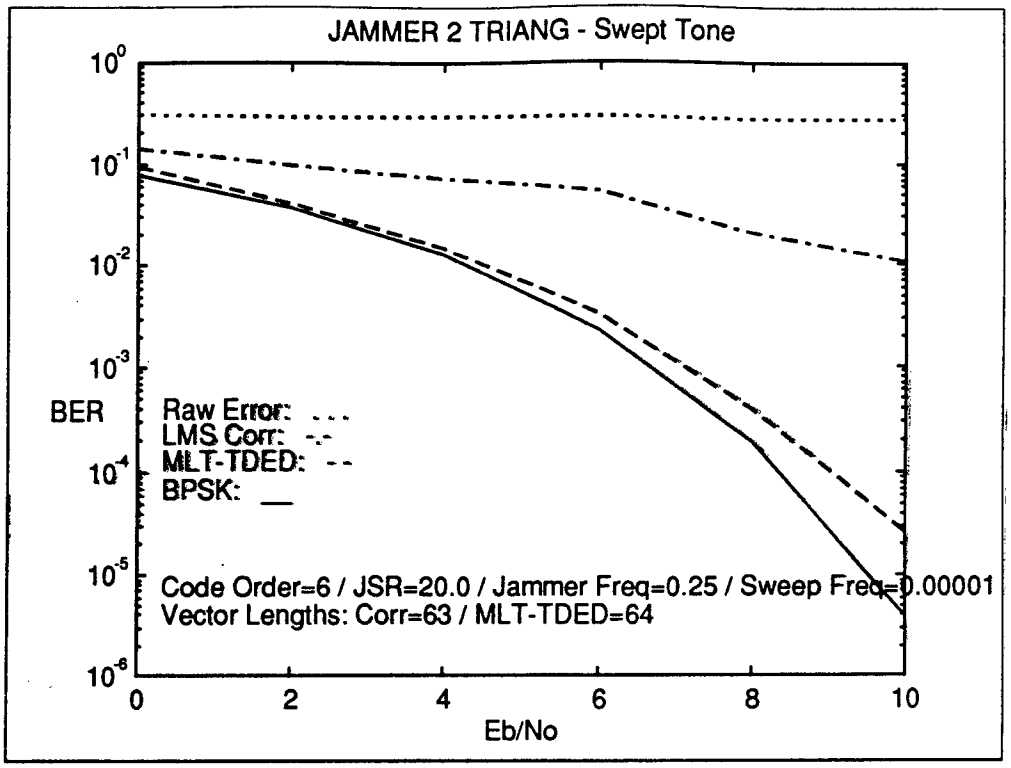

Figure 4.8 : BER vs. Eb/No for Jammer 2-Triang - Corr / MLT-TDED

Figures 4.9 and 4.10 present the plots of BER vs. JSR for the different structures, where a value of $E_b / N_o = 6\,dB$ is used for the channel. The default parameters used for the jammer are normalized frequency of $f = 0.25\,Hz$ and sweep frequency of $f_{sweep} = 0.00001\,Hz$. Tables 4.3 and 4.4 show the optimized values for the convergence factor μ of the adaptive filters and correlator, and exciser parameters of the MLT systems; the optimization is done for each JSR value. From the graphs, it can be concluded that none of the receiver systems is able to efficiently operate when exposed to this jammer. After values of $JSR \approx 20-35\,dB$, the performance of the various structures starts presenting poor results, even tough the MLT-TDED system seems to handle the interference slightly better.

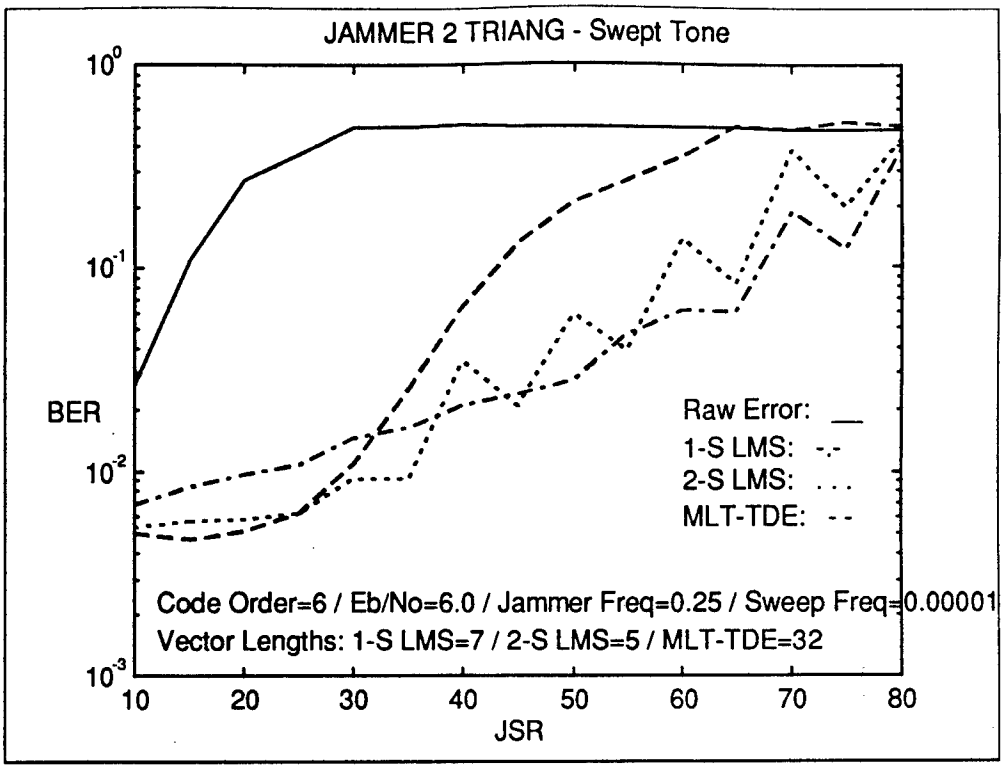

Figure 4.9 : BER vs. JSR for Jammer 2-Triang - Filters / MLT-TDE

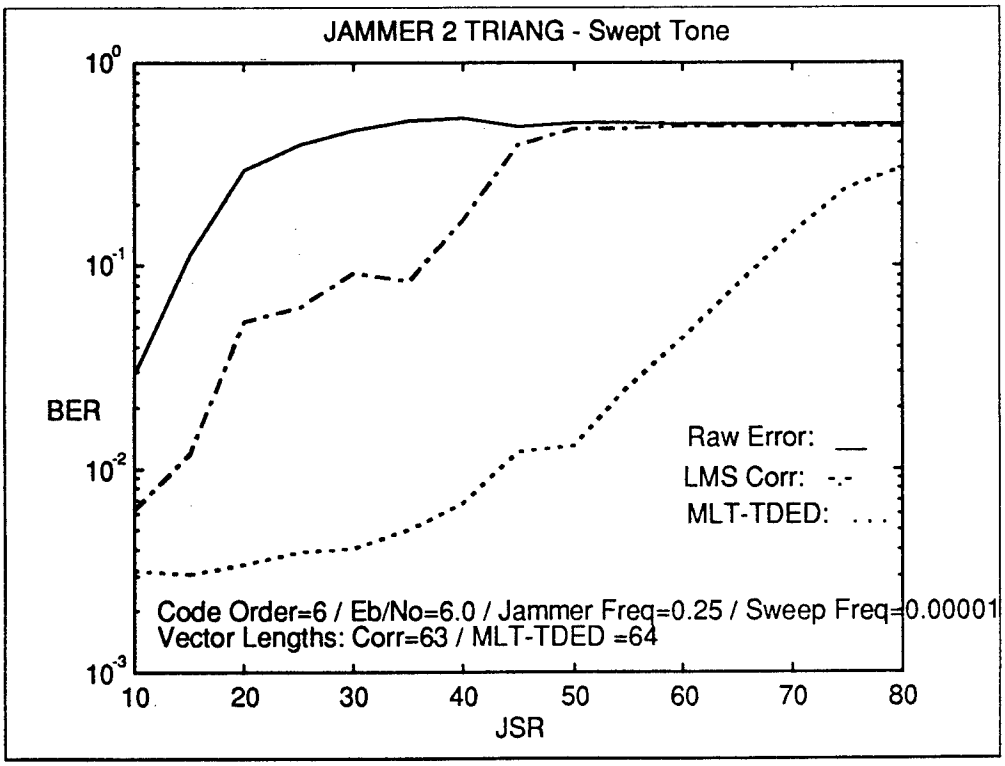

Figure 4.10 : BER vs. JSR for Jammer 2-Triang - Corr / MLT-TDED

PREDICTIVE FILTER	TWO-SIDED FILTER	MLT-TDE
JSR = 10 dB μ = 0.0001 JSR = 15 dB μ = 0.0001 JSR = 20 dB μ = 0.00001 JSR = 25 dB μ = 0.00001 JSR = 30 dB μ = 0.00001 JSR = 35 dB μ = 0.000001 JSR = 40 dB μ = 0.000001 JSR = 45 dB μ = 0.0000001 JSR = 50 dB μ = 0.0000001 JSR = 55 dB μ = 0.0000001 JSR = 60 dB μ = 0.00000001 JSR = 65 dB μ = 0.00000001 JSR = 70 dB μ = 0.000000001 JSR = 75 dB μ = 0.000000001 JSR = 80 dB μ = 0.0000000001	JSR = 10 dB μ = 0.0001 JSR = 15 dB μ = 0.0001 JSR = 20 dB μ = 0.0001 JSR = 25 dB μ = 0.0001 JSR = 30 dB μ = 0.00001 JSR = 35 dB μ = 0.00001 JSR = 40 dB μ = 0.000001 JSR = 45 dB μ = 0.000001 JSR = 50 dB μ = 0.0000001 JSR = 55 dB μ = 0.0000001 JSR = 60 dB μ = 0.00000001 JSR = 65 dB μ = 0.00000001 JSR = 70 dB μ = 0.000000001 JSR = 75 dB μ = 0.000000001 JSR = 80 dB μ = 0.0000000001	JSR = 10 dB Threshold = 9.0 Notch Width = 1 JSR = 15 dB Threshold = 11.0 Notch Width = 1 JSR = 20 dB Threshold = 13.0 Notch Width = 1 JSR = 25 dB Threshold = 11.0 Notch Width = 1 JSR = 30 dB Threshold = 11.0 Notch Width = 1 JSR = 35 dB Threshold = 15.0 Notch Width = 2 JSR = 40 dB Threshold = 15.0 Notch Width = 2 JSR = 45 dB Threshold = 15.0 Notch Width = 3 JSR = 50 dB Threshold = 20.0 Notch Width = 4 JSR = 55 dB Threshold = 37.0 Notch Width = 4 JSR = 60 dB Threshold = 45.0 Notch Width = 5 JSR = 65 dB Threshold = 45.0 Notch Width = 5 JSR = 70 dB Threshold = 45.0 Notch Width = 4 JSR = 75 dB Threshold = 50.0 Notch Width = 4 JSR = 80 dB Threshold = 55.0 Notch Width = 4

Table 4.3: Jammer 2 Triangle - Filters / MLT-TDE - Parameters Used for Each Value of JSR

ADAPTIVE CORRELATOR	MLT-TDED
JSR = 10 dB μ = 0.0001 JSR = 15 dB μ = 0.0001 JSR = 20 dB μ = 0.00001 JSR = 25 dB μ = 0.00001 JSR = 30 dB μ = 0.000001 JSR = 35 dB μ = 0.000001 JSR = 40 dB μ = 0.000001 JSR = 45 dB μ = 0.0000001 JSR = 50 dB μ = 0.0000001 JSR = 55 dB μ = 0.00000001 JSR = 60 dB μ = 0.00000001 JSR = 65 dB μ = 0.000000001 JSR = 70 dB μ = 0.000000001 JSR = 75 dB μ = 0.0000000001 JSR = 80 dB μ = 0.0000000001	JSR = 10 dB Threshold = 11.0 Notch Width = 1 JSR = 15 dB Threshold = 11.0 Notch Width = 1 JSR = 20 dB Threshold = 15.0 Notch Width = 1 JSR = 25 dB Threshold = 11.0 Notch Width = 2 JSR = 30 dB Threshold = 11.0 Notch Width = 2 JSR = 35 dB Threshold = 11.0 Notch Width = 2 JSR = 40 dB Threshold = 11.0 Notch Width = 2 JSR = 45 dB Threshold = 11.0 Notch Width = 4 JSR = 50 dB Threshold = 13.0 Notch Width = 4 JSR = 55 dB Threshold = 11.0 Notch Width = 4 JSR = 60 dB Threshold = 14.0 Notch Width = 4 JSR = 65 dB Threshold = 18.0 Notch Width = 6 JSR = 70 dB Threshold = 22.0 Notch Width = 6 JSR = 75 dB Threshold = 22.0 Notch Width = 6 JSR = 80 dB Threshold = 30.0 Notch Width = 6

Table 4.4: Jammer 2 Triangle - Corr / MLT-TDED - Parameters Used for Each Value of JSR

Figures 4.11 to 4.15 present the results obtained for BER vs. sweep frequency for the different receiver structures, using several values for the parameters of the interference suppression techniques, namely μ or the *threshold* and *notch width*. For these simulations, the default parameters used are $JSR = 20\,dB$, a normalized frequency of $f = 0.25\,Hz$, and $E_b / N_o = 6\,dB$. The MLT systems present good results and are relatively insensitive to sweep frequency. It can also be observed that their performance is rather independent of the parameters used for the excision process. On another hand, the LMS filters and correlator have hard time dealing with the jamming effects after values of $f_{sweep} \approx 10^{-6}\,Hz$. Apparently, the LMS algorithm is unable to track the jammer when its frequency changes too rapidly. Besides, the performance of these systems relies heavily on the convergence parameter μ utilized; the higher the sweep frequency, the lower the parameter needs to be in order to reduce the mean-square error and remove the jamming.

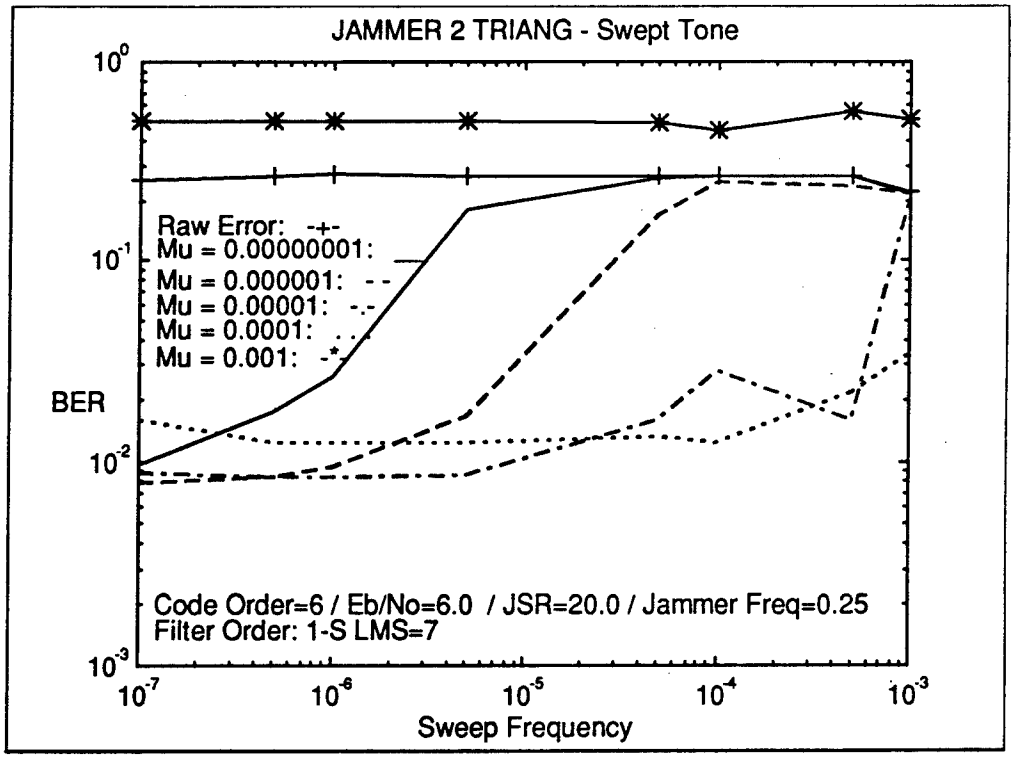

Figure 4.11 : BER vs. Sweep Frequency for Jammer 2-Triang - 1-S Filter

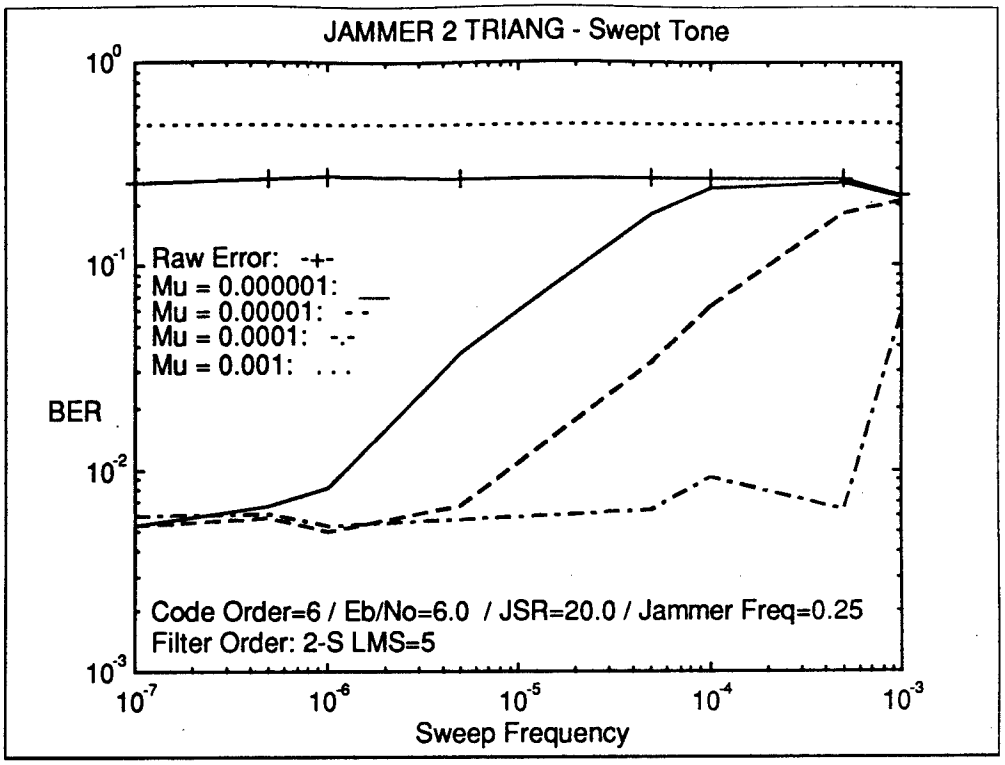

Figure 4.12 : BER vs. Sweep Frequency for Jammer 2-Triang - 2-S Filter

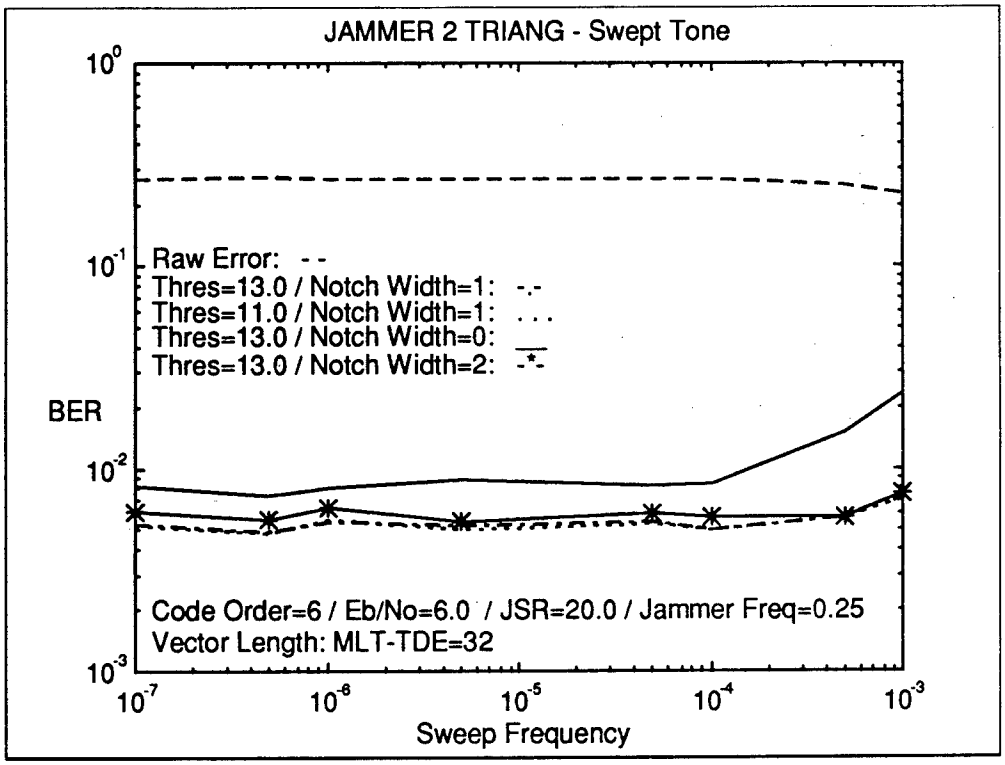

Figure 4.13 : BER vs. Sweep Frequency for Jammer 2-Triang - MLT-TDE

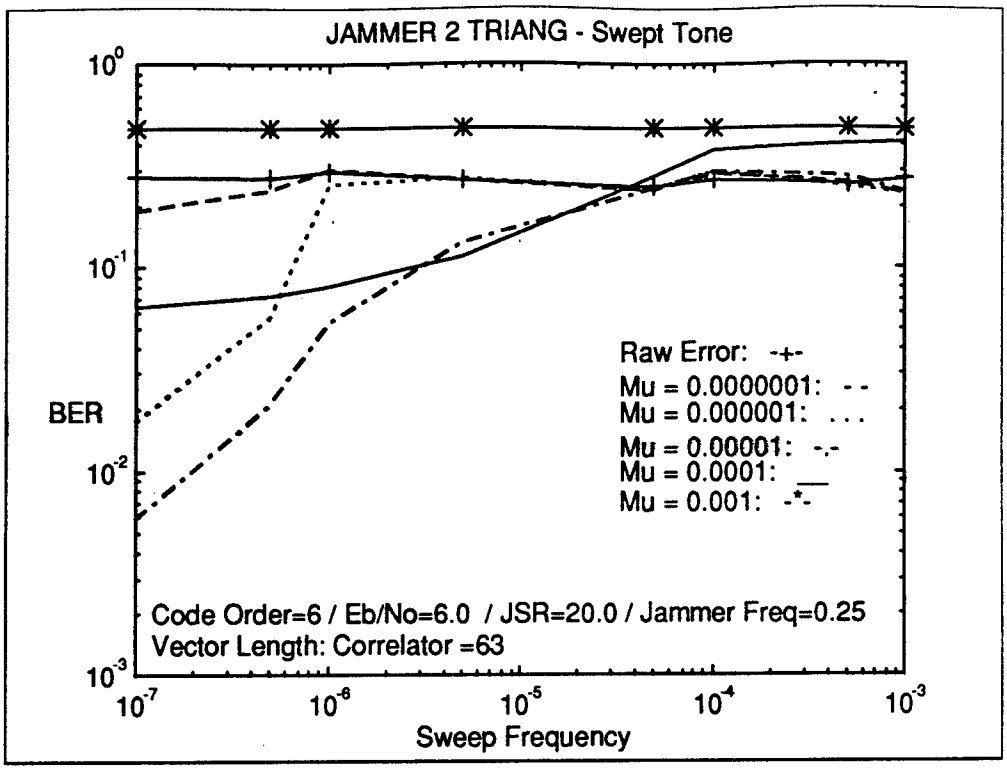

Figure 4.14 : BER vs. Sweep Frequency for Jammer 2-Triang - Corr

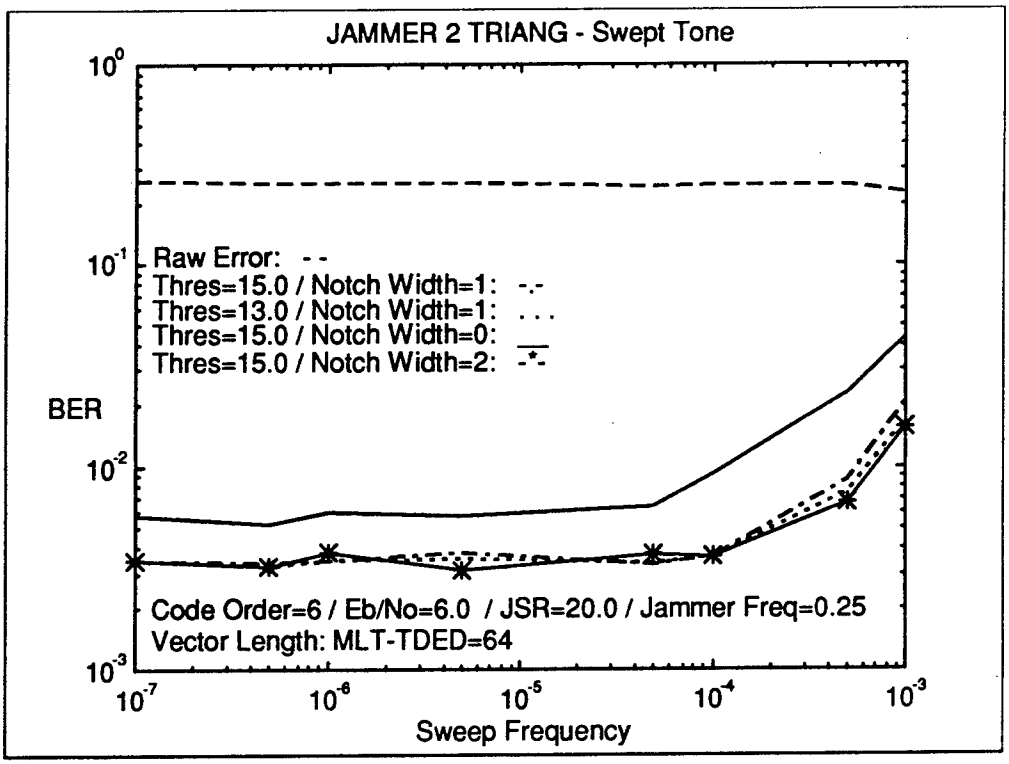

Figure 4.15 : BER vs. Sweep Frequency for Jammer 2-Triang - MLT-TDED

4.2.2- Chirp Jamming

In this section, the chirp jamming is added to the channel in order to produce the interference. Here, a ramp wave is used to vary the tone frequency.

Figures 4.16 and 4.17 show the BER vs. E_b/N_o for the four receiver structures, as well as for the results obtained with BPSK signal in AWGN and raw error. The default parameters used for the jammer are $JSR = 20\,dB$, a normalized frequency $f = 0.25\,Hz$ and a sweep frequency $f_{sweep} = 0.00001\,Hz$. The optimized values for the system parameters are $\mu = 0.00001$ for the predictive and $\mu = 0.0001$ for the two-sided filter, $threshold = 11.0$ and $notch\ width = 1$ for the MLT-TDE system, a value of $\mu = 0.00001$ for the correlator, and $threshold = 10.0$ and $notch\ width = 1$ for the MLT-TDED system. It can be noticed from the figures that all the techniques perform efficiently in removing the jammer, and their results are pretty similar, except for the predictive filter whose performance is slightly inferior than the others.

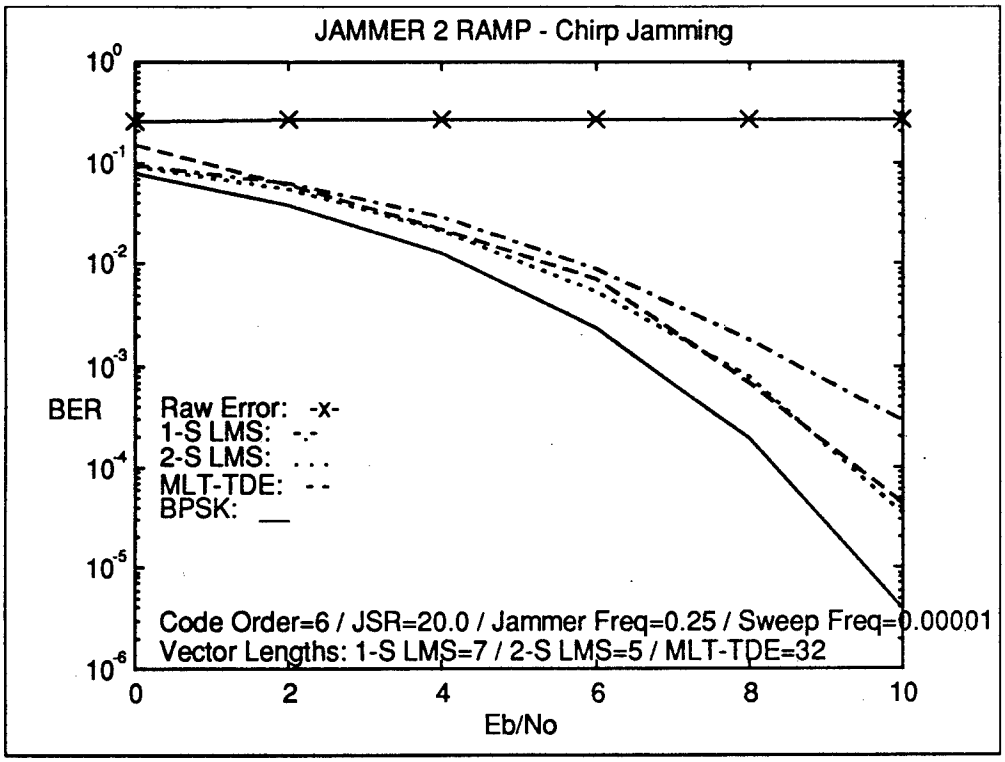

Figure 4.16 : BER vs. Eb/No for Jammer 2-Ramp - Filters / MLT-TDE

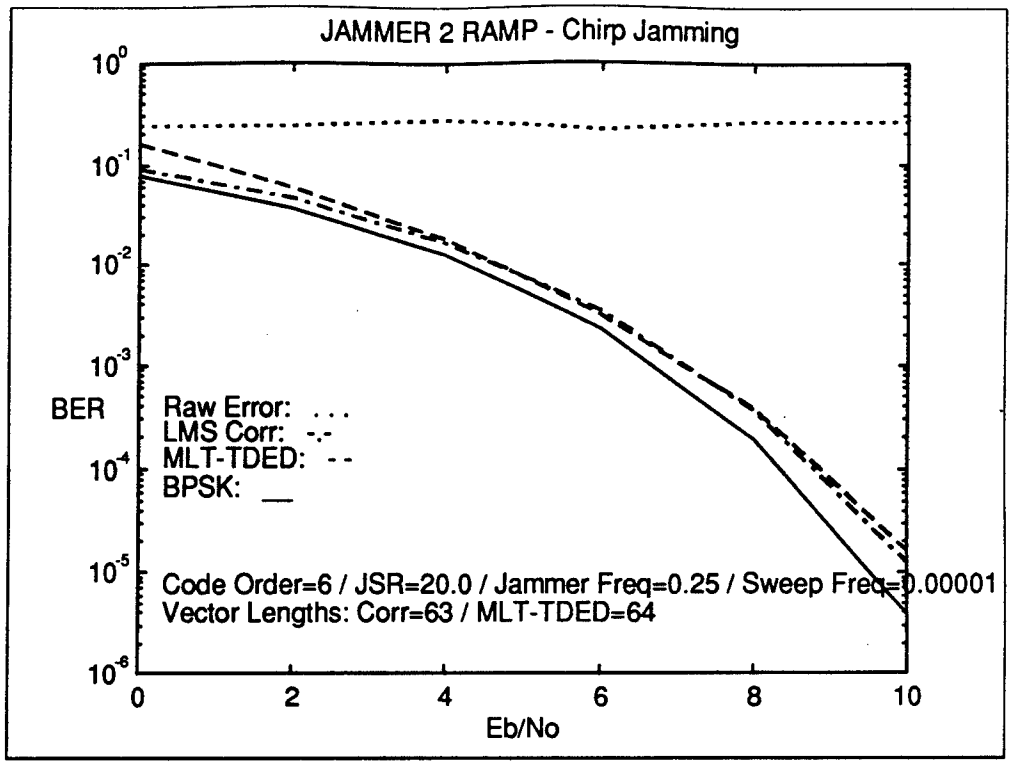

Figure 4.17 : BER vs. Eb/No for Jammer 2-Ramp - Corr / MLT-TDED

Figures 4.18 and 4.19 show BER vs. JSR for the different receiver systems, using a value of $E_b / N_o = 6\,dB$ for the Gaussian noise in the channel. The default parameters used for the jammer are normalized frequency of $f = 0.25\,Hz$ and sweep frequency of $f_{sweep} = 0.00001\,Hz$. Tables 4.5 and 4.6 show the optimized values for the systems parameters selected for each value of JSR. As the plots indicate, the four receiver structures show poor performance in removing the chirp jamming. After values of $JSR \approx 30\,dB$, the results start deteriorating rapidly, making an exception for of the MLT-TDED system, whose performance is slightly better.

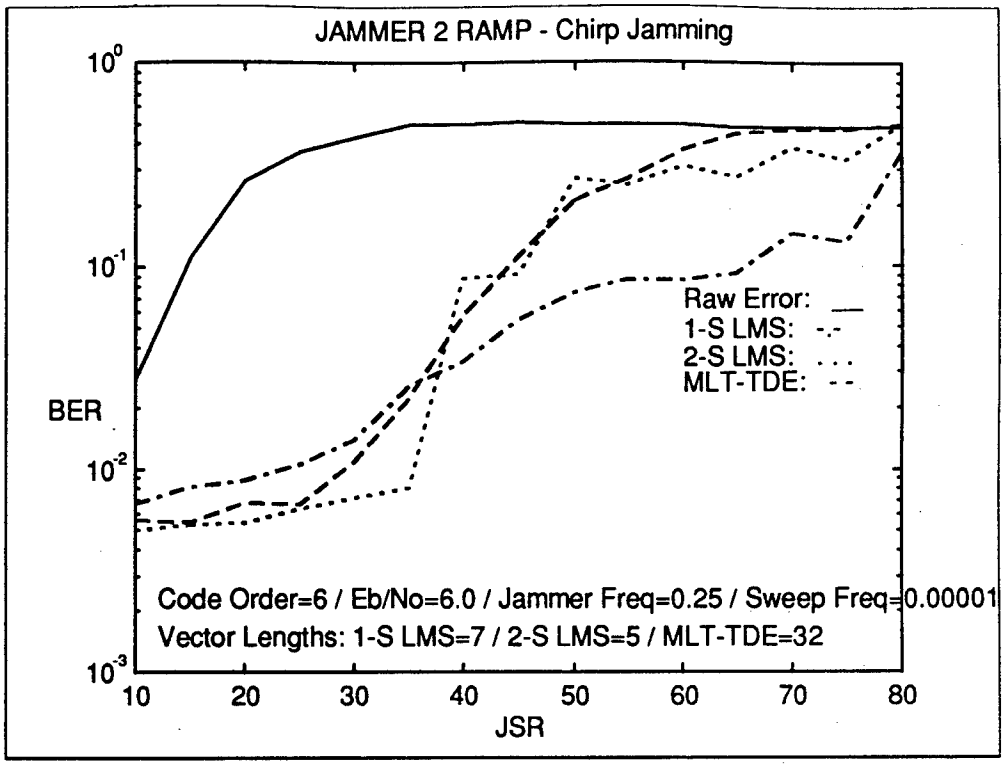

Figure 4.18 : BER vs. JSR for Jammer 2-Ramp - Filters / MLT-TDE

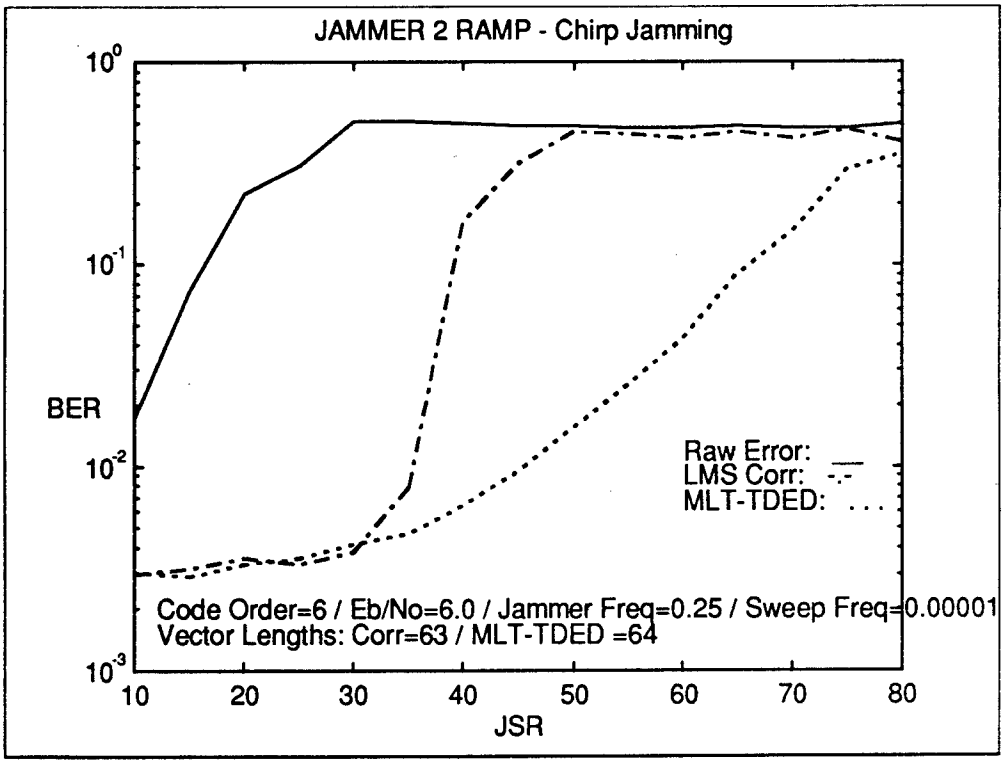

Figure 4.19 : BER vs. JSR for Jammer 2-Ramp - Corr / MLT-TDED

PREDICTIVE FILTER	TWO-SIDED FILTER	MLT-TDE
JSR = 10 dB μ = 0.0001 JSR = 15 dB μ = 0.00001 JSR = 20 dB μ = 0.00001 JSR = 25 dB μ = 0.00001 JSR = 30 dB μ = 0.00001 JSR = 35 dB μ = 0.00001 JSR = 40 dB μ = 0.000001 JSR = 45 dB μ = 0.000001 JSR = 50 dB μ = 0.0000001 JSR = 55 dB μ = 0.0000001 JSR = 60 dB μ = 0.00000001 JSR = 65 dB μ = 0.00000001 JSR = 70 dB μ = 0.000000001 JSR = 75 dB μ = 0.000000001 JSR = 80 dB μ = 0.0000000001	JSR = 10 dB μ = 0.0001 JSR = 15 dB μ = 0.0001 JSR = 20 dB μ = 0.0001 JSR = 25 dB μ = 0.0001 JSR = 30 dB μ = 0.00001 JSR = 35 dB μ = 0.00001 JSR = 40 dB μ = 0.000001 JSR = 45 dB μ = 0.000001 JSR = 50 dB μ = 0.0000001 JSR = 55 dB μ = 0.0000001 JSR = 60 dB μ = 0.00000001 JSR = 65 dB μ = 0.00000001 JSR = 70 dB μ = 0.000000001 JSR = 75 dB μ = 0.000000001 JSR = 80 dB μ = 0.0000000001	JSR = 10 dB Threshold = 9.0 Notch Width = 1 JSR = 15 dB Threshold = 9.0 Notch Width = 1 JSR = 20 dB Threshold = 11.0 Notch Width = 1 JSR = 25 dB Threshold = 12.0 Notch Width = 1 JSR = 30 dB Threshold = 11.0 Notch Width = 2 JSR = 35 dB Threshold = 14.0 Notch Width = 2 JSR = 40 dB Threshold = 14.0 Notch Width = 3 JSR = 45 dB Threshold = 17.0 Notch Width = 3 JSR = 50 dB Threshold = 26.0 Notch Width = 3 JSR = 55 dB Threshold = 43.0 Notch Width = 3 JSR = 60 dB Threshold = 48.0 Notch Width = 3 JSR = 65 dB Threshold = 50.0 Notch Width = 0 JSR = 70 dB Threshold = 47.0 Notch Width = 0 JSR = 75 dB Threshold = 45.0 Notch Width = 1 JSR = 80 dB Threshold = 80.0 Notch Width = 2

Table 4.5: Jammer 2 Ramp - Filters / MLT-TDE - Parameters Used for Each Value of JSR

ADAPTIVE CORRELATOR	MLT-TDED
JSR = 10 dB μ = 0.00001 JSR = 15 dB μ = 0.00001 JSR = 20 dB μ = 0.00001 JSR = 25 dB μ = 0.000001 JSR = 30 dB μ = 0.000001 JSR = 35 dB μ = 0.000001 JSR = 40 dB μ = 0.0000001 JSR = 45 dB μ = 0.0000001 JSR = 50 dB μ = 0.00000001 JSR = 55 dB μ = 0.00000001 JSR = 60 dB μ = 0.00000001 JSR = 65 dB μ = 0.000000001 JSR = 70 dB μ = 0.000000001 JSR = 75 dB μ = 0.0000000001 JSR = 80 dB μ = 0.0000000001	JSR = 10 dB Threshold = 10.0 Notch Width = 1 JSR = 15 dB Threshold = 10.0 Notch Width = 1 JSR = 20 dB Threshold = 10.0 Notch Width = 1 JSR = 25 dB Threshold = 14.0 Notch Width = 2 JSR = 30 dB Threshold = 12.0 Notch Width = 2 JSR = 35 dB Threshold = 15.0 Notch Width = 2 JSR = 40 dB Threshold = 11.0 Notch Width = 2 JSR = 45 dB Threshold = 11.0 Notch Width = 2 JSR = 50 dB Threshold = 10.0 Notch Width = 2 JSR = 55 dB Threshold = 13.0 Notch Width = 4 JSR = 60 dB Threshold = 13.0 Notch Width = 4 JSR = 65 dB Threshold = 17.0 Notch Width = 4 JSR = 70 dB Threshold = 20.0 Notch Width = 4 JSR = 75 dB Threshold = 20.0 Notch Width = 4 JSR = 80 dB Threshold = 24.0 Notch Width = 4

Table 4.6: Jammer 2 Ramp - Corr / MLT-TDED - Parameters Used for Each Value of JSR

Figures 4.20 to 4.24 show BER vs. sweep frequency for the various receiver structures, using many different values for μ and the exciser parameters. The default parameters used are $JSR = 20\,dB$ and a normalized frequency of $f = 0.25\,Hz$ for the jammer, and a value of $E_b / N_o = 6\,dB$ for the channel. The MLT systems provide a significant improvement over the no-suppression case, along with no real dependence on the sweep frequency and excision process parameters. On the contrary, the LMS algorithm is unable to track the jammer after values of $f_{sweep} \approx 10^{-6}\ Hz$, and its performance is closely tied to the value of the convergence parameter μ.

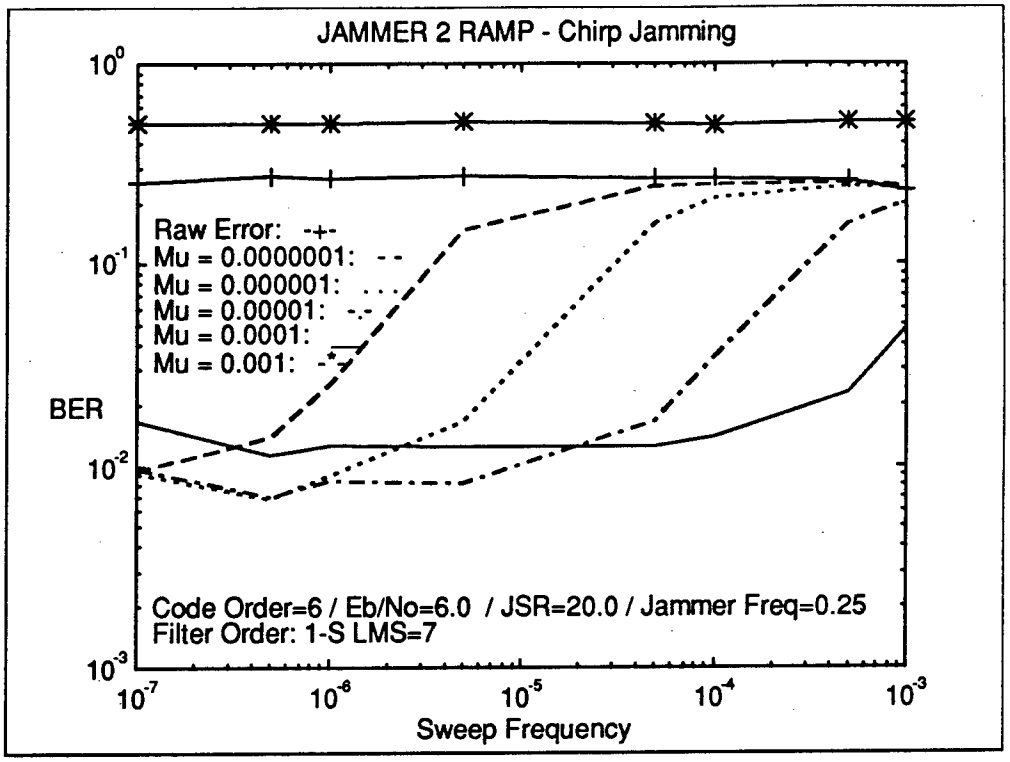

Figure 4.20 : BER vs. Sweep Frequency for Jammer 2-Ramp - 1-S Filter

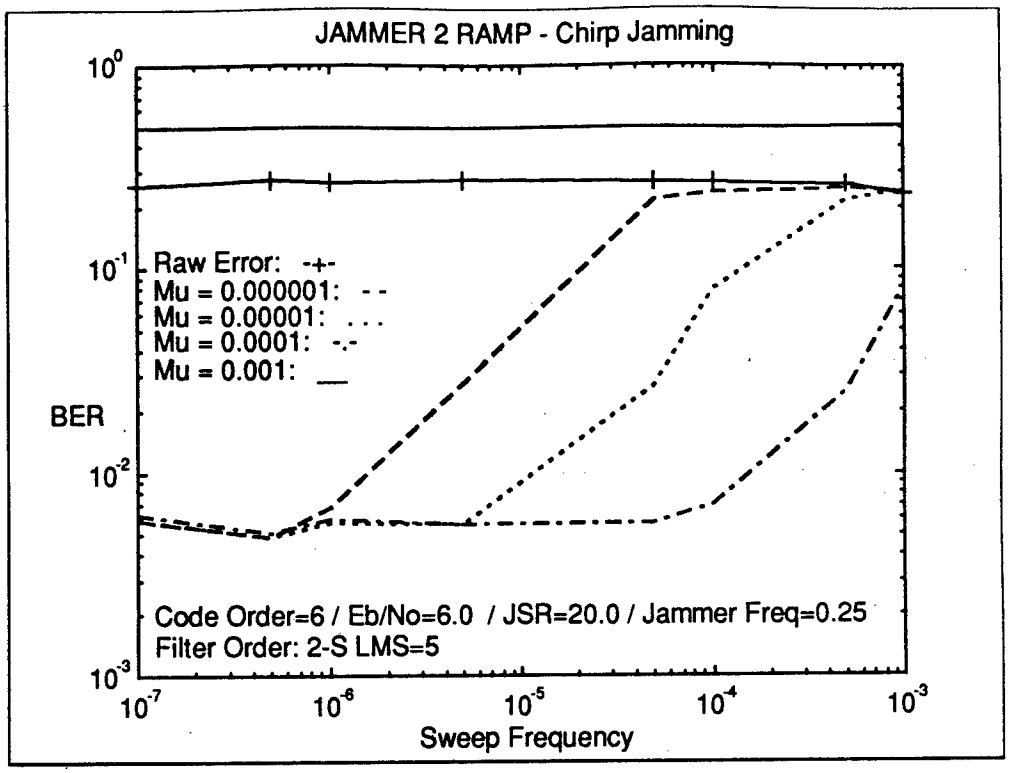

Figure 4.21 : BER vs. Sweep Frequency for Jammer 2-Ramp - 2-S Filter

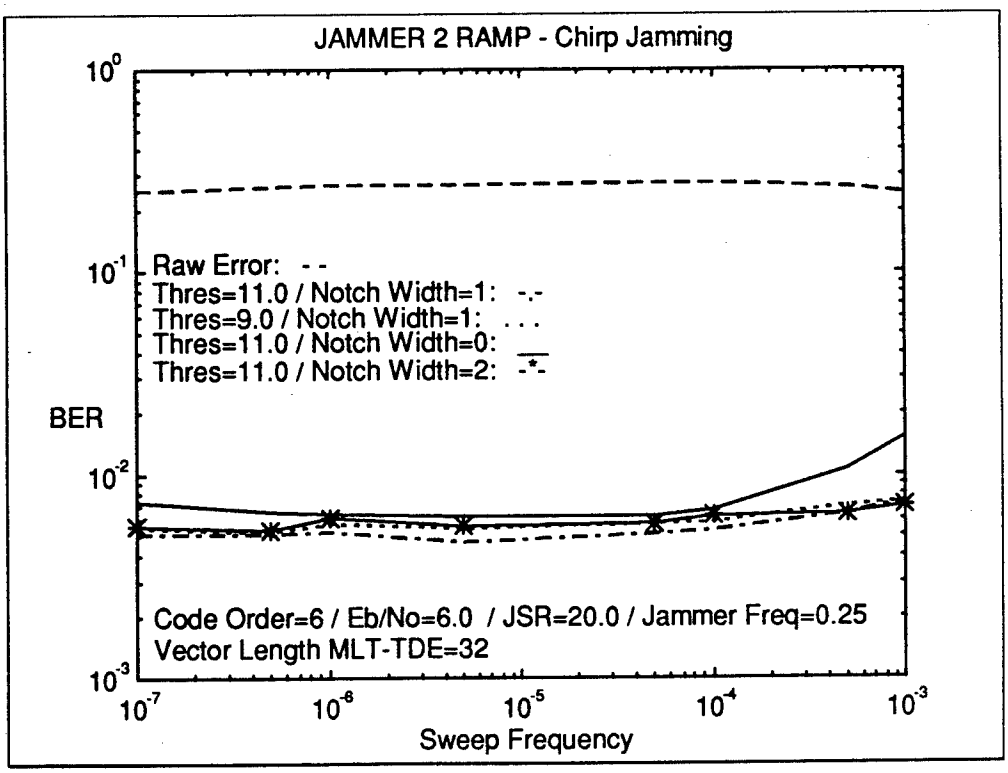

Figure 4.22 : BER vs. Sweep Frequency for Jammer 2-Ramp - MLT-TDE

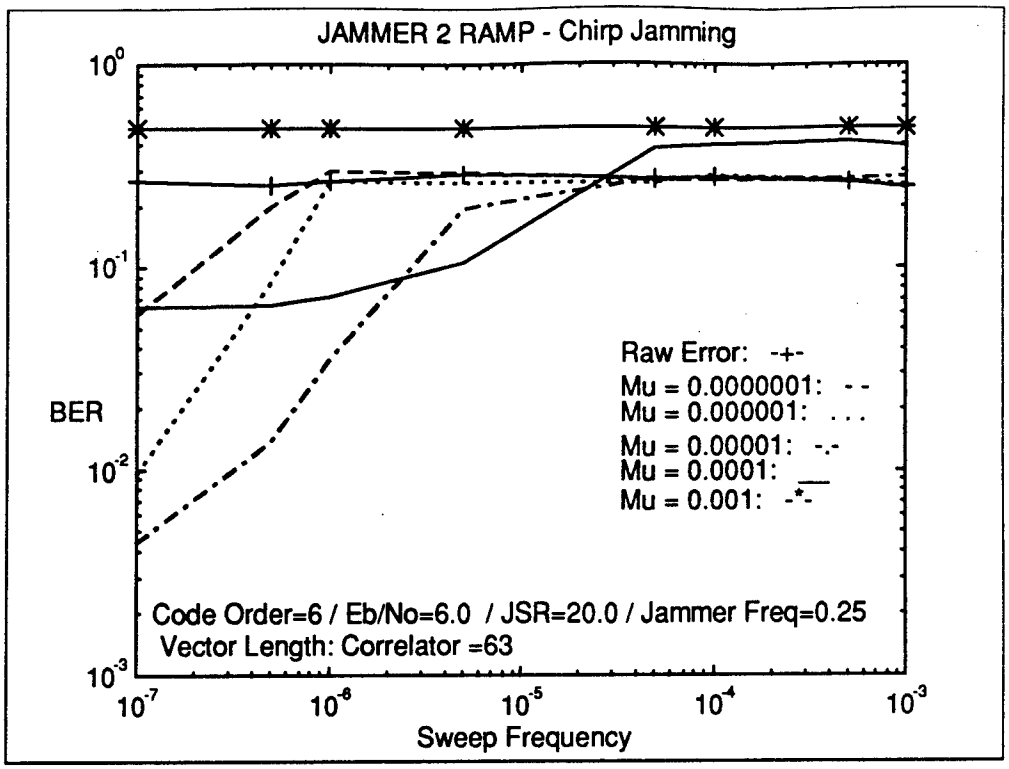

Figure 4.23 : BER vs. Sweep Frequency for Jammer 2-Ramp - Corr

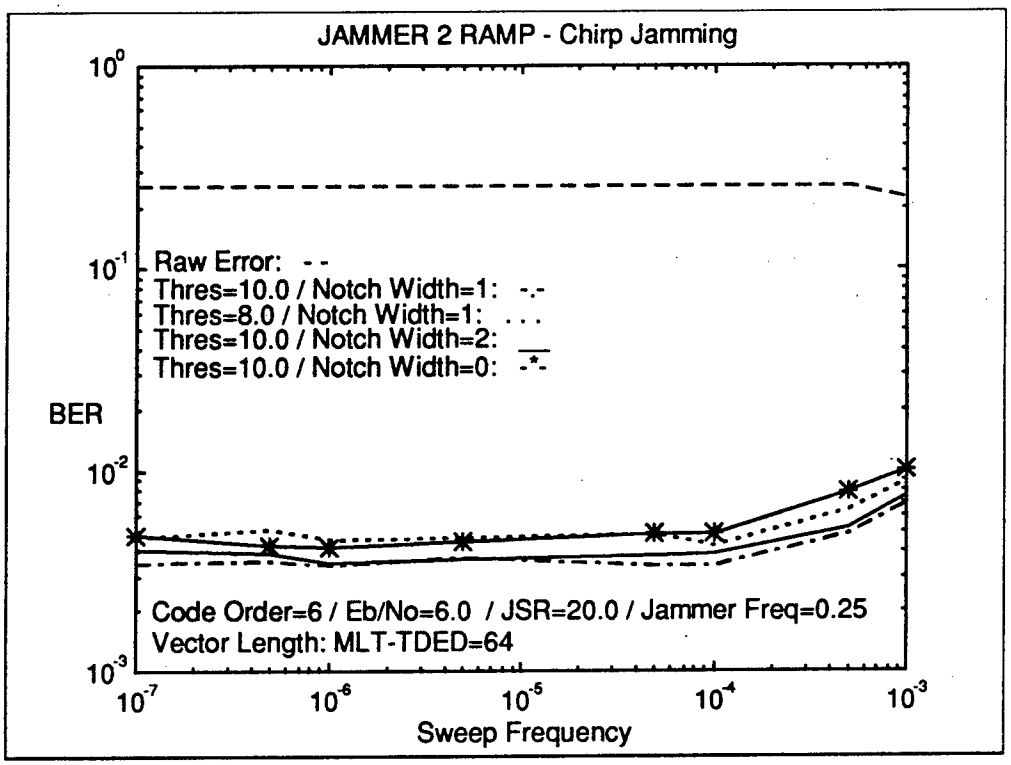

Figure 4.24 : BER vs. Sweep Frequency for Jammer 2-Ramp - MLT-TDED

4.3- Results for Jammer 3

This section shows the results obtained for each of the communication receiver systems in presence of Gaussian noise jamming.

Figure 4.25 shows BER vs. E_b/N_o for the filters and MLT-based transform domain exciser, along with the results for BPSK signal in AWGN and raw error. The jammer parameters used are $JSR = 20\,dB$, a normalized frequency $f = 0.234\,Hz$, and a jammer bandwidth of $BW = 0.1\,Hz$. A value of $\mu = 0.000001$ for the predictive and $\mu = 0.0001$ for the two-sided filter are used, while a $threshold = 9.0$ and $notch\ width = 2$ are employed for the MLT-transform domain exciser. The two-sided filter and MLT-TDE system present good and similar interference suppression capabilities; in contrast, for higher values of $E_b / N_o \approx 3\,dB$, the predictive filter presents poor performance, much inferior than the one obtained with the two previous structures.

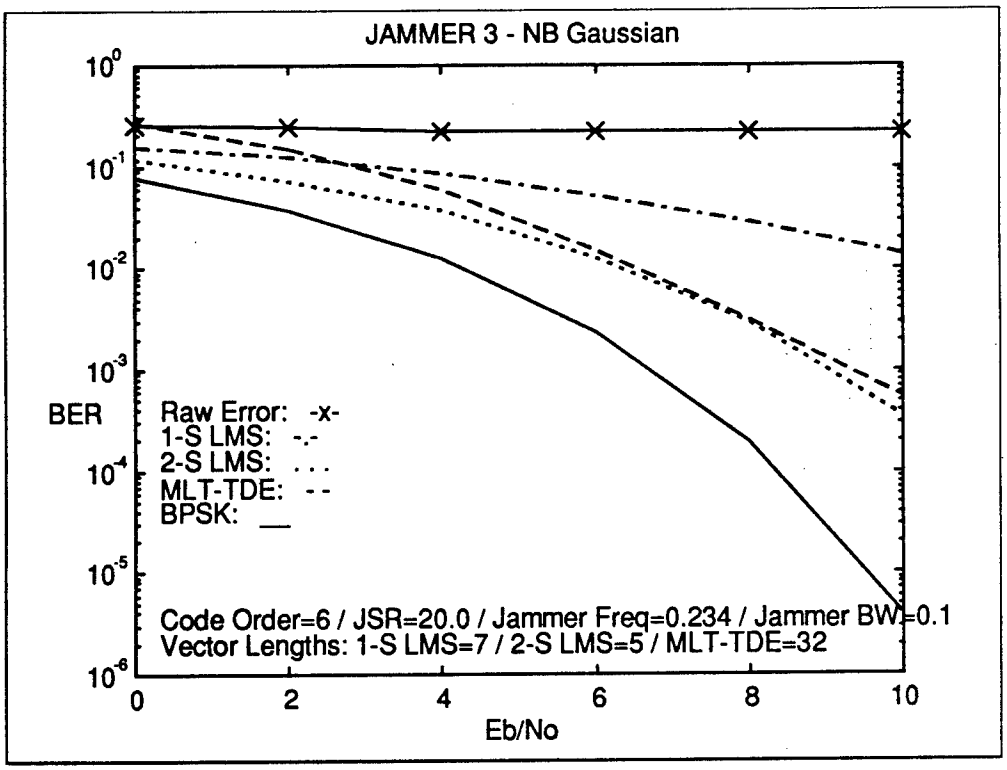

Figure 4.25 : BER vs. Eb/No for Jammer 3 - Filters / MLT-TDE

Figure 4.26 shows the plots of BER vs. E_b/N_o for the LMS correlator and MLT-TDED system. For these simulations, the default parameters used for the jammer are $JSR = 20\,dB$, a normalized frequency $f = 0.234\,Hz$, and a jammer bandwidth of $BW = 0.1\,Hz$. A value of $\mu = 0.000001$ for the correlator, and $threshold = 9.0$ and $notch\ width = 1$ for the MLT-TDED system are used. Note that the correlator structure presents similar results to the two-sided filter and MLT-TDE system as shown in Figure 4.25, while the performance of the MLT-TDED structure is slightly inferior, particularly after the value of $E_b / N_o \approx 8\,dB$.

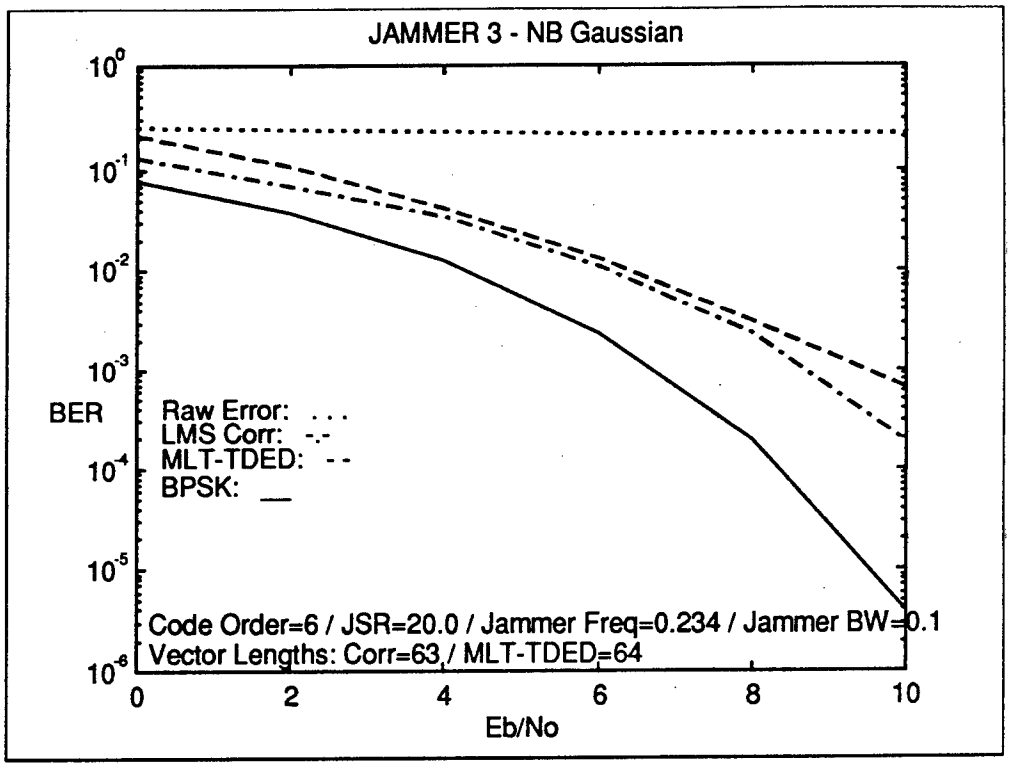

Figure 4.26 : BER vs. Eb/No for Jammer 3 - Corr / MLT-TDED

In Figures 4.27 and 4.28, the plots of BER vs. JSR for the different structures can be seen. The values used for the jammer are $E_b / N_o = 6\,dB$, a normalized frequency of $f = 0.234\,Hz$ and a jammer bandwidth of $BW = 0.1\,Hz$. The optimized parameters of the interference suppression techniques for each value of JSR are shown in Tables 4.7 and 4.8. After values of $JSR \approx 30\,dB$, all the different structures show poor performance in dealing with the interference; although the two-sided LMS filter and the MLT-TDED structure provide a slightly better performance than the other receivers.

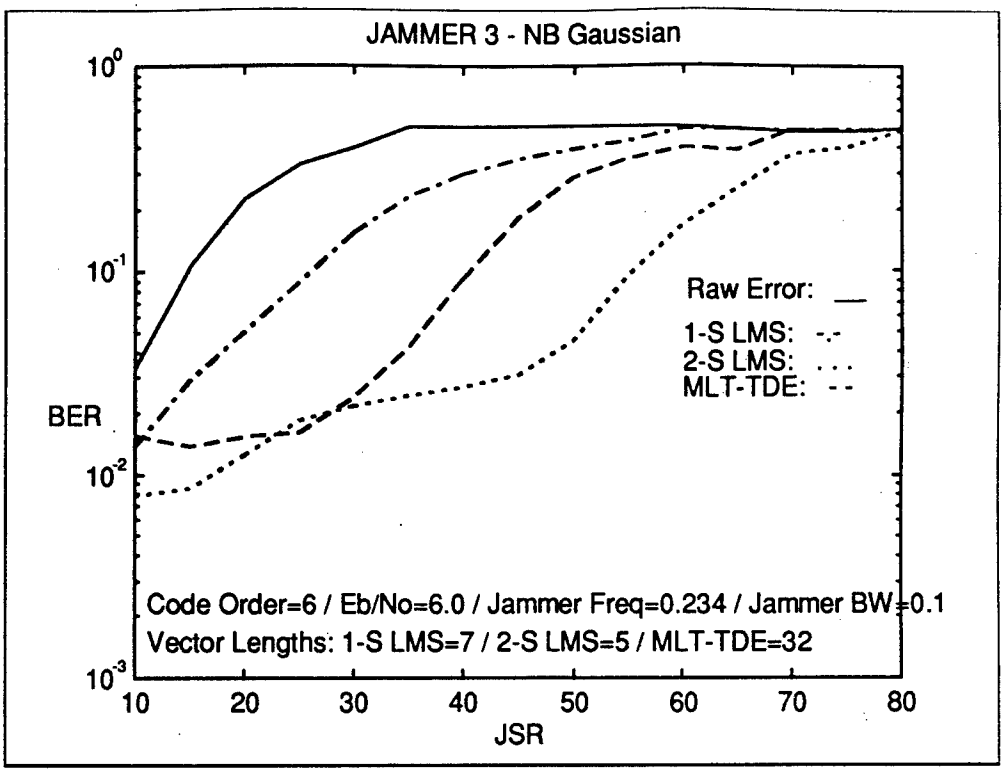

Figure 4.27 : BER vs. JSR for Jammer 3 - Filters / MLT-TDE

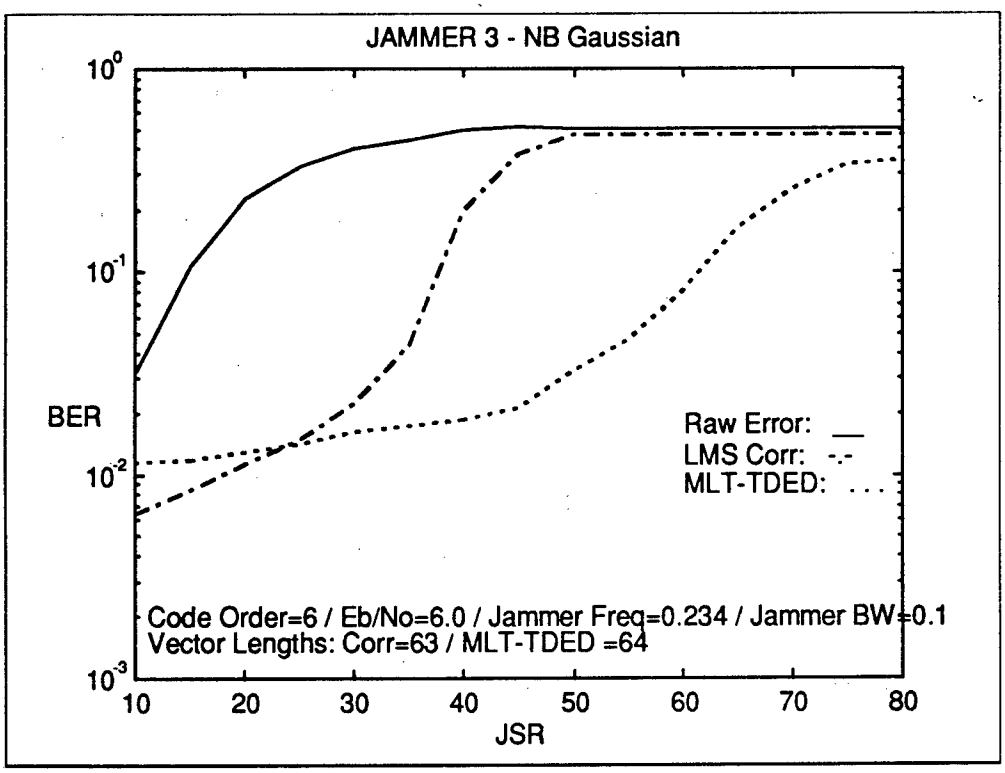

Figure 4.28 : BER vs. JSR for Jammer 3 - Corr / MLT-TDED

PREDICTIVE FILTER	TWO-SIDED FILTER	MLT-TDE
JSR = 10 dB μ = 0.000001 JSR = 15 dB μ = 0.0000001 JSR = 20 dB μ = 0.000001 JSR = 25 dB μ = 0.000001 JSR = 30 dB μ = 0.0000001 JSR = 35 dB μ = 0.000001 JSR = 40 dB μ = 0.0000001 JSR = 45 dB μ = 0.0000001 JSR = 50 dB μ = 0.0000001 JSR = 55 dB μ = 0.0000001 JSR = 60 dB μ = 0.0000001 JSR = 65 dB μ = 0.0000001 JSR = 70 dB μ = 0.0000001 JSR = 75 dB μ = 0.0000001 JSR = 80 dB μ = 0.00000001	JSR = 10 dB μ = 0.0001 JSR = 15 dB μ = 0.00001 JSR = 20 dB μ = 0.0001 JSR = 25 dB μ = 0.000001 JSR = 30 dB μ = 0.000001 JSR = 35 dB μ = 0.000001 JSR = 40 dB μ = 0.0000001 JSR = 45 dB μ = 0.0000001 JSR = 50 dB μ = 0.0000001 JSR = 55 dB μ = 0.00000001 JSR = 60 dB μ = 0.00000001 JSR = 65 dB μ = 0.00000001 JSR = 70 dB μ = 0.000000001 JSR = 75 dB μ = 0.000000001 JSR = 80 dB μ = 0.0000000001	JSR = 10 dB Threshold = 9.0 Notch Width = 2 JSR = 15 dB Threshold = 9.0 Notch Width = 2 JSR = 20 dB Threshold = 9.0 Notch Width = 2 JSR = 25 dB Threshold = 11.0 Notch Width = 2 JSR = 30 dB Threshold = 11.0 Notch Width = 2 JSR = 35 dB Threshold = 15.0 Notch Width = 2 JSR = 40 dB Threshold = 19.0 Notch Width = 2 JSR = 45 dB Threshold = 20.0 Notch Width = 3 JSR = 50 dB Threshold = 24.0 Notch Width = 3 JSR = 55 dB Threshold = 35.0 Notch Width = 3 JSR = 60 dB Threshold = 45.0 Notch Width = 4 JSR = 65 dB Threshold = 47.0 Notch Width = 4 JSR = 70 dB Threshold = 47.0 Notch Width = 5 JSR = 75 dB Threshold = 47.0 Notch Width = 5 JSR = 80 dB Threshold = 49.0 Notch Width = 5

Table 4.7: Jammer 3 - Filters / MLT-TDE - Parameters Used for Each Value of JSR

ADAPTIVE CORRELATOR	MLT-TDED
JSR = 10 dB μ = 0.00001 JSR = 15 dB μ = 0.000001 JSR = 20 dB μ = 0.000001 JSR = 25 dB μ = 0.000001 JSR = 30 dB μ = 0.000001 JSR = 35 dB μ = 0.000001 JSR = 40 dB μ = 0.000001 JSR = 45 dB μ = 0.0000001 JSR = 50 dB μ = 0.0000001 JSR = 55 dB μ = 0.0000001 JSR = 60 dB μ = 0.0000001 JSR = 65 dB μ = 0.0000001 JSR = 70 dB μ = 0.00000001 JSR = 75 dB μ = 0.00000001 JSR = 80 dB μ = 0.00000001	JSR = 10 dB Threshold = 9.0 Notch Width = 4 JSR = 15 dB Threshold = 9.0 Notch Width = 4 JSR = 20 dB Threshold = 9.0 Notch Width = 1 JSR = 25 dB Threshold = 9.0 Notch Width = 4 JSR = 30 dB Threshold = 9.0 Notch Width = 4 JSR = 35 dB Threshold = 9.0 Notch Width = 4 JSR = 40 dB Threshold = 12.0 Notch Width = 4 JSR = 45 dB Threshold = 13.0 Notch Width = 4 JSR = 50 dB Threshold = 15.0 Notch Width = 4 JSR = 55 dB Threshold = 15.0 Notch Width = 4 JSR = 60 dB Threshold = 20.0 Notch Width = 5 JSR = 65 dB Threshold = 28.0 Notch Width = 5 JSR = 70 dB Threshold = 35.0 Notch Width = 5 JSR = 75 dB Threshold = 40.0 Notch Width = 6 JSR = 80 dB Threshold = 40.0 Notch Width = 6

Table 4.8: Jammer 3- Corr / MLT-TDED - Parameters Used for Each Value of JSR

Figures 4.29 and 4.30 show the curves representing BER vs. jammer frequency for the different receiver structures and for the raw error. The plots only show a sampling of jammer frequencies with points taken at $f = 0.08\,Hz$, $f = 0.1\,Hz$, $f = 0.12\,Hz$, $f = 0.15\,Hz$, $f = 0.18\,Hz$, $f = 0.2\,Hz$, $f = 0.234\,Hz$, $f = 0.25\,Hz$, $f = 0.3\,Hz$, $f = 0.35\,Hz$, $f = 0.4\,Hz$, and $f = 0.45\,Hz$. For these simulations, the default parameters used for the jammer are $E_b / N_o = 6\,dB$, $JSR = 20\,dB$ and a jammer bandwidth of $BW = 0.1\,Hz$. A value of $\mu = 0.000001$ for the predictive and $\mu = 0.0001$ for the two-sided filter are used, while a $threshold = 9.0$ and $notch\ width = 2$ are employed for the MLT-transform domain exciser. Also, a value of $\mu = 0.000001$ for the correlator, and $threshold = 9.0$ and $notch\ width = 1$ for the MLT-TDED system are utilized to perform the simulations. The results show that the LMS filters and correlator are somewhat dependent on jammer frequency.

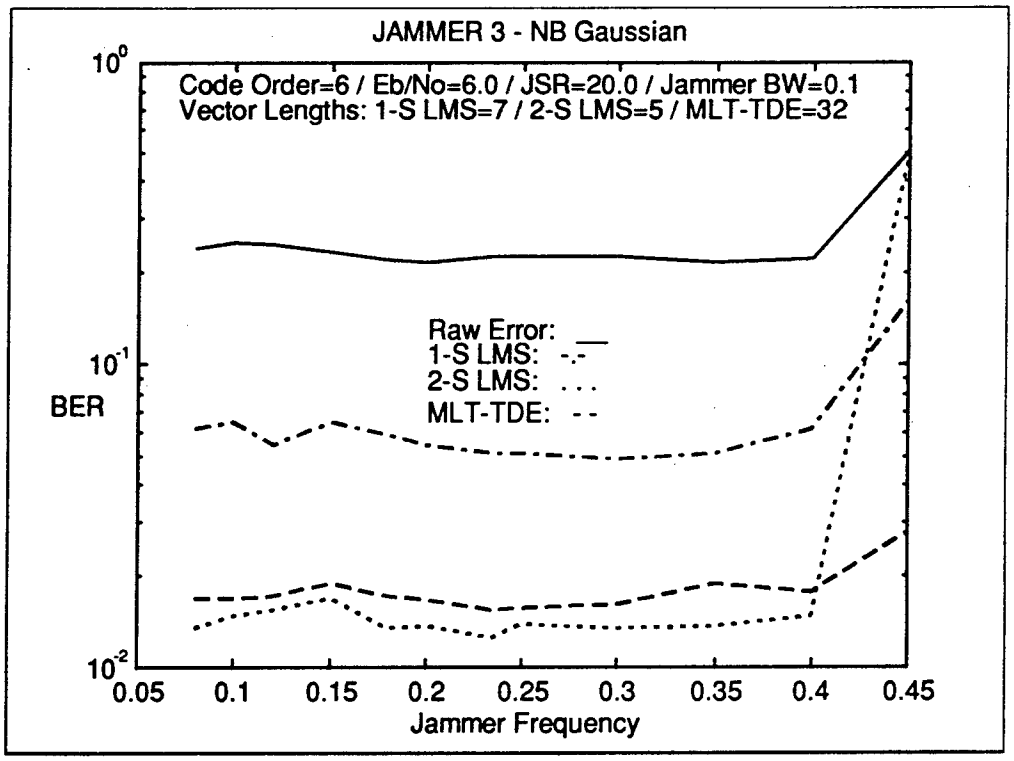

Figure 4.29 : BER vs. Jammer Frequency for Jammer 3 - Filters / MLT-TDE

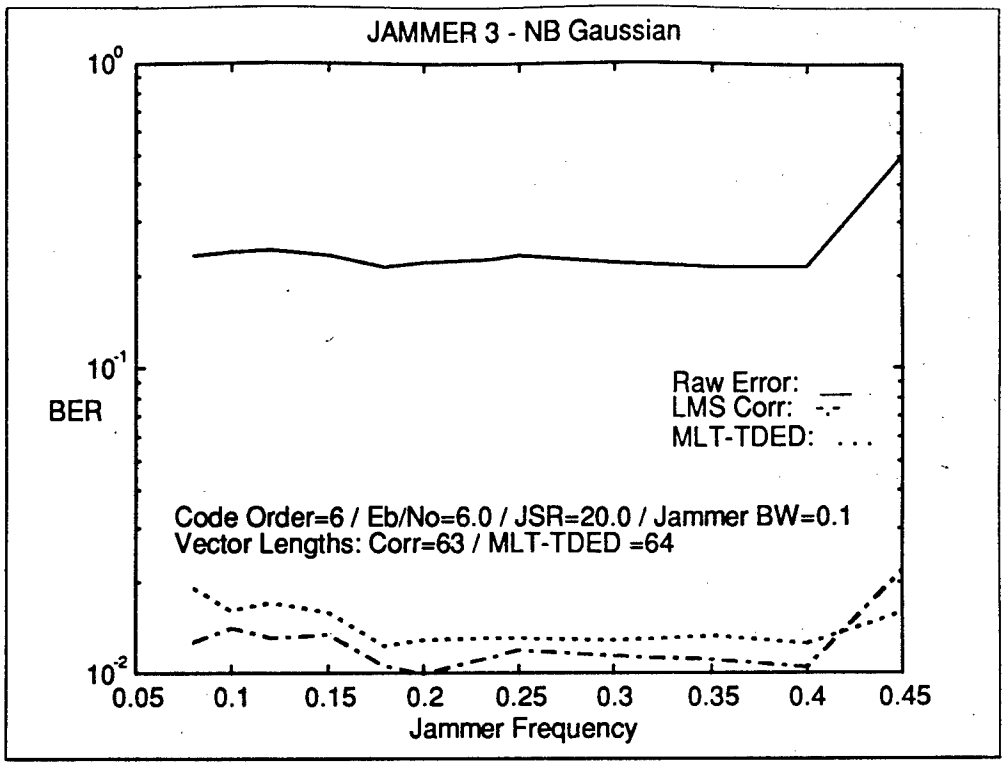

Figure 4.30 : BER vs. Jammer Frequency for Jammer 3 - Corr / MLT-TDED

In Figures 4.31 and 4.32, the plots of BER vs. jammer bandwidth can be seen for the different receiver systems and for the raw error case. The curves only show a sampling of jammer bandwidths with results obtained at $BW = 0.03\,Hz$, $BW = 0.05\,Hz$, $BW = 0.1\,Hz$, $BW = 0.15\,Hz$, $BW = 0.2\,Hz$, $BW = 0.25\,Hz$, $BW = 0.3\,Hz$, $BW = 0.35\,Hz$, $BW = 0.4\,Hz$, and $BW = 0.45\,Hz$. The default parameters are $E_b / N_o = 6\,dB$, $JSR = 20\,dB$ and a normalized frequency of $f = 0.234\,Hz$. The parameters for the interference suppression techniques include a value of $\mu = 0.000001$ for the predictive and $\mu = 0.0001$ for the two-sided filter, a $threshold = 9.0$ and $notch\ width = 2$ for the MLT-transform domain exciser, a value of $\mu = 0.000001$ for the correlator, and values of $threshold = 9.0$ and $notch\ width = 1$ for the MLT-TDED system. For all the structures, the results deteriorate as the jammer bandwidth increases; the predictive filter shows inferior performance, while the two-sided filter and the MLT-TDED system seem to tolerate larger bandwidth slightly better.

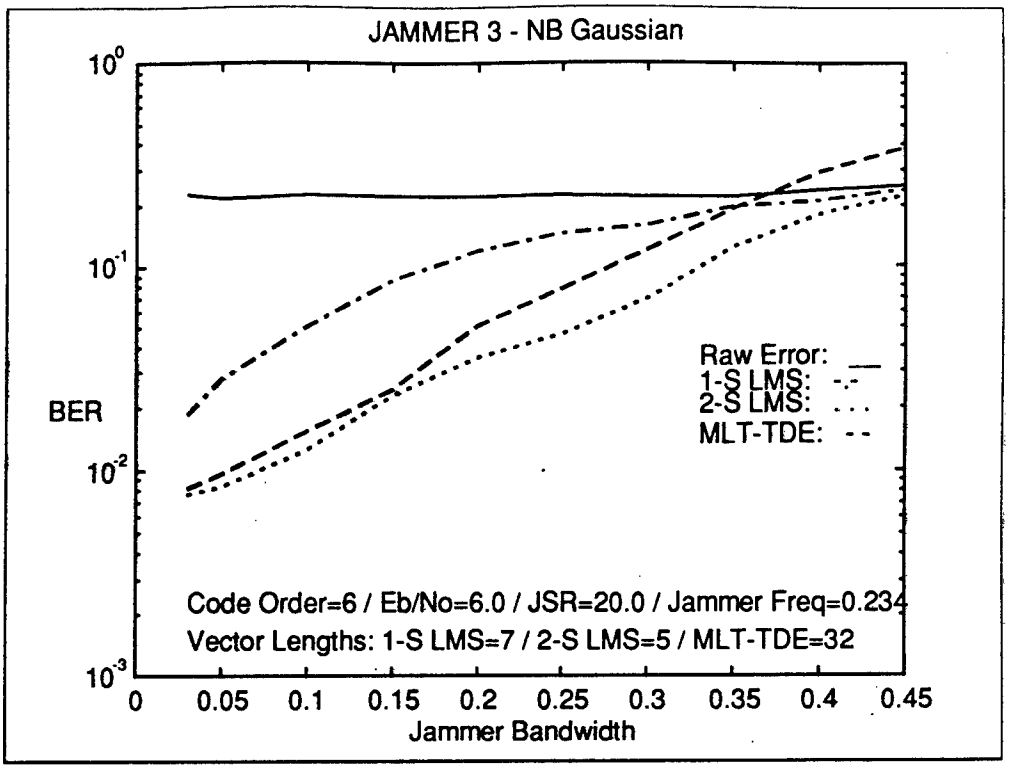

Figure 4.31 : BER vs. Jammer Bandwidth for Jammer 3 - Filters / MLT-TDE

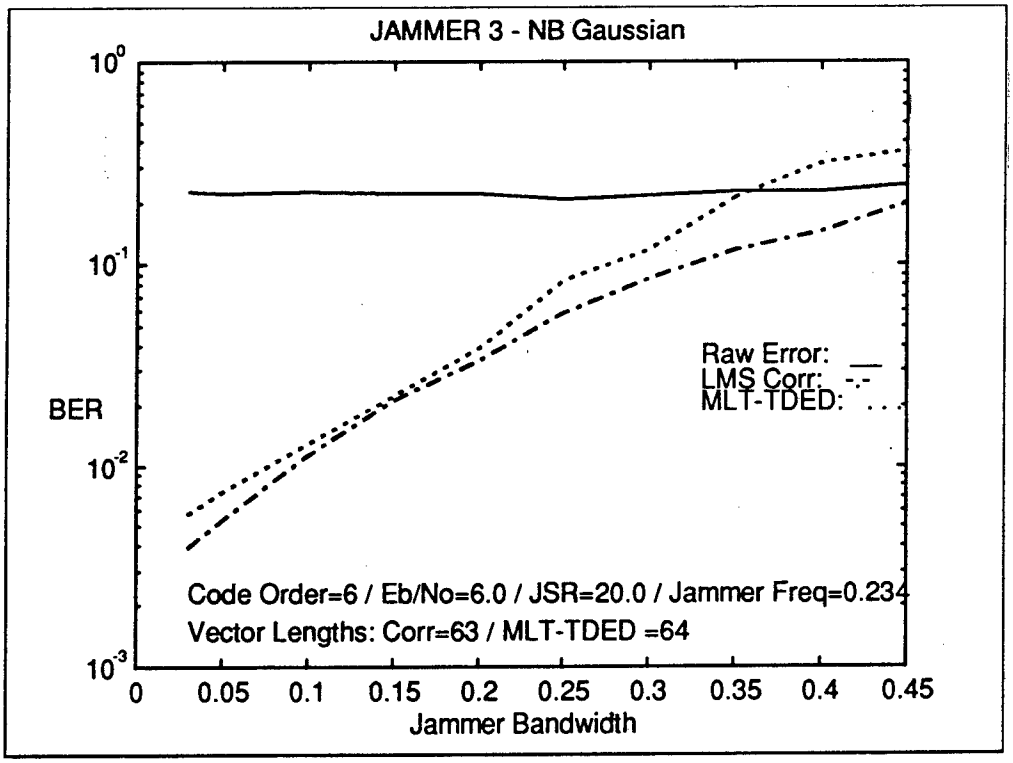

Figure 4.32 : BER vs. Jammer Bandwidth for Jammer 3 - Corr / MLT-TDED

4.4- Results for Jammer 4

4.4.1- Pulsed Tone

This section presents the results achieved for each of the receivers when the channel faces pulsed tone jamming.

In figure 4.33, the plot of BER vs. E_b/N_o for the one and two-sided LMS filters, and for the MLT-based transform domain exciser is shown. Besides, the results obtained with BPSK baseband signal in AWGN alone, along with the performance obtained without any interference suppression technique, are presented in the same curve. For these simulations, the default parameters used for the jammer are $JSR = 20\,dB$ and a normalized frequency $f = 0.1\,Hz$, while values of $f_{msk\ func} = 0.000001\,Hz$ and $Duty\ Cycle_{msk\ func} = 50\,\%$ are utilized for the masking function. A magnitude of $\mu = 0.00001$ for the predictive and $\mu = 0.0001$ for the two-sided filter are used, while a $threshold = 12.0$ and $notch\ width = 1$ are utilized for the MLT-TDE structure. As can be seen in the figure, the three suppression structures introduce significant improvement over the no-suppression case, although the predictive filter presents a slightly inferior performance than the other two systems.

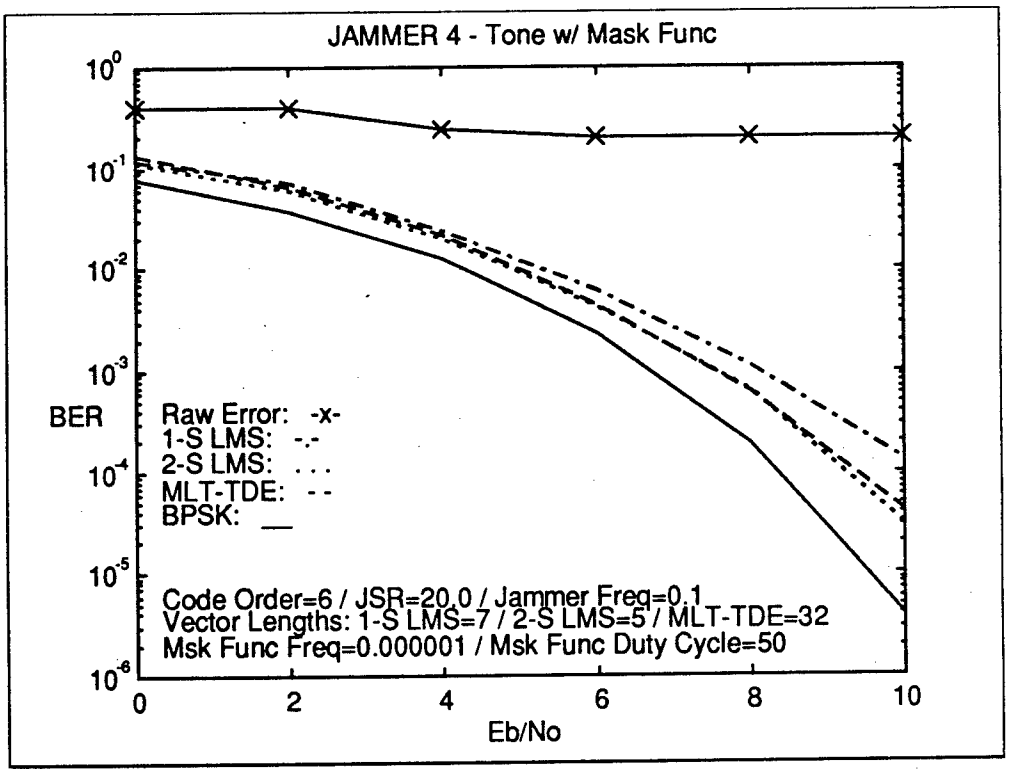

Figure 4.33 : BER vs. Eb/No for Jammer 4-Tone - Filters / MLT-TDE

Figure 4.34 shows BER vs. E_b/N_o for the adaptive LMS correlator and MLT-TDED system. Also, the performance of BPSK baseband signal in AWGN alone, as well as the performance of the raw error are added. For these simulations, the default parameters used for the jammer are $JSR = 20\,dB$ and a normalized frequency $f = 0.1\,Hz$, while values of $f_{msk\ func} = 0.000001\,Hz$ and $Duty\ Cycle_{msk\ func} = 50\,\%$ are utilized for the masking function. $\mu = 0.000001$ for the correlator, and $threshold = 15.0$ and $notch\ width = 2$ for the MLT-TDED system are used. These parameters were optimized in order to achieve best performance for the receivers. Both structures present similar results, which are closer to the AWGN-only performance than the two-sided filter and MLT-TDE structures presented in Figure 4.33.

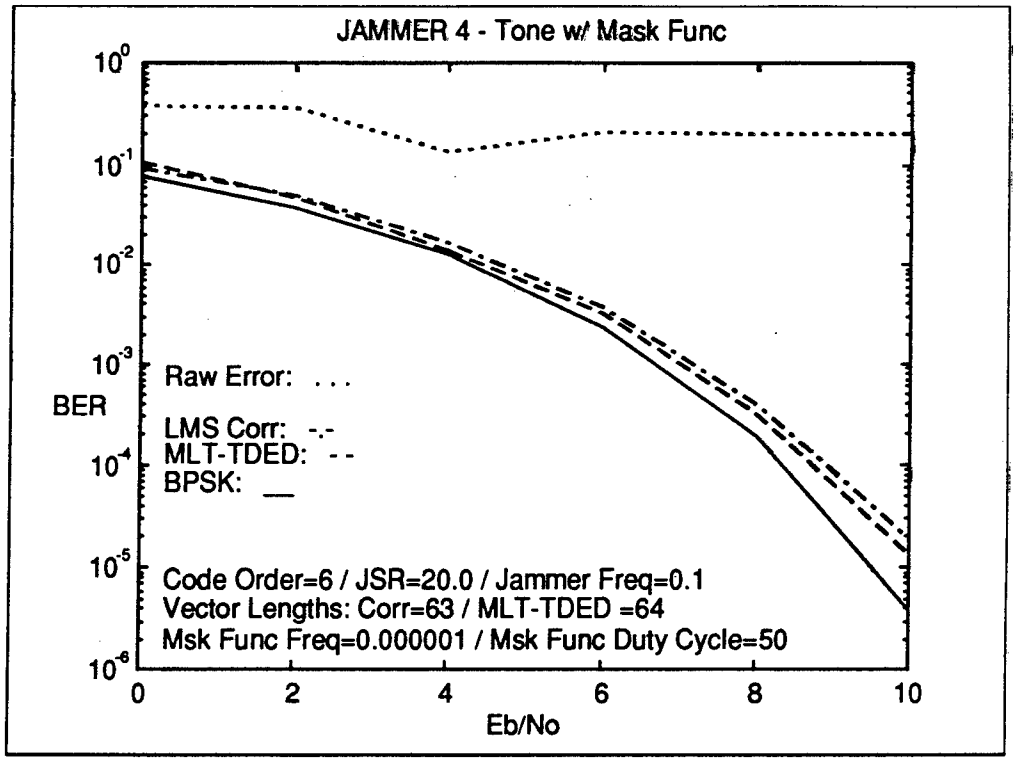

Figure 4.34 : BER vs. Eb/No for Jammer 4-Tone - Corr / MLT-TDED

Figures 4.35 and 4.36 show the curves of BER vs. JSR for the different structures. The convergence factor μ for the adaptive filters and correlator, and exciser parameters for the MLT systems are optimized for each value of JSR, and can be seen in Tables 4.9 and 4.10. A value of $E_b / N_o = 6\,dB$ is used for the Gaussian noise included in the channel. The default parameters used for the jammer are a normalized frequency $f = 0.1\,Hz$, and values of $f_{msk\ func} = 0.000001\,Hz$ and $Duty\ Cycle_{msk\ func} = 50\,\%$ for the masking function. It can be seen that the LMS filters provide the best performance, in particular the two-sided filter, showing moderate dependence of BER on JSR. All the other systems provide poor performance after values of $JSR \approx 35\,dB$, even though the MLT-TDED system seems to reasonably reduce the jamming effects up to $JSR \approx 65\,dB$.

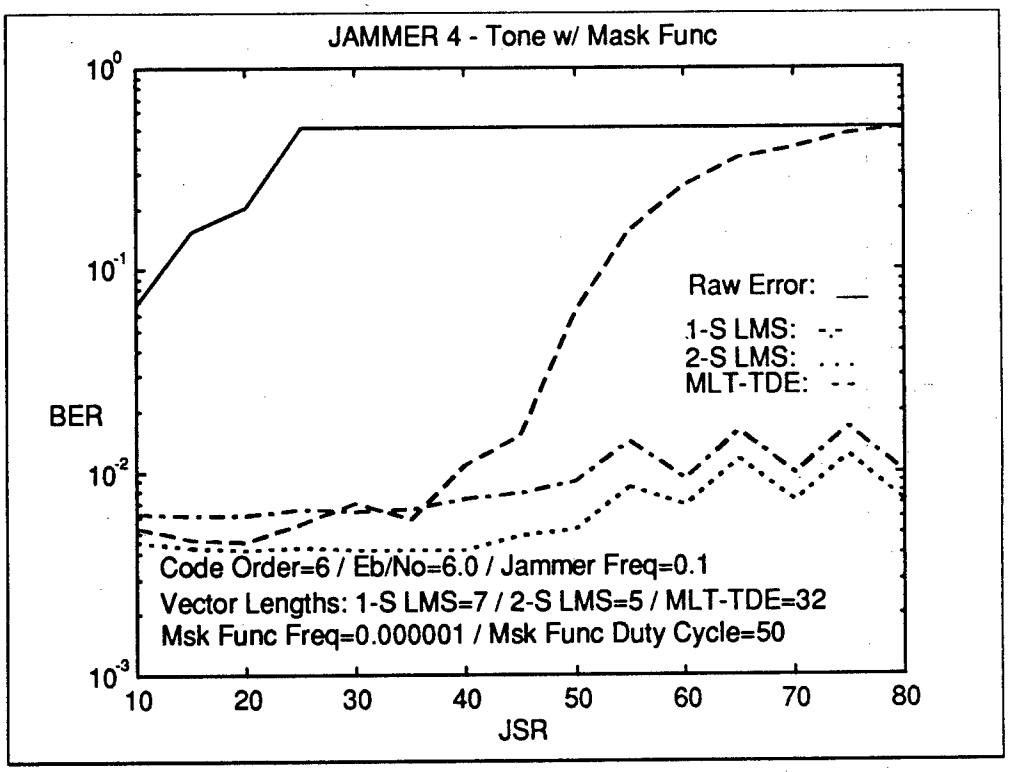

Figure 4.35 : BER vs. JSR for Jammer 4-Tone - Filters / MLT-TDE

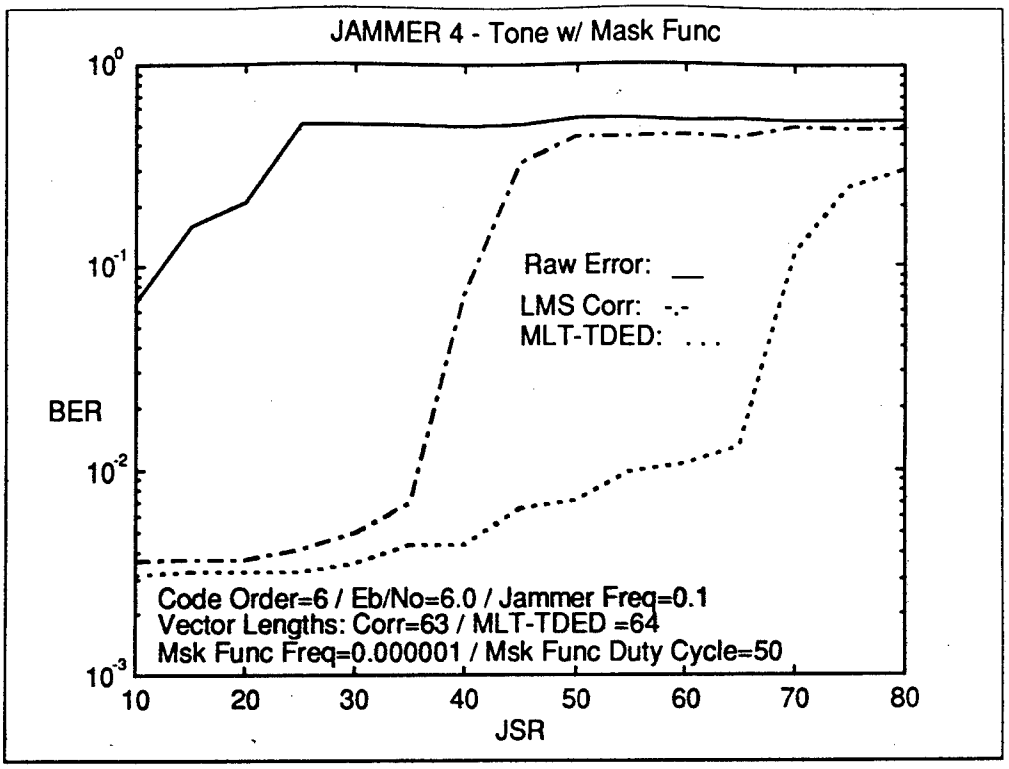

Figure 4.36 : BER vs. JSR for Jammer 4-Tone - Corr / MLT-TDED

PREDICTIVE FILTER	TWO-SIDED FILTER	MLT-TDE
JSR = 10 dB μ = 0.00001 JSR = 15 dB μ = 0.00001 JSR = 20 dB μ = 0.00001 JSR = 25 dB μ = 0.00001 JSR = 30 dB μ = 0.000001 JSR = 35 dB μ = 0.000001 JSR = 40 dB μ = 0.0000001 JSR = 45 dB μ = 0.0000001 JSR = 50 dB μ = 0.0000001 JSR = 55 dB μ = 0.0000001 JSR = 60 dB μ = 0.00000001 JSR = 65 dB μ = 0.00000001 JSR = 70 dB μ = 0.000000001 JSR = 75 dB μ = 0.000000001 JSR = 80 dB μ = 0.0000000001	JSR = 10 dB μ = 0.0001 JSR = 15 dB μ = 0.0001 JSR = 20 dB μ = 0.0001 JSR = 25 dB μ = 0.0001 JSR = 30 dB μ = 0.00001 JSR = 35 dB μ = 0.00001 JSR = 40 dB μ = 0.000001 JSR = 45 dB μ = 0.000001 JSR = 50 dB μ = 0.0000001 JSR = 55 dB μ = 0.0000001 JSR = 60 dB μ = 0.00000001 JSR = 65 dB μ = 0.00000001 JSR = 70 dB μ = 0.000000001 JSR = 75 dB μ = 0.000000001 JSR = 80 dB μ = 0.0000000001	JSR = 10 dB Threshold = 9.0 Notch Width = 1 JSR = 15 dB Threshold = 12.0 Notch Width = 1 JSR = 20 dB Threshold = 12.0 Notch Width = 1 JSR = 25 dB Threshold = 12.0 Notch Width = 1 JSR = 30 dB Threshold = 12.0 Notch Width = 1 JSR = 35 dB Threshold = 16.0 Notch Width = 2 JSR = 40 dB Threshold = 20.0 Notch Width = 2 JSR = 45 dB Threshold = 18.0 Notch Width = 4 JSR = 50 dB Threshold = 18.0 Notch Width = 5 JSR = 55 dB Threshold = 18.0 Notch Width = 5 JSR = 60 dB Threshold = 22.0 Notch Width = 6 JSR = 65 dB Threshold = 22.0 Notch Width = 7 JSR = 70 dB Threshold = 24.0 Notch Width = 7 JSR = 75 dB Threshold = 24.0 Notch Width = 7 JSR = 80 dB Threshold = 24.0 Notch Width = 7

Table 4.9: Jammer 4 Tone - Filters / MLT-TDE - Parameters Used for Each Value of JSR

ADAPTIVE CORRELATOR	MLT-TDED
JSR = 10 dB μ = 0.000001 JSR = 15 dB μ = 0.000001 JSR = 20 dB μ = 0.000001 JSR = 25 dB μ = 0.000001 JSR = 30 dB μ = 0.000001 JSR = 35 dB μ = 0.000001 JSR = 40 dB μ = 0.000001 JSR = 45 dB μ = 0.0000001 JSR = 50 dB μ = 0.00000001 JSR = 55 dB μ = 0.000000001 JSR = 60 dB μ = 0.0000000001 JSR = 65 dB μ = 0.0000000001 JSR = 70 dB μ = 0.0000000001 JSR = 75 dB μ = 0.000000001 JSR = 80 dB μ = 0.000000001	JSR = 10 dB Threshold = 11.0 Notch Width = 1 JSR = 15 dB Threshold = 15.0 Notch Width = 2 JSR = 20 dB Threshold = 15.0 Notch Width = 2 JSR = 25 dB Threshold = 15.0 Notch Width = 2 JSR = 30 dB Threshold = 17.0 Notch Width = 2 JSR = 35 dB Threshold = 21.0 Notch Width = 2 JSR = 40 dB Threshold = 23.0 Notch Width = 3 JSR = 45 dB Threshold = 25.0 Notch Width = 4 JSR = 50 dB Threshold = 27.0 Notch Width = 4 JSR = 55 dB Threshold = 27.0 Notch Width = 4 JSR = 60 dB Threshold = 27.0 Notch Width = 5 JSR = 65 dB Threshold = 35.0 Notch Width = 5 JSR = 70 dB Threshold = 35.0 Notch Width = 6 JSR = 75 dB Threshold = 35.0 Notch Width = 6 JSR = 80 dB Threshold = 37.0 Notch Width = 6

Table 4.10: Jammer 4 Tone - Corr / MLT-TDED - Parameters Used for Each Value of JSR

Figures 4.37 and 4.38 present BER vs. jammer frequency, for the different receiver structures and for the raw error. The curves only show a sampling of jammer frequencies with points taken at $f = 0.08\,Hz$, $f = 0.1\,Hz$, $f = 0.12\,Hz$, $f = 0.15\,Hz$, $f = 0.18\,Hz$, $f = 0.2\,Hz$, $f = 0.234\,Hz$, $f = 0.25\,Hz$, $f = 0.3\,Hz$, $f = 0.35\,Hz$, $f = 0.4\,Hz$, and $f = 0.45\,Hz$. For these simulations, the default parameters used are values of $E_b / N_o = 6\,dB$ for the channel, $JSR = 20\,dB$ for the jammer, and $f_{msk\ func} = 0.000001\,Hz$ and $Duty\ Cycle_{msk\ func} = 50\,\%$ for the masking function. The parameters used for the interference suppression techniques are $\mu = 0.00001$ for the predictive and $\mu = 0.0001$ for the two-sided filter, $threshold = 12.0$ and $notch\ width = 1$ for the MLT-TDE structure, $\mu = 0.000001$ for the correlator, and $threshold = 15.0$ and $notch\ width = 2$ for the MLT-TDED system. It can be observed that all the structures are able to efficiently remove the jamming effects, showing no real dependence on jammer frequency.

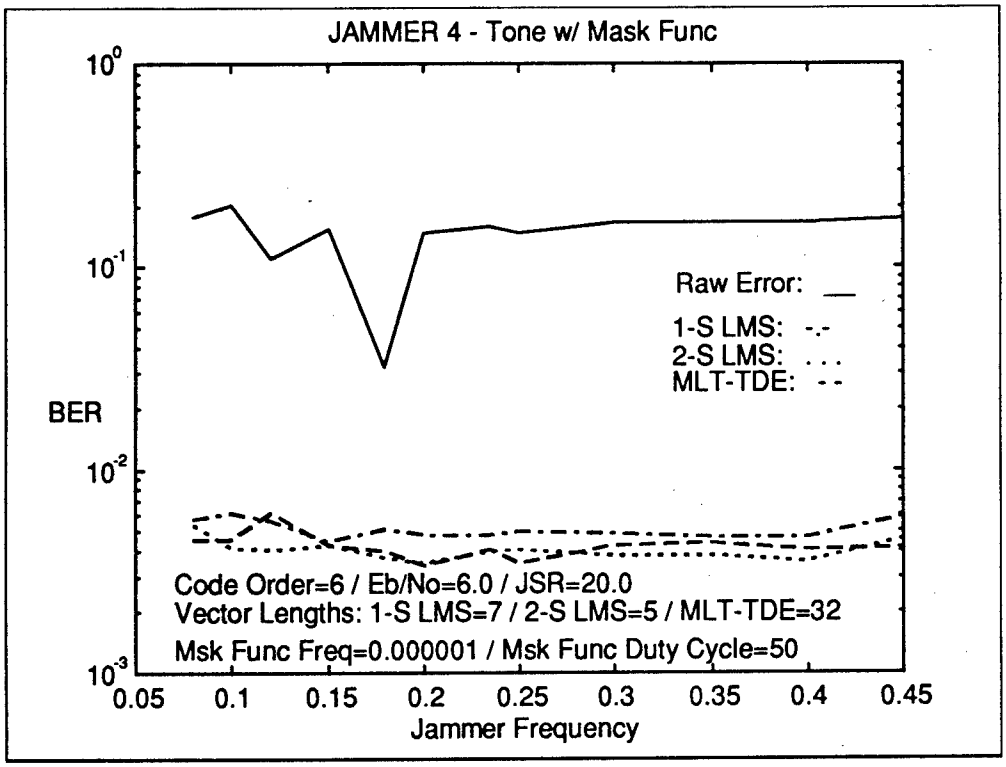

Figure 4.37 : BER vs. Jammer Frequency for Jammer 4-Tone - Filters / MLT-TDE

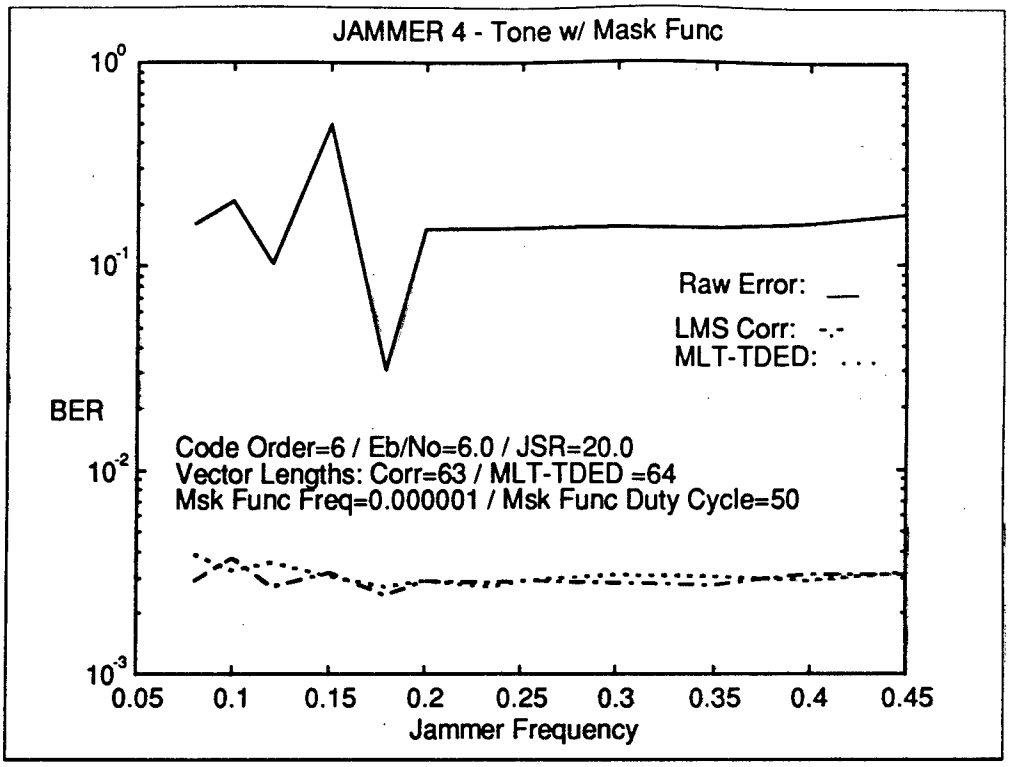

Figure 4.38 : BER vs. Jammer Frequency for Jammer 4-Tone - Corr / MLT-TDED

4.4.2- Pulsed Gaussian Jamming

This section shows the results obtained for each of the communication receiver systems in presence of pulsed Gaussian noise jamming in the channel.

In Figure 4.39, the plot of BER vs. E_b/N_o for the filters and MLT-based transform domain exciser, as well as the results for BPSK signal in AWGN and raw error are presented. The jammer parameters used are $JSR = 20\,dB$, a normalized frequency of $f = 0.1\,Hz$, and a jammer bandwidth of $BW = 0.05\,Hz$, while the values for the masking function are $f_{msk\ func} = 0.000001\,Hz$ and $Duty\ Cycle_{msk\ func} = 50\,\%$. A value of $\mu = 0.00001$ for the predictive and $\mu = 0.00001$ for the two-sided filter are used, while a $threshold = 10.0$ and $notch\ width = 1$ are employed for the MLT-TDE structure. The two-sided filter and MLT-TDE system present reasonable and somewhat similar interference suppression capabilities; on another hand, for higher values of $E_b / N_o \approx 4\,dB$, the predictive filter presents poor performance, with higher values for the BER than the other two structures.

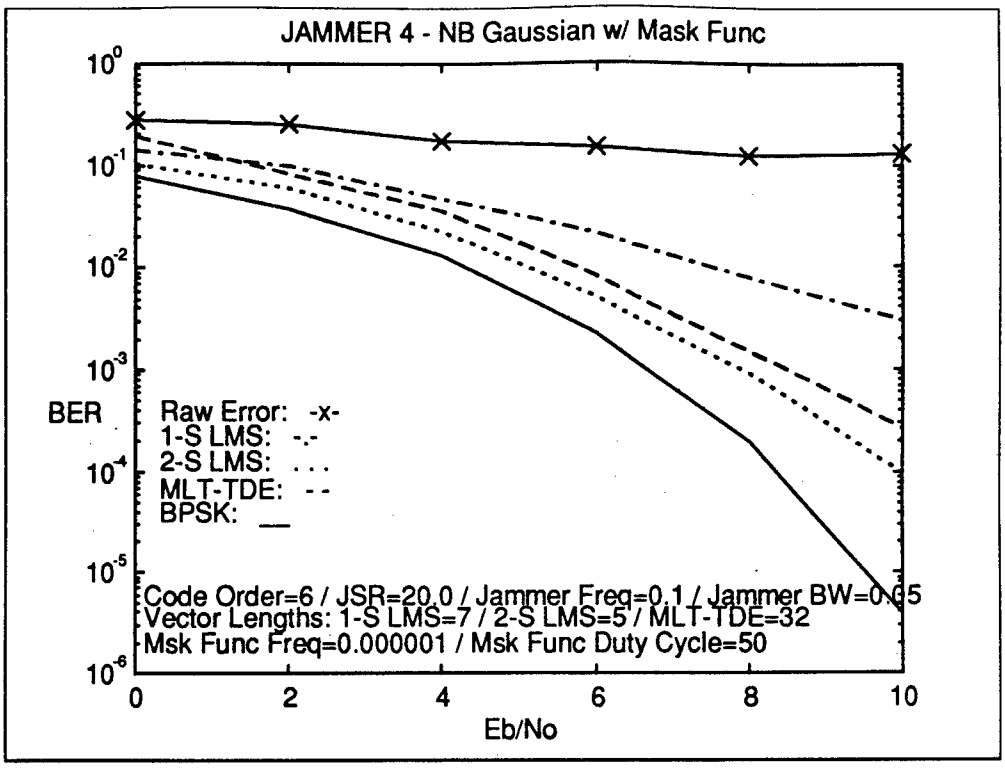

Figure 4.39 : BER vs. Eb/No for Jammer 4-NB - Filters / MLT-TDE

Figure 4.40 plots BER vs. E_b/N_o for the LMS correlator and MLT-TDED system. For these simulations, the default parameters used for the jammer are $JSR = 20\,dB$, a normalized frequency $f = 0.1\,Hz$, and a jammer bandwidth of $BW = 0.05\,Hz$, while the default values utilized to represent the masking function are $f_{msk\ func} = 0.000001\,Hz$ and $Duty\ Cycle_{msk\ func} = 50\,\%$. A value of $\mu = 0.00001$ for the correlator, and $threshold = 13.0$ and $notch\ width = 2$ for the MLT-TDED system are used. Both structures produce results that are similar to those for the two-sided filter and MLT-TDE system, even though the results of the adaptive correlator slightly deteriorate after $E_b / N_o \approx 5\,dB$.

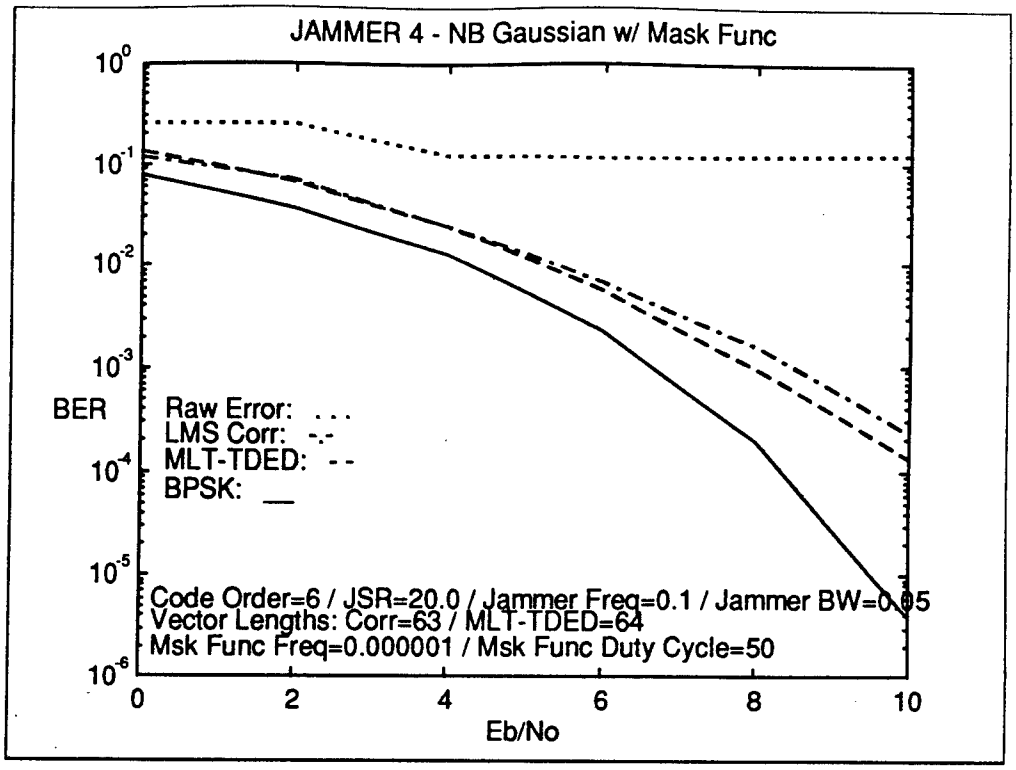

Figure 4.40 : BER vs. Eb/No for Jammer 4-NB - Corr / MLT-TDED

Figures 4.41 and 4.42 show the curves representing BER vs. JSR for the different structures. Values of $E_b / N_o = 6\,dB$, normalized frequency of $f = 0.1\,Hz$, and jammer bandwidth of $BW = 0.05\,Hz$ are used for the jammer, while for the masking function $f_{msk\ func} = 0.000001\,Hz$ and $Duty\ Cycle_{msk\ func} = 50\,\%$ are employed. The optimized parameters of the interference suppression techniques for each value of JSR are shown in Tables 4.11 and 4.12. As can be observed from the curves, after values of $JSR \approx 30 - 40\,dB$ all the different structures show poor performance in improving the BER; although the two-sided LMS filter and the MLT-TDED structure present better results than the other receivers.

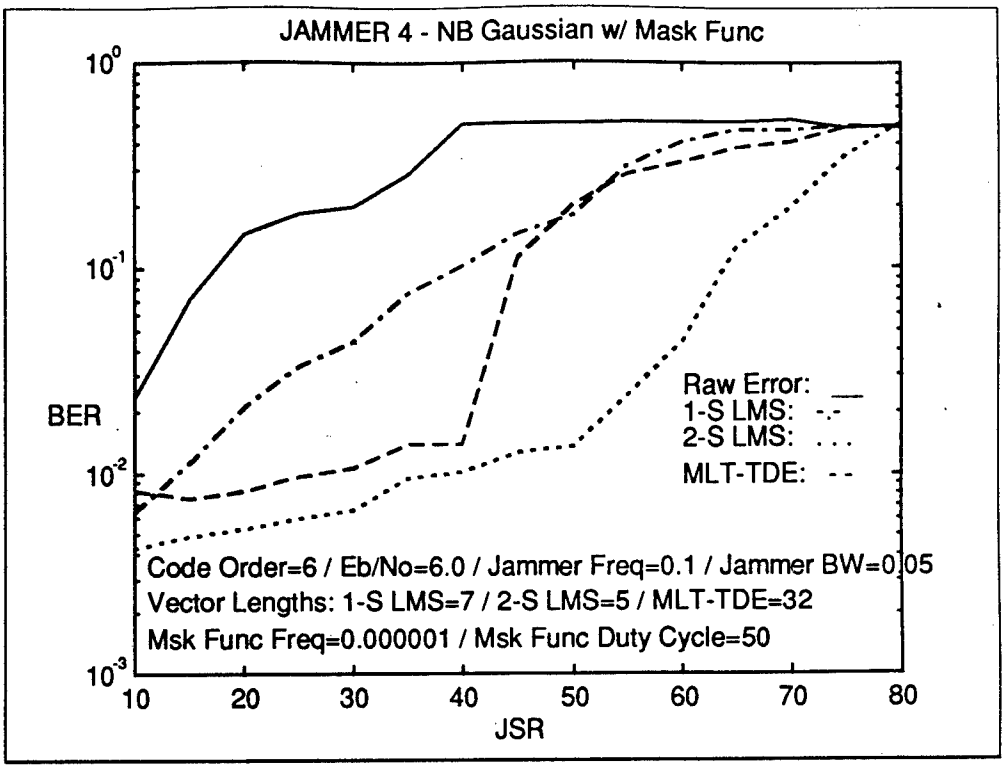

Figure 4.41 : BER vs. JSR for Jammer 4-NB - Filters / MLT-TDE

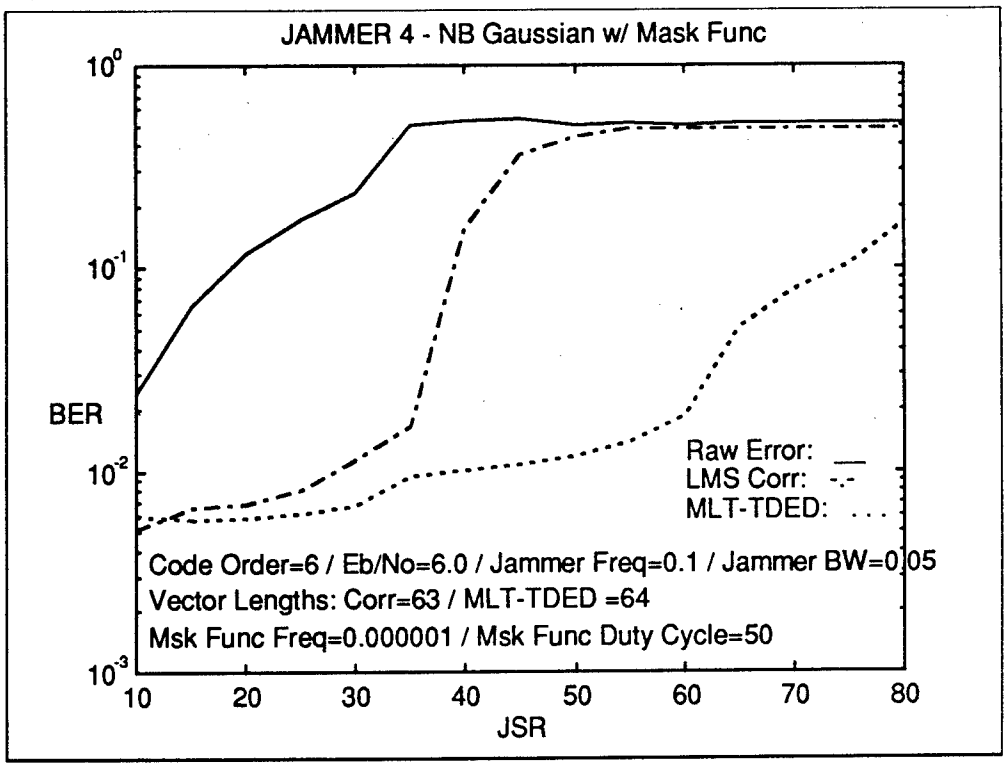

Figure 4.42 : BER vs. JSR for Jammer 4-NB - Corr / MLT-TDED

PREDICTIVE FILTER	TWO-SIDED FILTER	MLT-TDE
JSR = 10 dB μ = 0.00001 JSR = 15 dB μ = 0.00001 JSR = 20 dB μ = 0.00001 JSR = 25 dB μ = 0.00001 JSR = 30 dB μ = 0.00001 JSR = 35 dB μ = 0.000001 JSR = 40 dB μ = 0.000001 JSR = 45 dB μ = 0.0000001 JSR = 50 dB μ = 0.0000001 JSR = 55 dB μ = 0.00000001 JSR = 60 dB μ = 0.00000001 JSR = 65 dB μ = 0.000000001 JSR = 70 dB μ = 0.0000000001 JSR = 75 dB μ = 0.000000000001 JSR = 80 dB μ = 0.000000000001	JSR = 10 dB μ = 0.00001 JSR = 15 dB μ = 0.00001 JSR = 20 dB μ = 0.00001 JSR = 25 dB μ = 0.00001 JSR = 30 dB μ = 0.00001 JSR = 35 dB μ = 0.000001 JSR = 40 dB μ = 0.000001 JSR = 45 dB μ = 0.0000001 JSR = 50 dB μ = 0.0000001 JSR = 55 dB μ = 0.00000001 JSR = 60 dB μ = 0.00000001 JSR = 65 dB μ = 0.000000001 JSR = 70 dB μ = 0.000000001 JSR = 75 dB μ = 0.0000000001 JSR = 80 dB μ = 0.0000000001	JSR = 10 dB Threshold = 10.0 Notch Width = 1 JSR = 15 dB Threshold = 11.0 Notch Width = 2 JSR = 20 dB Threshold = 10.0 Notch Width = 1 JSR = 25 dB Threshold = 11.0 Notch Width = 2 JSR = 30 dB Threshold = 11.0 Notch Width = 2 JSR = 35 dB Threshold = 13.0 Notch Width = 2 JSR = 40 dB Threshold = 15.0 Notch Width = 2 JSR = 45 dB Threshold = 17.0 Notch Width = 4 JSR = 50 dB Threshold = 21.0 Notch Width = 4 JSR = 55 dB Threshold = 21.0 Notch Width = 5 JSR = 60 dB Threshold = 21.0 Notch Width = 5 JSR = 65 dB Threshold = 25.0 Notch Width = 6 JSR = 70 dB Threshold = 29.0 Notch Width = 7 JSR = 75 dB Threshold = 29.0 Notch Width = 8 JSR = 80 dB Threshold = 29.0 Notch Width = 8

Table 4.11: Jammer 4 Noise - Filters / MLT-TDE - Parameters Used for Each Value of JSR

ADAPTIVE CORRELATOR	MLT-TDED
JSR = 10 dB μ = 0.00001 JSR = 15 dB μ = 0.00001 JSR = 20 dB μ = 0.00001 JSR = 25 dB μ = 0.000001 JSR = 30 dB μ = 0.000001 JSR = 35 dB μ = 0.000001 JSR = 40 dB μ = 0.000001 JSR = 45 dB μ = 0.0000001 JSR = 50 dB μ = 0.0000001 JSR = 55 dB μ = 0.0000001 JSR = 60 dB μ = 0.0000001 JSR = 65 dB μ = 0.00000001 JSR = 70 dB μ = 0.00000001 JSR = 75 dB μ = 0.00000001 JSR = 80 dB μ = 0.00000001	JSR = 10 dB Threshold = 9.0 Notch Width = 1 JSR = 15 dB Threshold = 13.0 Notch Width = 2 JSR = 20 dB Threshold = 13.0 Notch Width = 2 JSR = 25 dB Threshold = 14.0 Notch Width = 2 JSR = 30 dB Threshold = 14.0 Notch Width = 2 JSR = 35 dB Threshold = 14.0 Notch Width = 2 JSR = 40 dB Threshold = 14.0 Notch Width = 2 JSR = 45 dB Threshold = 14.0 Notch Width = 2 JSR = 50 dB Threshold = 14.0 Notch Width = 2 JSR = 55 dB Threshold = 14.0 Notch Width = 2 JSR = 60 dB Threshold = 14.0 Notch Width = 5 JSR = 65 dB Threshold = 14.0 Notch Width = 5 JSR = 70 dB Threshold = 14.0 Notch Width = 6 JSR = 75 dB Threshold = 14.0 Notch Width = 6 JSR = 80 dB Threshold = 14.0 Notch Width = 6

Table 4.12: Jammer 4 Noise - Corr / MLT-TDED - Parameters Used for Each Value of JSR

Figures 4.43 and 4.44 show the curves representing BER vs. jammer frequency for the different receiver structures and for the raw error. The plots only show a sampling of jammer frequencies with points taken at $f = 0.08\,Hz$, $f = 0.1\,Hz$, $f = 0.12\,Hz$, $f = 0.15\,Hz$, $f = 0.18\,Hz$, $f = 0.2\,Hz$, $f = 0.234\,Hz$, $f = 0.25\,Hz$, $f = 0.3\,Hz$, $f = 0.35\,Hz$, $f = 0.4\,Hz$, and $f = 0.45\,Hz$. For these simulations, the default parameters used for the jammer are $E_b / N_o = 6\,dB$, $JSR = 20\,dB$ and a jammer bandwidth of $BW = 0.05\,Hz$, while values of $f_{msk\ func} = 0.000001\,Hz$ and $Duty\ Cycle_{msk\ func} = 50\,\%$ are utilized for the masking frequency. A value of $\mu = 0.00001$ for the predictive and $\mu = 0.00001$ for the two-sided filter are used, while a $threshold = 10.0$ and $notch\ width = 1$ are employed for the MLT-TDE structure. Also, a value of $\mu = 0.00001$ for the correlator, and $threshold = 13.0$ and $notch\ width = 2$ for the MLT-TDED system are utilized to perform the simulations. The results show that the structures are rather independent on jammer frequency.

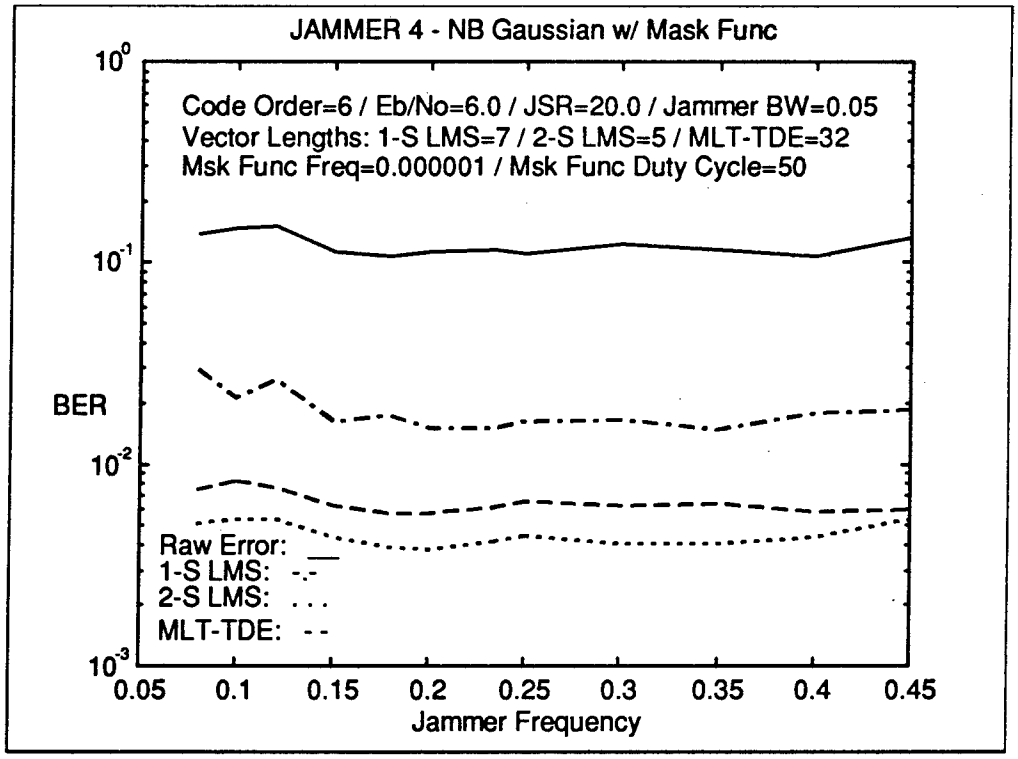

Figure 4.43 : BER vs. Jammer Frequency for Jammer 4-NB - Filters / MLT-TDE

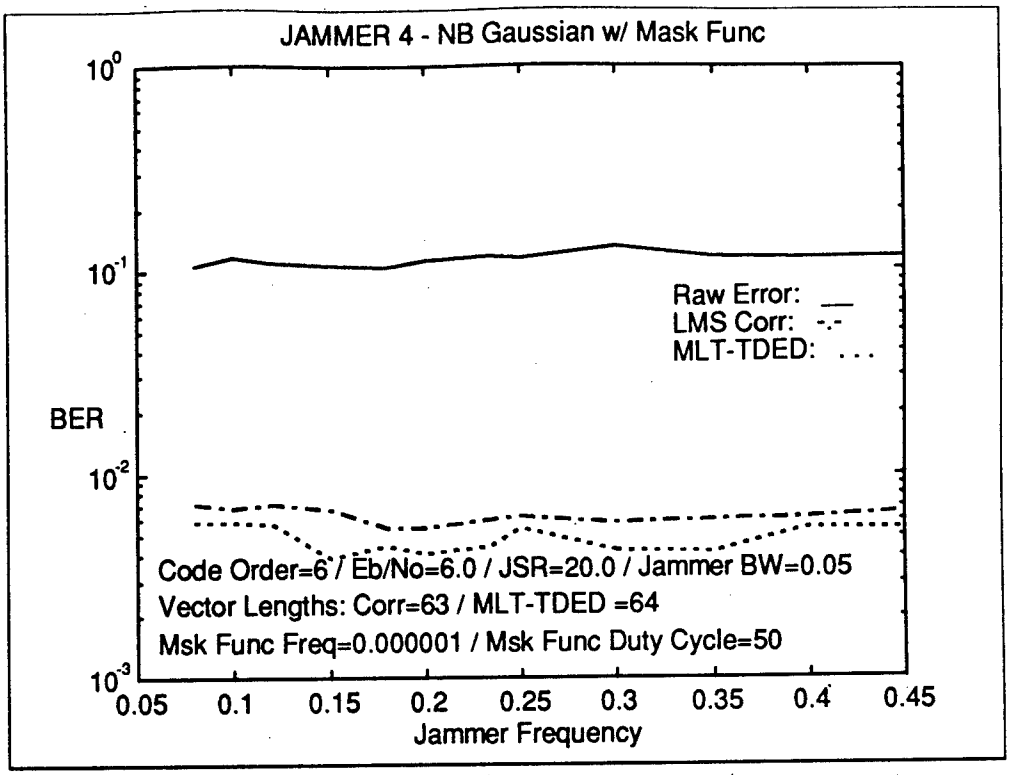

Figure 4.44 : BER vs. Jammer Frequency for Jammer 4-NB - Corr / MLT-TDED

In Figures 4.45 and 4.46, the plots of BER vs. jammer bandwidth can be seen for the different receiver systems and for the raw error case. The curves only show a sampling of jammer bandwidths with results obtained at $BW = 0.03\,Hz$, $BW = 0.05\,Hz$, $BW = 0.1\,Hz$, $BW = 0.15\,Hz$, $BW = 0.2\,Hz$, $BW = 0.25\,Hz$, $BW = 0.3\,Hz$, $BW = 0.35\,Hz$, $BW = 0.4\,Hz$, and $BW = 0.45\,Hz$. The default parameters for the jammer are $E_b / N_o = 6\,dB$, $JSR = 20\,dB$ and a normalized frequency of $f = 0.1\,Hz$; $f_{msk\ func} = 0.000001\,Hz$ and $Duty\ Cycle_{msk\ func} = 50\,\%$ are used for the masking frequency. The parameters for the interference suppression techniques include a value of $\mu = 0.00001$ for the predictive and $\mu = 0.00001$ for the two-sided filter, a $threshold = 10.0$ and $notch\ width = 1$ for the MLT-TDE structure, a value of $\mu = 0.00001$ for the correlator, and $threshold = 13.0$ and $notch\ width = 2$ for the MLT-TDED system. In all the structures, the BER increases with the jammer bandwidth; the predictive filter shows inferior performance, while the two-sided filter and the MLT-TDED system seem to somewhat perform better under higher jammer bandwidth scenarios.

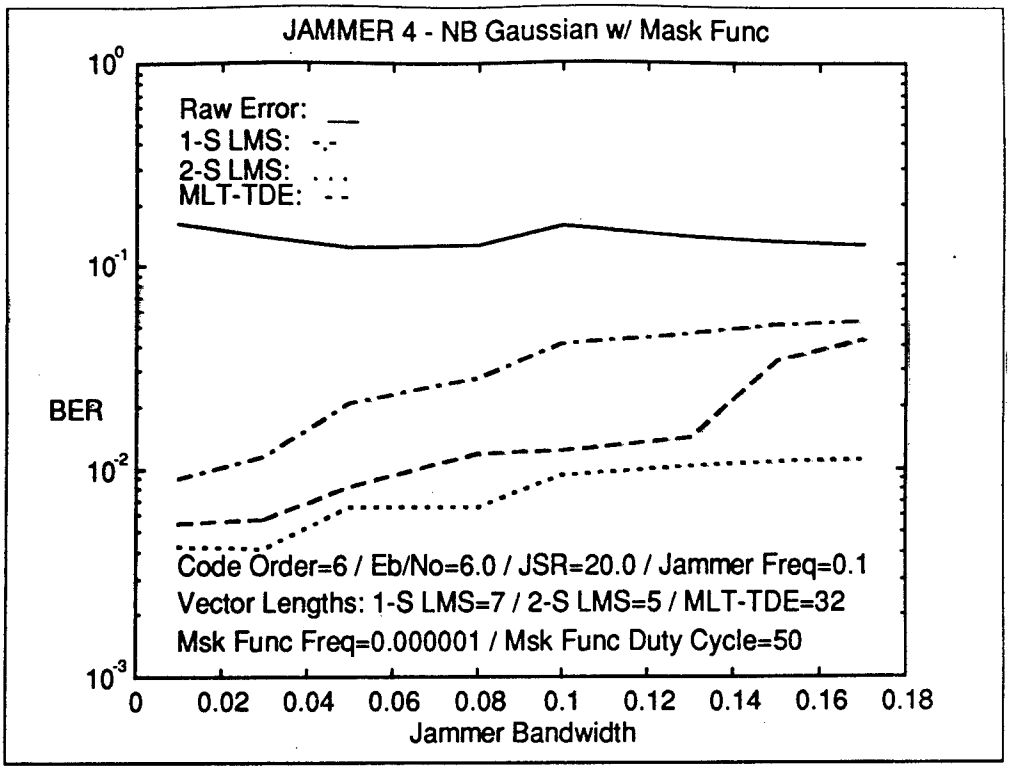

Figure 4.45 : BER vs. Jammer Bandwidth for Jammer 4-NB - Filters / MLT-TDE

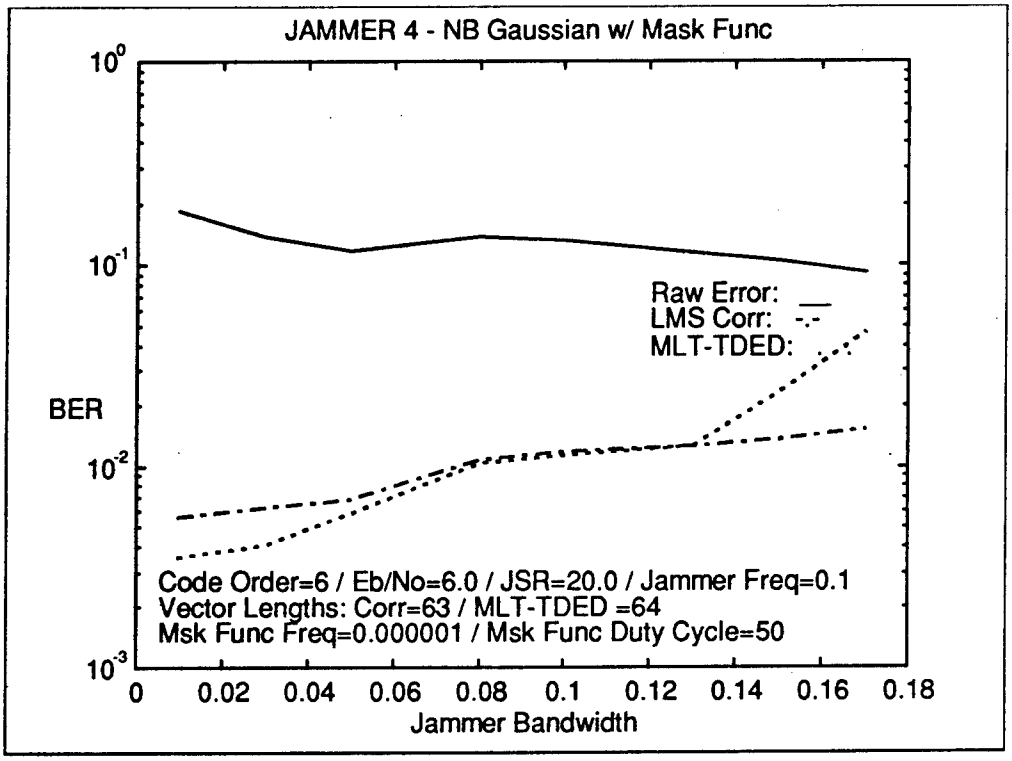

Figure 4.46 : BER vs. Jammer Bandwidth for Jammer 4-NB - Corr / MLT-TDED

CHAPTER 5

Conclusions and Discussions

5.1- Conclusions

The performance, in terms of low bit error rate, of the different receiver systems depends heavily on the jamming signal and parameters used, and therefore there is no "ideal" structure in the sense of a particular system that would be able to handle any type of situation. However, the satisfactory achievement of the LMS filters for the fixed tone, and of the MLT-TDED system for the sweep and Gaussian noise jammers can be emphasized.

5.1.1- Adaptive Filters

The simulation results indicate that LMS adaptive filtering improves bit error rate performance in a variety of narrowband jammer environments. Nevertheless, for higher values of JSR, the value of the μ parameter has to be lowered down, to decrease the additional distortion introduced by the jammer. The adaptive LMS filter performs pretty well with the fixed tone, but has problems keeping track of the changes involved in the swept-tone jammers. Indeed, since the jammer frequency is now changing constantly with these jammers, the transfer function of the adaptive filter must also be changing continually to track them. Hence, the LMS algorithm must not only converge, but must converge quickly enough to adjust any change in the jammer; thus, the convergence factor μ of the adaptive filter becomes an important parameter, as it governs the rate at which the filter converges. As mentioned earlier in this report, the larger the value of μ, the faster the convergence. Therefore, it is necessary to maintain a large value of μ, as the jammer frequency is changing quickly; however, a larger μ introduces more code distortion, making difficult the overall performance of the filter. Moreover, it can be observed that the performance relies heavily on the value of μ used; consequently, careful tuning is necessary in order for the filters to operate adequately.

In general, the two-sided filter performs better than the predictive, and requires lower implementation complexity with only $25\ OpS$ (Operation per Sample), while the predictive filter needs $28\ OpS$. It can therefore be concluded that the two-sided structure is much more efficient than the predictive.

5.1.2- MLT-Transform Domain Exciser

The MLT-TDE system performs pretty well as long as the interference power remains lower than a certain limit. Essentially, if the jammer-to-signal ratio is high enough, the windowing effects of the

block processing may cause the jammer sidelobes to also transcend the threshold, and as a result, a large portion of the signal energy is removed, increasing the bit error rate.

The results also point to the fact that the MLT systems are relatively insensitive to sweep frequency, and that their performance is rather independent of the parameters used for the excision process, which means that the system does not require fine tuning.

5.1.3- Adaptive Correlator

Regarding the tracking performance of this receiver, the adaptive correlator shows the highest convergence time, as its tracking capabilities are unable to remove the interference when the jammer sweeps too rapidly; this is why a higher number of symbols to wait is used for this structure. Indeed, this receiver involves a training period where the known sequence is generated in the receiver. Moreover, this structure presents poor results with large values of E_b / N_o for the swept-tone jammers.

However, the adaptive correlator involves much less computation in comparison with all the other receivers, with only $4\ OpS$ (Operation per Sample), due to its relatively simple structure.

5.1.4- MLT-Transform Domain Excision and Detection

The MLT-TDED system performs pretty well as long as the jammer-to-signal ratio is not high enough to originate signal energy destruction, even though its performance is pretty satisfactory compared with the other receiver structures, specially for the swept-tone and Gaussian jammers.

Besides, as the results indicate, the tracking capabilities of the MLT-TDED system are excellent, and it can definitely be concluded that this structure presents the shortest convergence time.

However, regarding the implementation complexity, the MLT-TDED system requires $29\ OpS$, and therefore is the computationally most expensive system. Anyhow, the lapped transform domain excision and detection algorithm must be considered as an efficient method for narrowband interference suppression applications.

5.1.5- Additional Comments

It can be noticed from Tables 4.1 to 4.12 that the higher the value of JSR, the lower the value of μ in the LMS algorithm to compensate for the excess power of the jammer, and the higher the values of *threshold* and/or *notch width* in the excision process, in order to be able to remove larger amounts of interference energy. Also, the values of μ used for the predictive filter are usually equal or lower than the ones used in the two-sided structure. Indeed, the results obtained with the first structure are frequently

inferior than the ones achieved with the two-sided, and therefore a lower values of μ has to be used in order to reduce the excess mean-square error.

It seems like the overall performance of the various receiver systems presents better outcomes with the fixed tone than with the pulsed tone; apparently, the changing shape of the jammer produces higher error rate. However, better performance is obtained with the pulsed Gaussian noise than with the uninterrupted version of it. This result might be due to the fact that a value of $BW = 0.05\ Hz$ is used for the pulsed noise, while a higher value of $BW = 0.1\ Hz$ is applied to the non-pulsed noise jammer. Also, the results obtained with chirp jamming are slightly better than the ones with swept tone. This might be due to the form of the triangular wave itself, which exhibits more alterations than the ramp wave, and therefore is harder to track.

5.2- Future Research

Some simulations were run for the filters and correlator receivers using the RLS algorithm for the adaptive filters. The RLS algorithm is much more computationally expensive than the LMS, even though it is supposed to converge faster. However, as for the different systems studied, the performance of the RLS algorithm was somewhat similar to the LMS algorithm's. Also, nonlinear LMS and RLS filters could be analyzed [12].

LMS and RLS adaptive filtering in the frequency domain can give significant reductions in computation over the conventional time-domain approach [4], and could also be incorporated as another communication receiver structure. However, this system has the drawback that it may not be able to react as quickly to changes in the input as the simple exciser.

Additional processing could be incorporated in the different systems, like compensation for the adaptive filter, and error-correcting codes combined with interleaving.

☆U.S. GOVERNMENT PRINTING OFFICE 1998-610-130-81005

CHAPTER 6

Bibliography

1.- Simon Haykin; "Digital Communications"; John Wiley & Sons; 1988.

2.- Rodger E. Ziemer and Roger L. Peterson; "Digital Communications and Spread Spectrum Systems"; Macmillan Publishing Company; 1985.

3.- Simon Haykin; "Adaptive Filter Theory"; Prentice-Hall; 1986.

4.- Francis Reed and Paul Feintuch; "A Comparison of LMS Adaptive Cancellers Implemented in the Frequency Domain and the Time Domain"; IEEE Transactions on Acoustics, Speech, and Signal Processing, June 1981.

5.- Gary J. Saulnier, Pankaj Das, and Laurence Milstein; "An Adaptive Digital Suppression Filter for Direct-Sequence Spread-Spectrum Communications"; IEEE Journal on Selected Areas in Communications; September 1985.

6.- Henrique S. Malvar; "Signal Processing with Lapped Transform"; Artech House; 1987.

7.- Michael J. Medley; "Adaptive Narrow-Band Interference Suppression Using Linear Transforms and Multirate Filter Banks"; PhD Thesis RPI; November 1995.

8.- Michael J. Medley, Gary J. Saulnier and Pankaj K. Das; "Narrow-band Interference Excision in Spread Spectrum Systems Using Lapped Transforms".

9.- Charles Pateros and Gary J. Saulnier; "A Decision Directed Adaptive Correlator for a Direct Sequence Spread Spectrum Receiver"; IEEE; 1992.

10.- Charles Pateros and Gary J. Saulnier; "An Adaptive Correlator Receiver for Direct Sequence Spread Spectrum Communication".

11.- Laurence Milstein; "Interference Rejection Techniques in Spread Spectrum Communications"; Proceedings of the IEEE, vol. 76, June 1988.

12.- Wen-Rong Wu and Fu-Fuang Yu; "New Nonlinear Algorithms for Estimating and Suppressing Narrowband Interference in DS Spread Spectrum Systems"; IEEE Transactions on Communications; April 1996.

13.- Don J. Torrieri; "Principles of Secure Communication Systems"; Artech House,; 1992.